AD-A150 139 SAMPLE INTRODUCTION METHODS FOR IMPROVING THE PARTICLE 1/2
DETECTION CAPABILI.. (U) DAYTON UNIV OH RESEARCH INST
W E RHINE ET AL. 04 JAN 85 UDR-TR-84-37 NAEC-92-185
UNCLASSIFIED N68335-83-C-0625 F/G 20/6 NL

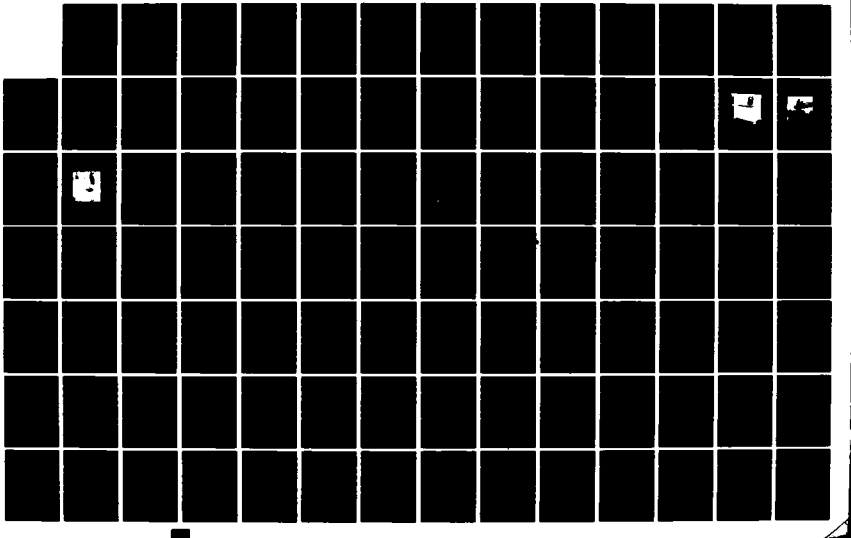

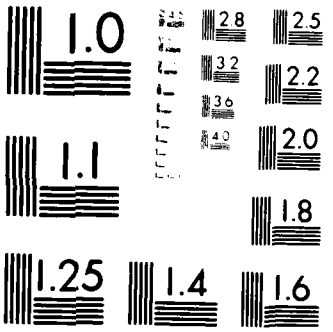

(12)

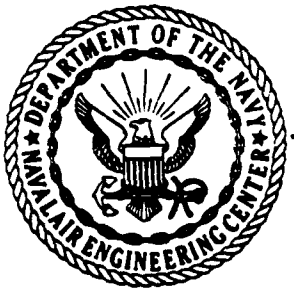

LAKEHURST N J

NAVAL AIR ENGINEERING CENTER

REPORT NAEC-92-185

SAMPLE INTRODUCTION METHODS FOR IMPROVING THE PARTICLE DETECTION CAPABILITY OF THE SPECTROMETRIC OIL ANALYSIS PROGRAM

Advanced Technology Office
Support Equipment Engineering Department
Naval Air Engineering Center
Lakehurst, New Jersey 08733

4 January 1985

Final Technical Report
AIRTASK A03V3400/051B/4F41-460-000

APPROVED FOR PUBLIC RELEASE;
DISTRIBUTION UNLIMITED

Prepared for

Commander, Naval Air Systems Command
AIR-310G
Washington, DC 20361

NAEC-92-185

SAMPLE INTRODUCTION METHODS FOR IMPROVING THE PARTICLE DETECTION CAPABILITY OF THE SPECTROMETRIC OIL ANALYSIS PROGRAM

Prepared by: Wendell E. Rhine
W. E. Rhine
University of Dayton Research Institute

Reviewed by: P. M. O'Donnell
P. M. O'Donnell
Advanced Technology Office (92A3)

Approved by: F. G. Evans
F. E. Evans
Support Equipment Engineering Superintendent

NOTICE

UNCLASSIFIED

SECURITY CLASSIFICATION OF THIS PAGE (When Data Entered)

REPORT DOCUMENTATION PAGE	READ INSTRUCTIONS BEFORE COMPLETING FORM
1. REPORT NUMBER NAEC-92-185	2. GOVT ACCESSION NO. A150139 / 3. RECIPIENT'S CATALOG NUMBER
4. TITLE (and Subtitle) Sample Introduction Methods for Improving the Particle Detection Capability of the Spectrometric Oil Analysis Program	5. TYPE OF REPORT & PERIOD COVERED Final Technical Report 25 Apr 83 - 25 Apr 84 6. PERFORMING ORG. REPORT NUMBER UDR-TR-84-37
7. AUTHOR(s) Wendell E. Rhine and Robert E. Kauffman	8. CONTRACT OR GRANT NUMBER(s) N68335-83-C-0625
9. PERFORMING ORGANIZATION NAME AND ADDRESS University of Dayton Research Institute 300 College Park Dayton, OH 45469	10. PROGRAM ELEMENT, PROJECT, TASK AREA & WORK UNIT NUMBERS Air Task A03V3400/051B/ 4F41-460-000
11. CONTROLLING OFFICE NAME AND ADDRESS Naval Air Systems Command (AIR-310G) Washington, DC 20361	12. REPORT DATE 4 January 1985 13. NUMBER OF PAGES 181
14. MONITORING AGENCY NAME & ADDRESS(if different from Controlling Office) Naval Air Engineering Center Support Equipment Engineering Department Code 92A3 Lakehurst, NJ 08733	15. SECURITY CLASS. (of this report) UNCLASSIFIED 15a. DECLASSIFICATION DOWNGRADING SCHEDULE

16. DISTRIBUTION STATEMENT (of this Report)

Approved for Public Release: Distribution unlimited.

17. DISTRIBUTION STATEMENT (of the abstract entered in Block 20, if different from Report)

18. SUPPLEMENTARY NOTES

19. KEY WORDS (Continue on reverse side if necessary and identify by block number)

Lubricant Contaminants
Particle Analysis
Wear Metal Analysis
Rotating Disk Electrode
Atomic Emission Spectroscopy
Engine Condition Monitoring

20. ABSTRACT (Continue on reverse side if necessary and identify by block number)

A program is being conducted to improve the particle detection capability of the rotating disk electrode arc/spark source atomic emission spectrometer, i.e., the A/E35U-3. This spectrometer is the primary spectrometer used by over 200 of the tri-service Joint Oil Analysis Program (JOAP) laboratories. Specifically, the A/E35U-3 emission spectrometer is used by 82 percent of the Air Force, 96 percent of the Navy, and 100 percent of the Army JOAP laboratories.

(continued)

DD FORM 1 JAN 73 1473 EDITION OF 1 NOV 65 IS OBSOLETE

UNCLASSIFIED

SECURITY CLASSIFICATION OF THIS PAGE (When Data Entered)

20. ABSTRACT (Continued)

The initial investigation determined the factors which limit the particle detection capability of the A/E35U-3 spectrometers. The results of this investigation were delineated in NAEC-92-169, Spectrometer Sensitivity Investigations on the Spectrometric Oil Analysis Program.

This report discusses the next effort which was conducted to improve the particle detection capability of the A/E35U-3 spectrometer. Acid dissolution, spark-to-residue and spark-in-vapor methods were investigated. The resultant data indicated that these methods can improve the particle detection capability of the spark source emission spectrometers.

Of the methods investigated, an acid dissolution method, followed by ashing the acid treated oil on a rotating platform electrode, gave the best metal recoveries and the most accurate analyses. All of the metals tested gave 100±5 percent recoveries except tin and aluminum which gave 119 percent and 74 percent recoveries, respectively. The modifications required for this acid dissolution (spark-to-residue) method are minimal. They involve replacing the rotating disk electrode with the rotating platform electrode. This method is particle size independent, since the particles are dissolved by the acid prior to analysis.

The spark-to-residue methods investigated that do not involve prior acid dissolution also improved the particle detection capability of the spark source emission spectrometer. However, the emission intensities observed for the standards and suspensions of metal particles did not agree resulting in low accuracy and high standard deviations for the analyses.

Another method investigated that has potential for improving the particle detection capability of spark source emission spectrometers was the spark-in-vapor method. For this method the oil is deposited onto an electrothermal atomization device and heated to vaporize the matrix and any metallic species. The atomic vapor is transported to the spark source by a carrier gas such as argon. Although electrothermal atomizers have been used with atomic absorption and plasma emission spectrometers, this effort is believed to be the first time electrothermal atomizers have been used with spark source spectrometers.

The spark-in-vapor method improved the particle detection capability of the spark source atomic emission spectrometer. With this method, the A/E35U-3 spectrometer could detect particles greater than 45 µm and gave accurate analyses for metal particles as large as 20 to 30 µm depending upon the metal. Specifically, this effort demonstrated the feasibility of the spark-in-vapor method by analyzing suspensions of silver, aluminum, copper, iron, magnesium and titanium powders in MIL-L-23699 oil.

The spark-to-residue and spark-in-vapor methods developed during this effort eliminate the matrix effects usually associated with spark source emission spectrometers. Therefore, analytical results obtained for various lubricants, i.e., hydrocarbon, versus synthetic ester base oils, can be directly compared.

The spark-in-vapor method also gives the spark emission spectrometers the capability to analyze ceramic materials such as silicon nitride. Also, it was demonstrated that rotating the disk counterclockwise improved the analysis of a 12-element suspension of metal particles.

PREFACE

This report describes the research conducted by personnel of the University of Dayton Research Institute on Contract No. N68335-83-C-0625. The work reported herein was performed during the period of 25 April 1983 to 25 April 1984, and was supported by the Naval Air Engineering Center, Support Equipment Engineering Department (92A3), Lakehurst, New Jersey. The effort was monitored by Mr. P. M. O'Donnell of the Naval Air Engineering Center whose advice and direction were significant in the successful completion of this effort.

The authors acknowledge the use of figures copyrighted by Baird Corporation. The figures appear in Section II and are appropriately referenced.

The A/E35U-3 used in the effort was located at Naval Air Engineering Center, Lakehurst, New Jersey, and, we thank Mr. P. M. O'Donnell for permission to use the spectrometer and making the necessary arrangements for our visit. We also thank Dr. Kent Eisentraut for permission to use his facilities at Wright-Patterson Air Force Base in preparing samples and for use of the A/E35U-1 spectrometer.

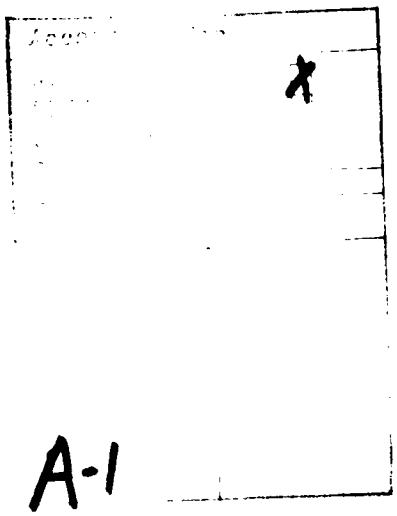

TABLE OF CONTENTS

TABLE OF CONTENTS (CONT'D)

TABLE OF CONTENTS (CONT'D)

TABLE OF CONTENTS (CONT'D)

TABLE OF CONTENTS (CONT'D)

TABLE OF CONTENTS (CONCLUDED)

LIST OF TABLES

LIST OF TABLES (CONT'D)

LIST OF TABLES (CONCLUDED)

LIST OF ILLUSTRATIONS

LIST OF ILLUSTRATIONS (CONT'D)

LIST OF ILLUSTRATIONS (CONT'D)

LIST OF ILLUSTRATIONS (CONCLUDED)

LIST OF ABBREVIATIONS

A%	Percent Metal Analyzed
ADM	Acid Dissolution Method
AD-STRM	Acid Dissolution/Spark-To-Residue Method
AE	Atomic Emission
AEE	Atlantic Equipment Engineers
A/E35U-1	Rotating Disk Electrode Spark Emission Spectrometer Used Prior to the A/E35U-3
A/E35U-3	Rotating Disk Electrode Spark Emission Spectrometer Currently Used for Oil Analysis
BC-1	Boiler Cap Electrode (1.0 mm Upper Orifice Diameter)
BC-2	Boiler Cap Electrode (2.1 mm Upper Orifice Diameter)
BC-3	Boiler Cap Electrode (3.2 mm Upper Orifice Diameter)
D-2	Bay Carbon's Rotating Disk Electrode (Catalog No. D-2)
JOAP	Joint Oil Analysis Program
NAEC	Naval Air Engineering Center
NAS	Naval Air Station
PC-1	Porous Cup Electrode With 30^{o} Chamber Floor
PC-30	Porous Cup Electrode With Flat Chamber Floor
PSIM	Particle Size Independent Method
RDE	Rotating Disk Electrode
RDE-SSAES	Rotating Disk Electrode - Spark Source Atomic Emission Spectrometry
ROC/RIC	Research Organic/Inorganic Chemical Corporation
RPE	Rotating Platform Electrode

LIST OF ABBREVIATIONS (CONT'D)

RSE	Reciprocating Semicylindrical Electrode
S.D.	Standard Deviation
SIVM	Spark-In-Vapor Method
STRM	Spark-To-Residue Method
TSC	Technical Support Center
UDRI	University of Dayton Research Institute
VC-2	Vacuum Cup Electrode
VMC	Vacuum Metallurgical Company
Ag	Silver
Al	Aluminum
B	Boron
Ba	Barium
Be	Beryllium
C	Carbon
Cd	Cadmium
Co	Cobalt
Cr	Chromium
Cu	Copper
Fe	Iron
H	Hydrogen
Mg	Magnesium
Mn	Manganese
Mo	Molybdenum
Na	Sodium
Ni	Nickel

LIST OF ABBREVIATIONS (CONCLUDED)

O	Oxygen
Pb	Lead
Si	Silicon
Sn	Tin
Ti	Titanium
V	Vanadium
W	Tungsten
Zn	Zinc
HCl	Hydrochloric Acid
HF	Hydrofluoric Acid
HNO_3	Nitric Acid
PTS	p-Toluenesulfonic Acid
TiC	Titanium Carbide
Si_3N_4	Silicon Nitride
ppm	Parts per Million
Neodol 91-8	$RO(CH_2CH_2O)_8H$ where R = C_9H_{19}, $C_{10}H_{21}$, $C_{11}H_{23}$ (Shell Oil Company)
µl	Microliter
µm	Micrometer
ml	Milliliter
mm	Millimeter

I. INTRODUCTION

A. The Joint Oil Analysis Program (JOAP) uses rotating disk electrode spark source atomic emission (RDE-SSAE) spectrometers to determine the presence of wear metal in used oil samples taken from operational aircraft. The presence of metallic debris, which is usually referred to as wear metal, in used oil samples is indicative of oil-wetted component wear. By detecting component wear before equipment failure occurs, JOAP has been successful in increasing fleet reliability and in reducing maintenance costs [reference (a)].

B. However, every year JOAP experiences equipment failures without prior detection of severe wear. One possible reason for these unpredicted failures is the inability of the RDE-SSAE spectrometers to detect large wear metal particles. Several cases have been reported where metallic wear particles produced by severe component wear were not detected by spectrometric methods [references (b)-(e)]. In two of these cases [references (d) and (e)] the inability of the spectrometers to detect the large wear metal particles led to aircraft, oil-wetted component failures where no abnormal wear was indicated by spectrometric oil analysis. Research conducted by the University of Dayton Research Institute (UDRI) also demonstrated that RDE-SSAE spectrometers could not quantitatively determine the concentration of wear metal particles larger than 3-10 μm [references (f) and (g)].

C. The factors responsible for the low particle detection capabilities of the RDE-SSAE spectrometers have been identified by UDRI [reference (g)]. The two most important factors identified were that the rotating disk is not an

---

Ref: (a) AFLC Historical Study No. 393 of December 1982: The Air Force Spectrometric Oil Analysis Program 1963-1980.

(b) Beerbower, A. "Spectrometry and Other Analysis Tools for Failure Prognosis". J. American Soc. of Lub. Engineers, V. 32, No. 6, P. 285-293, 1975.

(c) Seifert, W. W. and Wescott, V. C. "Investigation of Iron Content of Lubricating Oils Using a Ferrograph and an Emission Spectrometer". Wear, V. 23, No. 2, P. 239, 1973.

(d) Naval Aviation Integrated Logistic Support Center Report No. 03-41 of 27 May 1976: An Investigation of the Navy Oil Analysis Program (NOAP).

(e) Lee, R., Technical Support Center, Naval Air Station, Pensacola, Florida, Private Communication, 1979.

(f) AFWAL Report No. TR-82-4017 of February 1982: Evaluation of Plasma Source Spectrometers for the Air Force Oil Analysis Program.

(g) NAEC Report No. 92-169 of April 1983: Spectrometer Sensitivity Investigations on the Spectrometric Oil Analysis Program.

efficient particle transport system and the source has insufficient energy to vaporize both the oil and particles present.

D. Preliminary results presented in Report No. NAEC-92-169 [reference (g)] showed that the particle detection capabilities of RDE-SSAE spectrometers could be improved by using the homogeneous samples obtained from acid dissolution methods or by vaporizing (ashing) the oil prior to analysis of the wear metal debris. The work reported herein discusses the results obtained for acid dissolution methods and for ashing methods which were investigated as techniques for improving the particle detection capabilities of RDE-SSAE spectrometers.

E. The equipment and procedures used to improve the particle detection capabilities of RDE-SSAE spectrometers are discussed in Section II. The results and discussion of the methods investigated are included in Section III while Sections IV and V discuss the conclusions and recommendations derived from the research conducted.

II. EQUIPMENT AND PROCEDURES

A. INTRODUCTION.

1. The spectometric analysis of wear metals in lubricating oils requires procedures for the preparation of standards and samples and for calibration of the instrument. The accuracy of the analytical results depends primarily on the requirement that the standards and samples be as similar as possible.

2. This section describes the emission spectrometers used, the procedures followed to prepare and analyze the standards and samples, and the techniques used to improve the particle detection capabilities of RDE-SSAE spectrometers.

B. INSTRUMENTATION.

1. EMISSION SPECTROMETERS.

a. Introduction. The two instruments studied during this investigation are the A/E35U-1 (Figure 1) and A/E35U-3 (Figure 2) rotating disk electrode spark source atomic emission spectrometers manufactured by Baird Corporation, Bedford, Massachusetts. The A/E35U-1 is capable of simultaneously analyzing for Ag, Al, Cr, Cu, Fe, Mg, Ni, Pb, Si, and Sn, while the A/E35U-3 is equipped with 20 channels for the simultaneous analysis of Ag, Al, B, Ba, Be, Cd, Cr, Cu, Fe, Mg, Mn, Mo, Na, Ni, Pb, Si, Sn, Ti, V, and Zn. The A/E35U-1 is located at the University of Dayton Research Institute, Dayton, Ohio. The A/E35U-3 is located at the Naval Air Engineering Center, Lakehurst, New Jersey, and was used with the permission of Mr. P.M. O'Donnell. Standard JOAP analysis procedures were followed for operating the A/E35U-1 and the A/E35U-3 spectrometers [reference (h)].

b. Theory of Operation.

(1) Atomic emission (AE) spectrometry refers to analytical methods based on the measurement of atomic emission spectra. Emission spectrometry is based on a principle of atomic physics. An atom in its ground state consists of a nucleus and orbiting electrons in discrete energy levels. When the atom is subjected to high temperatures, it absorbs energy in specific quantities (Quanta), which forces the atom's electrons into higher energy levels, leaving the atom in an unstable excited state. Atoms in excited states spontaneously revert to their ground state by releasing the absorbed energy in the form of light in one or more characteristic wavelengths. To determine the concentration of metal in oil, the intensity of a suitable emission line for each element of interest is measured and compared with the emission intensities observed for standards.

(2) Inherently, atomic emission spectrometry has some distinct advantages when compared to atomic absorption spectrometry which make it a

---

Ref: (h) Naval Air Systems Command Report No. NA17-15-50 of 1 May 1977: Joint Oil Analysis Program Laboratory Manual.

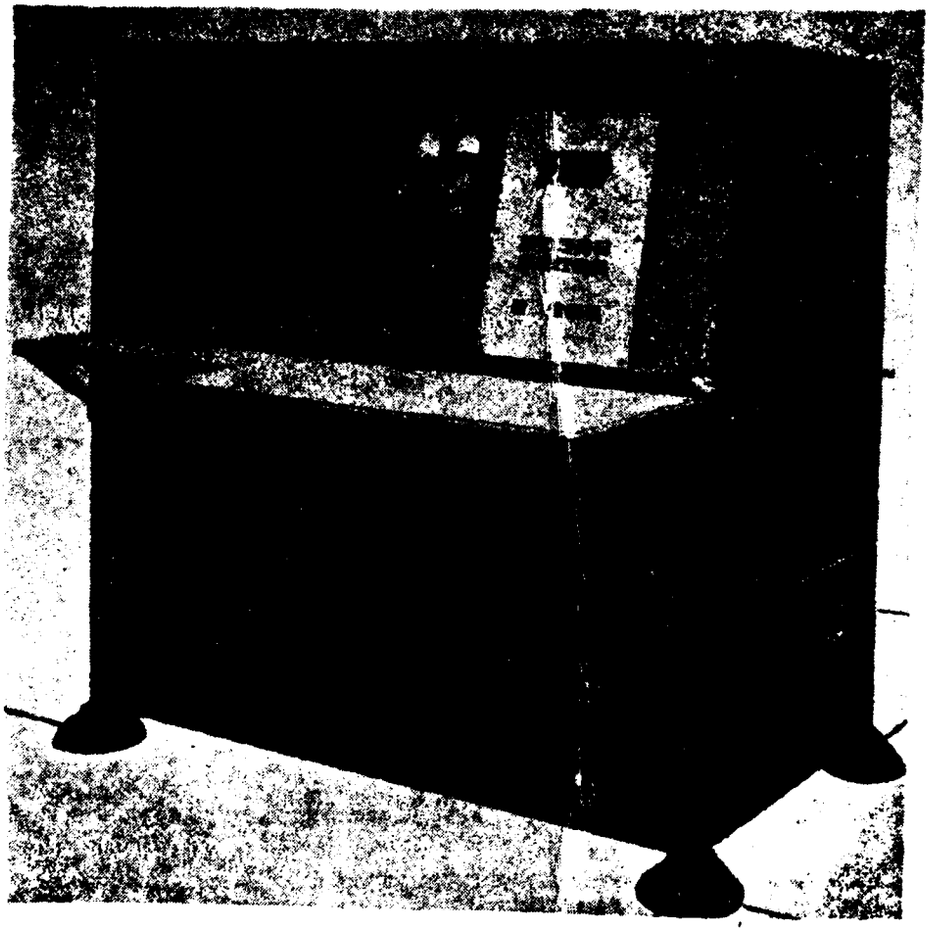

Figure 1. The A/E35U-1 Rotating Disk Electrode Spark Source Atomic Emission Spectrometer (Reproduced from Reference i).

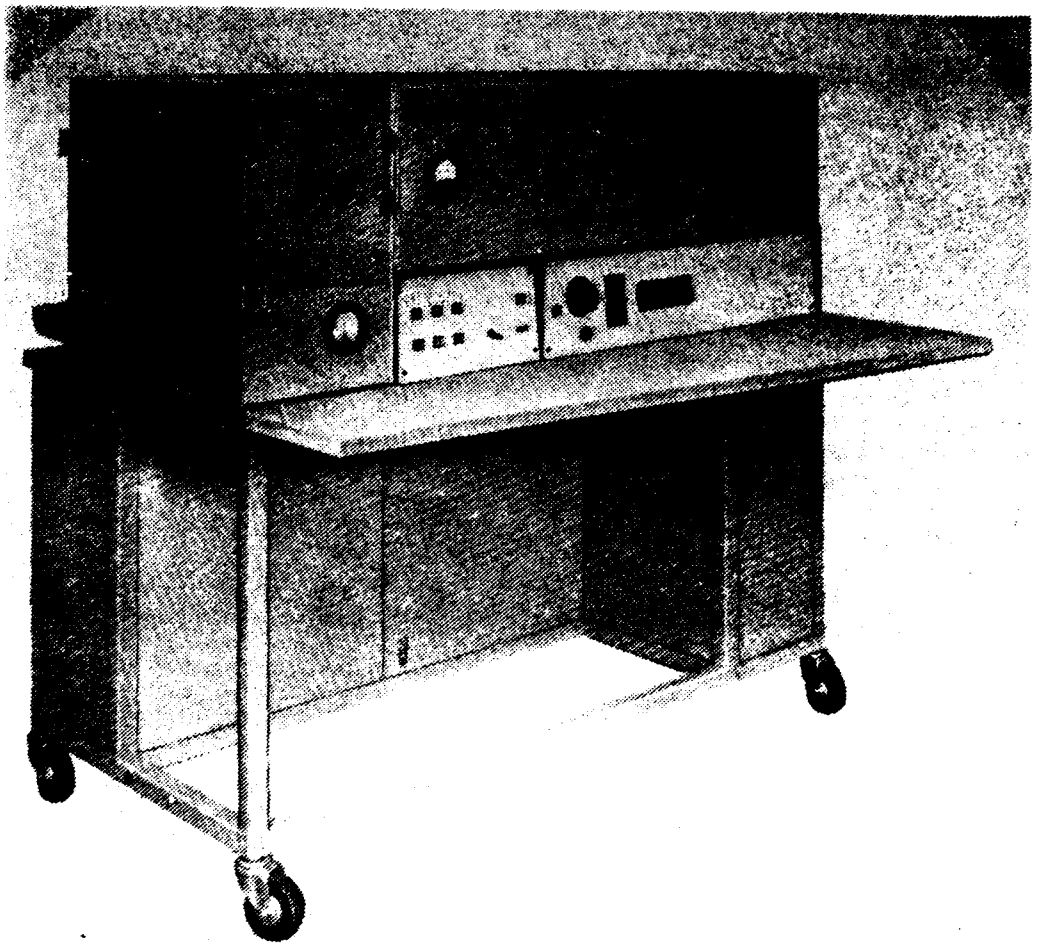

Figure 2. The A/E35U-3 Rotating Disk Electrode Spark Source Atomic Emission Spectrometer (Reproduced from Reference j).

desirable method for wear metal analyses. Since all the elements present in the sample are excited simultaneously, emission spectrometers have been designed to simultaneously detect the light emitted from all of the elements of interest. Since emission spectrometers can determine all of the potential wear metals simultaneously, the determination of wear metals in used oil samples by emission spectrometry saves tremendous amounts of analysis time when compared to atomic absorption spectrometry. In atomic absorption spectrometry typically only one element can be determined per analysis.

(3) The A/E35U-3 and the A/E35U-1 spectrometers are equipped with a rotating disk electrode (RDE) (Figure 3) to transport the oil sample to the spark excitation source. The oil sample is placed in the sample vessel beneath the rotating electrode (Figure 3) on a movable platform. The platform is raised so that the rotating disk electrode transports the sample to the spark source where the elements in the oil can be vaporized and excited.

(4) The A/E35U-3 and A/E35U-1 spectrometers employ a diffraction grating to disperse the emitted light which is detected by side-on photomultiplier tubes. Figure 4 depicts the schematic diagram of the optical system of the A/E35U-3. The spectral lines used by the A/E35U-3 and the A/E35U-1 for wear metal analysis are listed in Tables 1 and 2, respectively. Since each instrument is calibrated with the same single element standards, the analytical results from both instruments can be directly compared as was demonstrated in previous reports [reference (g)].

c. Comparison of the Sources Used on the A/E35U-1 and the A/E35U-3.

(1) The source on the A/E35U-1 operates using a 12 KV alternating RF current at 3.4-3.6 amperes [reference (i)]. The inductance is 360 millihenries and the capacitance is 0.0025 microfarads. A high voltage transformer charges a bank of capacitors through a current limiting resistor to furnish the high voltage ac spark necessary to analyze an oil sample. When the voltage across the capacitors reaches a certain level, the auxiliary gap breaks down and provides a short circuit path to the analytical gap. The discharge current can run as high as 40,000 peak amperes which provides sufficient power to volatilize the oil sample in the gap. The intense electrical field produced by such high power excites the atoms of the metals present, and they emit their characteristic radiation which is detected by photomultiplier tubes.

(2) The excitation source on the A/E35U-3 is of a multisource design [reference (j)]. The power supply is divided into an igniter circuit and a low voltage power circuit. The igniter circuit provides energy (22 KV)

Ref: (i) Baird Corp. Report No. FSN6650-937-4401 of 15 May 1972: Spectrometer, Engine Oil Analysis, A/E35U-1 Technical Manual.

(j) Baird Corp. Report No. FSN6650-251-0712 of 1 February 1973: Operation Instructions, Maintenance Instructions, Fluid Analysis Spectrometer (FAS-2).

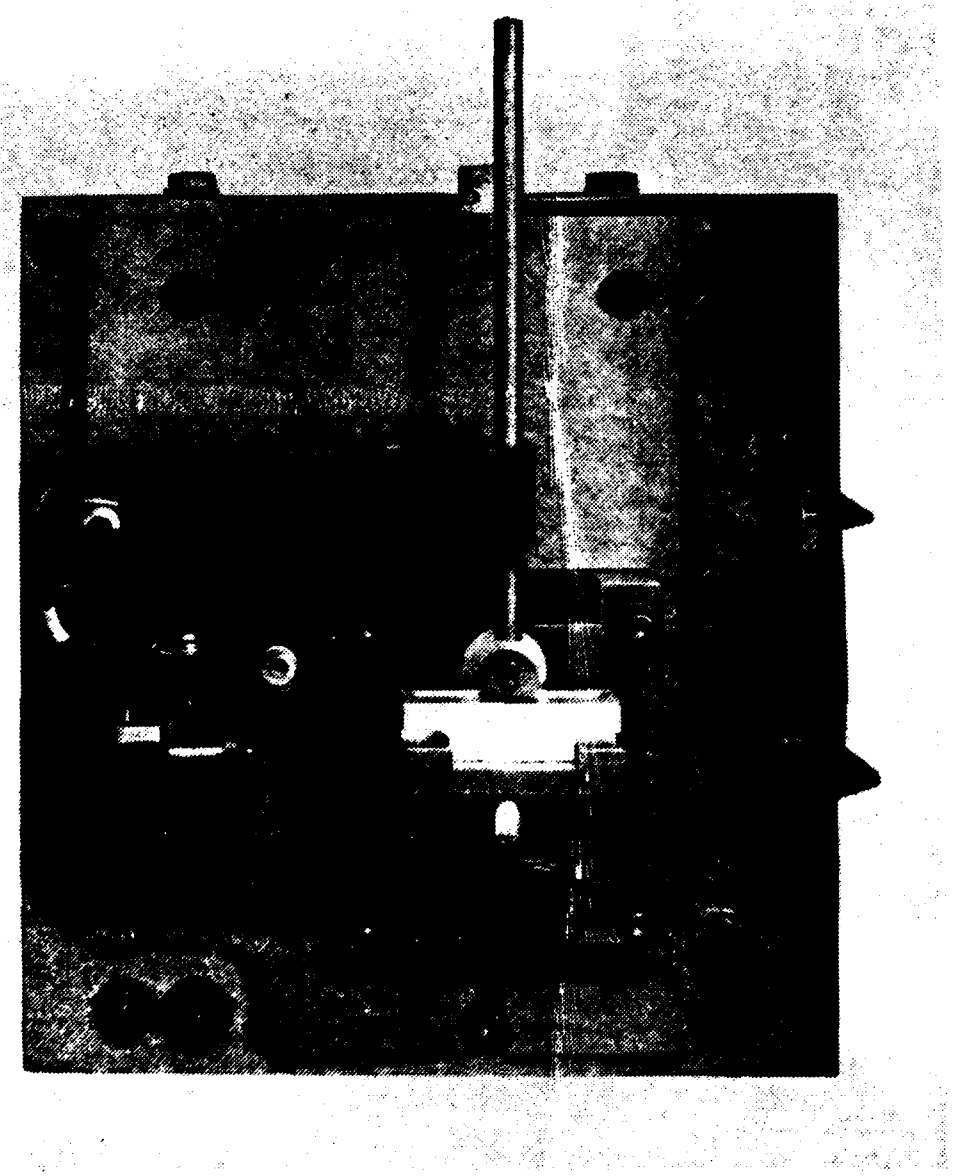

Figure 3. Analytical Source Assembly for the A/E35U-3 (Reproduced from Reference j).

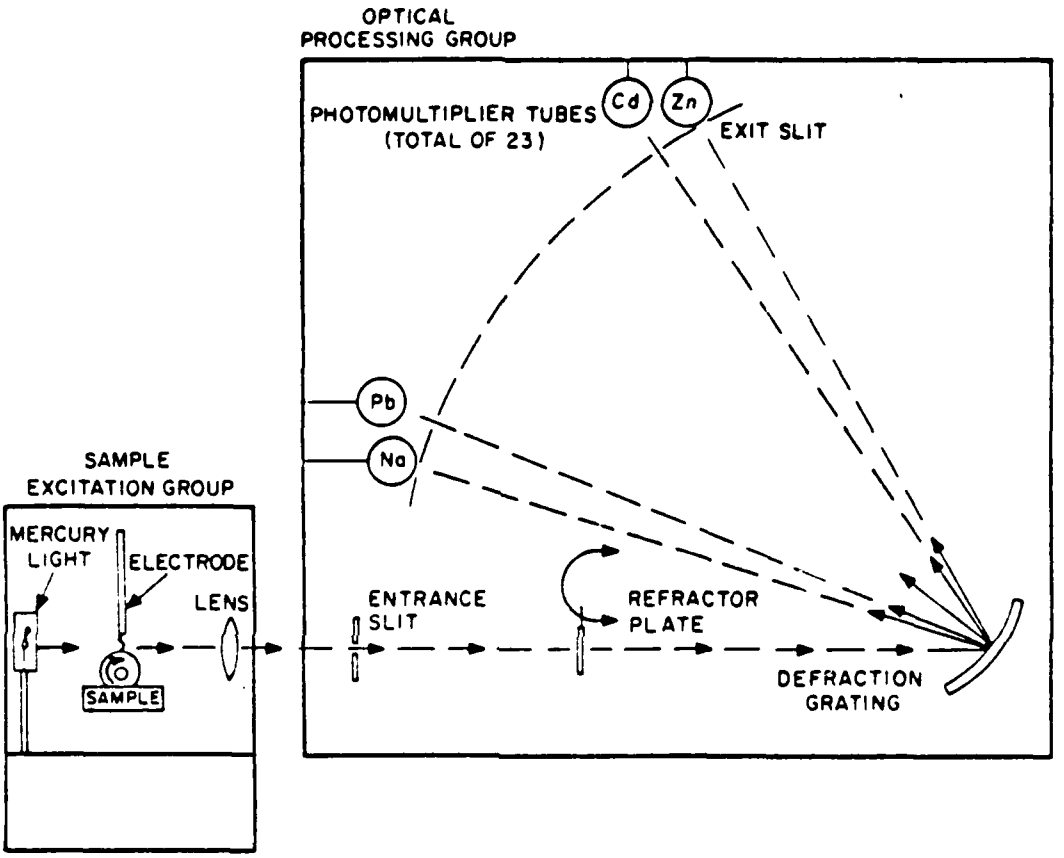

Figure 4. Schematic Diagram of the Optical System Used by the A/E35U-3 (Reproduced from Reference j).

TABLE 1. WAVELENGTHS USED BY THE A/E35U-3 FOR WEAR METAL ANALYSES

Element	Type*	Wavelength(Å)	Element	Type	Wavelength(Å)
Ag	I	3281	Mn	II	2576
Al	I	3082	Mo	II	2816
B	I	2497	Na	I	5896
Ba	II	4554	Ni	I	3415
Be	I	2651	Pb	I	2833
Cd	II	2265	Si	I	2516
Cr	I	4254	Sn	I	3175
Cu	I	3274	Ti	II	3349
Fe	II	2599	V	I	4379
Mg	II	2803	Zn	I	2139

*I Emission from Neutral Atom
II Emission from Ionized Atom

TABLE 2. WAVELENGTHS USED BY THE A/E35U-1 FOR WEAR METAL ANALYSES

Element	Type*	Wavelength(Å)
Al	I	3082
Fe	II	2598
Cr	I	4254
Ag	I	3280
Cu	I	3248
Sn	-	2859
Mg	II	2803
Pb	II	2203
Ni	I	3414
Si	I	2881

*I Emission from Neutral Atom
II Emission from Ionized Atom

for the auxiliary gap to initially strike the arc, while the low-voltage power circuit provides the energy to maintain the analytical arc with an average of five to six pulses per half cycle.

(3) The igniter is a high voltage circuit which provides approximately 14,000 volts to break down the auxiliary gap. As soon as the auxiliary gap breaks down, the analytical gap ignites. After the analytical gap has been ionized, the low-voltage (175 volt peaks) power circuit is able to discharge and provides the required excitation energy to raise the energy of the atoms above the ground state.

C. SUPPLIES.

1. CONOSTAN CONCENTRATES.

a. Single element metal alkyl aryl sulfonate concentrates were obtained from the Continental Oil Company, Conostan Standard Division, Ponca City, Oklahoma. These concentrates are viscous liquids which are miscible with each other and other lubricants.

b. Table 3 lists the metal concentrations in each concentrate as determined by the National Bureau of Standards. Each concentrate contains Na and Fe as contaminants. When multielement standards are prepared, the concentrations of Na and Fe in each concentrate must be taken into account to obtain a multielement standard with the correct final concentrations of Na and Fe.

2. LUBRICATING OILS. The MIL-L-23699 ester based lubricating oil used in this study was obtained from the Mobil Oil Corporation, New York, New York. The Base 245 hydrocarbon oil was obtained from the Continental Oil Company, Conostan Standard Division, Ponca City, Oklahoma.

3. METAL POWDERS. The metal powders were obtained from Research Organic/Inorganic Chemical Company (ROC/RIC), Sun Valley, California; Vacuum Metallurgical Company (VMC), Tokyo, Japan; and Atlantic Equipment Engineers (AEE), Bergenfield, New Jersey.

4. CERAMIC POWDERS. The TiC and Si_3N_4 ceramic powders used for this investigation were produced by Herman C. Starck and GTE-Sylvania, respectively, and were obtained through the courtesy of Dr. Alan Katz and K. Mazdiyasni (AFWAL/MLL, Wright-Patterson Air Force Base, Ohio). The metallic impurities and the Ti concentration in the TiC powder are shown in Table 4.

5. IRON OXIDE POWDER. The ferric oxide powder (Fe_2O_3) used for this investigation was obtained from Morton Thiokol, Inc., Alfa Products, Danvers, Massachusetts.

TABLE 3. CONCENTRATION OF METAL IN CONOSTAN CONCENTRATES

Element	%Metal	Fe (ppm)	Na (ppm)
Ag	5.07	8	120
Al	2.29	25	8
B	1.10	14	11
Ba	7.56	14	11
Be	0.526	20	46
Cd	8.32	17	14
Cr	1.89	59	29
Cu	4.61	37	170
Fe	2.55	BD*	59
Mg	2.10	11	248
Mn	2.93	49	6
Mo	2.10	77	45
Na	3.79	10	BD
Ni	3.43	19	110
Pb	9.92	13	32
Si	13.11	9	1
Sn	5.91	19	23
Ti	6.13	16	7
V	2.02	25	19
Zn	4.41	16	102

*BD = Below Detection Limit (1 ppm)

TABLE 4. ELEMENTAL ANALYSIS OF TiC CERAMIC POWDER

Element	% By Weight
Ti	79.30
Cr	0.05
Co	0.12
Fe	0.05
W	0.65
O	0.25
C	19.58

6. SAMPLE SUPPORTING ELECTRODES.

a. Sample Supporting Electrodes

(1) Rotating Disk Electrode. The rotating disk electrodes (Figure 5) used to transport the oil sample to the source and used to support the residue of the oil sample for the spark-to-residue methods were obtained from Bay Carbon, Bay City, Michigan. The rotating disk electrodes (Catalog No. D-2) were produced from Bay Carbon graphite grades, BCI 100 MD-X (apparent density=1.64) and BCI 100 HD (apparent density=1.85). The instructions for installation of the disk electrode on the A/E35U-1 and A/E35U-3 spectrometers are given in references (i) and (j).

(2) Rotating Platform Electrode. The rotating platform electrodes (Figure 5) used to support the residue of the oil sample for the spark-to-residue methods were obtained from Bay Carbon. The rotating platform electrode (Catalog No. D-3) were produced from Bay Carbon graphite grades, BCI 100 MD-X (apparent density=1.64), BCI 100 MD (apparent density=1.79), and BCI 100 HD (apparent density=1.85).

(3) Reciprocating Semicylindrical Electrode. The reciprocating semicylindrical electrodes were produced at UDRI by flattening one side of a rod electrode obtained from Bay Carbon in the graphite grade BCI 100 MD. To retain the sample, two shallow craters with the dimensions of 1.0"(l) x .200"(w) x .012"(d) were ground into the flat side of the semi-cylindrical electrode. The resulting reciprocating semicylindrical electrode is shown in Figure 5.

(4) Vacuum Cup Electrode. The vacuum cup electrodes (Figure 5) used to transport the acid/oil/Neodol 91-8 solution produced by the RDE-SSAE acid dissolution method were obtained from Bay Carbon. The vacuum cup electrodes (Catalog No. VC-2) were produced from Bay Carbon graphite grade BCI 100 MD.

(5) Porous Cup Electrode. The porous cup electrodes (Figure 5) used to transport the acid/oil/Neodol 91-8 solution produced by the RDE-SSAE acid dissolution method were obtained from Bay Carbon. The porous cup electrodes (Catalog No. PC-1 and PC-30) were produced from Bay Carbon graphite grade BCI 100 MD.

b. Vapor Transporting Electrodes.

(1) Boiler Cap Electrode. The boiler cap electrodes (Figure 6) used to introduce the metal vapor into the spark source were obtained from Bay Carbon. The boiler cap electrodes (Catalog No. BC-1) were produced from Bay Carbon graphite grade BCI 100 MD. Modified boiler cap electrodes in which the diameter of the upper orifice (G in Figure 6) was enlarged from 1.0 mm to 2.1 mm (referred to as BC-2) were also obtained from Bay Carbon using the BCI 100 MD grade graphite. Boiler cap electrodes with upper orifices of 3.2 mm (referred to BC-3) were produced at UDRI using a No. 30 drill bit.

(2) Modified Rotating Disk Electrode. The modified rotating disk electrodes (Figure 6) used to introduce the metal vapor into the spark source

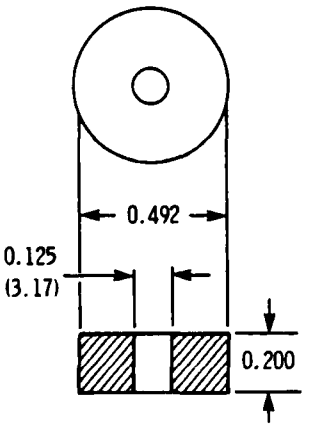

ROTATING DISK ELECTRODE
(D-2)

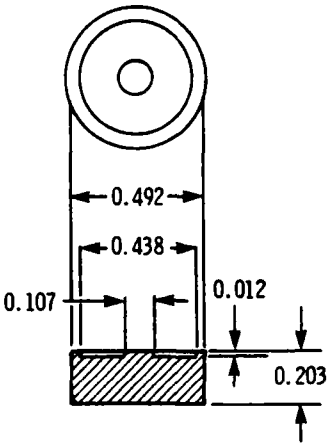

ROTATING PLATFORM
ELECTRODE
(D-3)

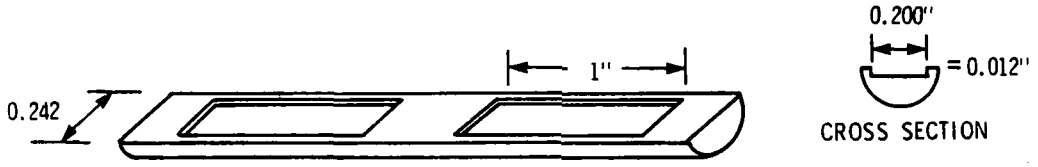

RECIPROCATING SEMICYLINDRICAL ELECTRODE
(RSE)

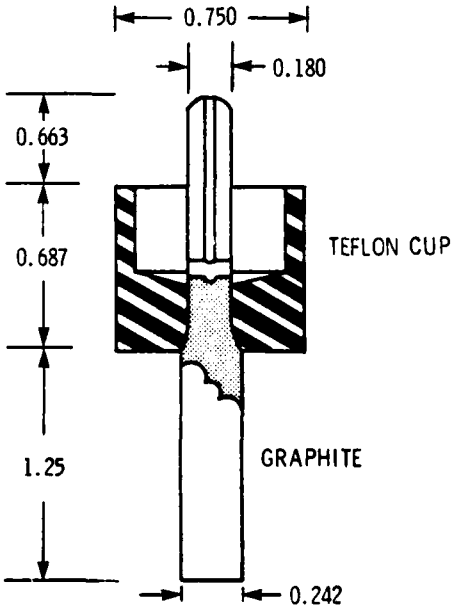

VACUUM CUP ELECTRODE
(VC-2)

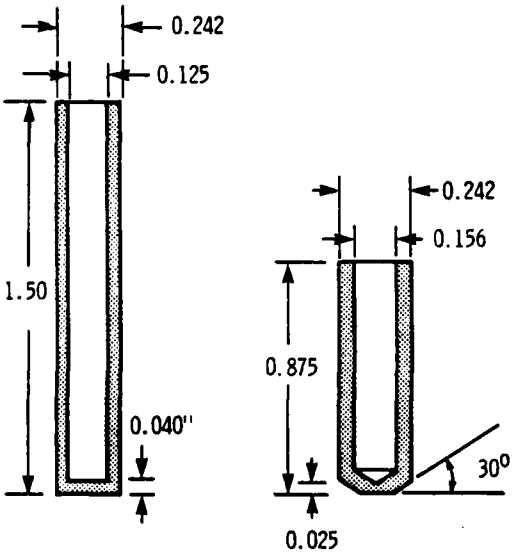

POROUS CUP ELECTRODES
(PC-30) (PC-1)

Figure 5. Sample Supporting Electrodes.

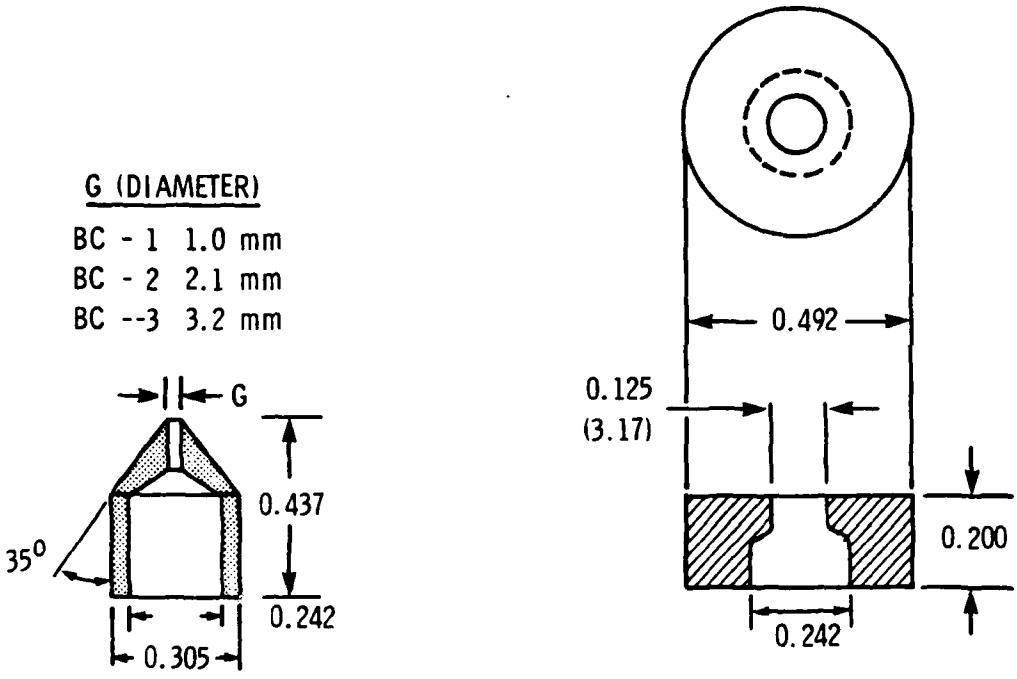

BOILER CAP ELECTRODE

MODIFIED ROTATING DISK ELECTRODE

VAPOR TRANSPORTING ELECTRODES

15° TAPER ELECTRODE

160° TIP-ANGLE ELECTRODE

CONFIGURATION OF COUNTER ELECTRODE

Figure 6. Vapor Transporting Electrodes and Configuration of the Counter Electrode.

were produced at UDRI from the D-2 rotating disk electrodes obtained from Bay Carbon. The D-2 electrode was modified by enlarging the bottom half of the orifice in order to obtain a tight fit on the source end of the glass atomization chamber (Figures 7 and 8).

7. COUNTER-ELECTRODE. The 160^{o} and 15^{o} tip angles (Figure 6) were formed on the rod electrodes obtained from Bay Carbon using the A/E35U-3 and A/E35U-1 Baird Electrode Sharpeners, respectively. The installation and gapping procedures for the rod (upper) electrode for the A/E35U-1 and A/E35U-3 spectrometers are given in references (i) and (j).

8. ELECTROTHERMAL ATOMIZER COMPONENTS.

a. The electrothermal atomization devices used in this study were constructed using graphite braids, graphite square-weave tapes, and commercially available tungsten filaments. The graphite braid was obtained from Leeman Laboratories, Tewksbury, Massachusetts, in a 6-foot length and contained high strength, flexible, continuous filaments of graphite which are woven to form a braid of 1.5 to 2.0 mm in diameter. The graphite braid contained Al, Fe, and Si oxide impurities and was cleaned prior to use by repeated resistive heating until a constant blank signal was obtained. Constant blank signals were usually obtained after three to five repetitions of the cleaning cycle.

b. The graphite square-weave tape was obtained from Johnson Matthey, Inc., Seabrook, New Hampshire, in a 10-inch length and contained high strength, flexible, continuous filaments of graphite which are woven to form a flat square-weave tape 25 mm in width and 0.09 mm in thickness. The graphite square-weave tape was 99.9 percent pure but also contained Al, Fe, and Si oxide impurities. It was cleaned prior to use in the same manner as the graphite braid.

c. The commercially available tungsten filaments used in this study were taken from General Electric Company 100, 200, and 300 watt light bulbs. The filaments were taken from their respective light bulbs by carefully crushing the base of the glass envelope and cutting the tungsten filament from its support wires and electric leads. A package of 200 watt tungsten filaments (approximately 50 in number) was also obtained from the General Electric Company, Cleveland, Ohio. The tungsten filaments are manufactured by first wrapping a tungsten wire around a steel mandrel to form a tight coil approximately 0.4 mm in diameter. The coil so produced is then wrapped around a second, larger steel mandrel to form a coiled, coil approximately 0.8, 1.6, and 4.0 mm in diameter for the 100, 200, and 300 watt filaments. The tungsten filaments required one heating cycle to remove the tungsten oxide from the surface of the filament.

D. SPECIAL APPARATUS.

1. MODIFIED VORTEX MIXER. In order to simultaneously heat and agitate the oil samples, a Fisher Touch Mixer obtained from Fisher Scientific Company, Pittsburgh, Pennsylvania, was modified by gluing the edges of a heating mat obtained from Cole Parmer Instrument Company, Chicago, Illinois, to the foam

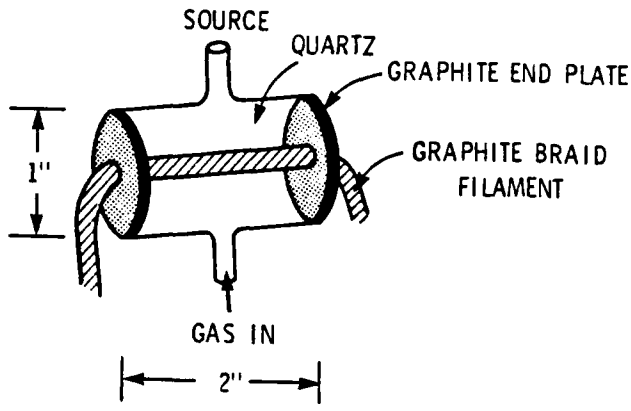

Figure 7. Design of the Cylindrical Atomization Chamber.

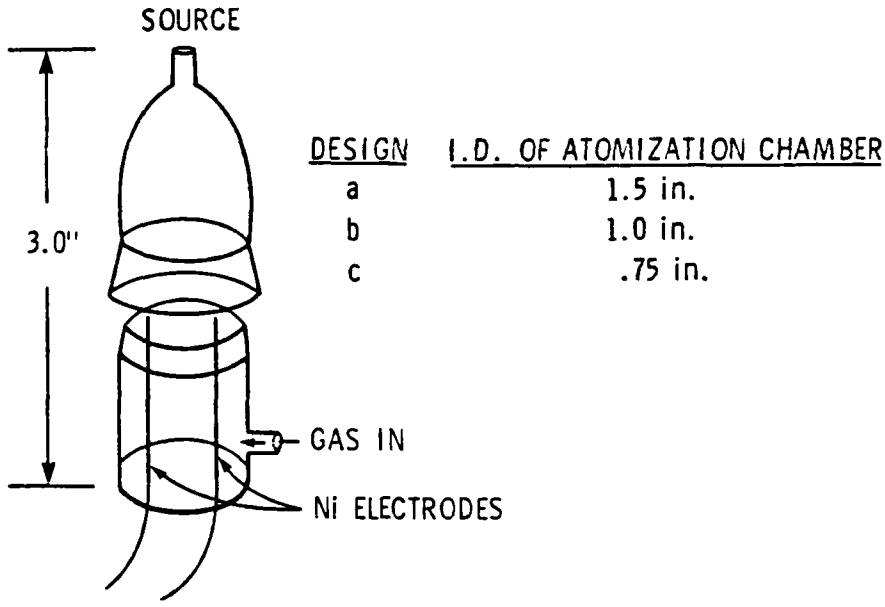

DESIGN	I.D. OF ATOMIZATION CHAMBER
a	1.5 in.
b	1.0 in.
c	.75 in.

Figure 8. Design of the Glass Atomization Chamber.

pad of the mixer. Before being glued to the foam pad, the heating mat was bent into the shape of a figure eight to provide two heated compartments into which samples could be placed. The temperature of the heating pad was adjusted by using a 115 volt, 10 amp variable transformer (Fisher Scientific).

2. OPEN-ENDED FURNACE. In order to ash the oil samples on the rotating disk electrode, an open-ended furnace was constructed by placing a semicircular [2-3/8" (I.D.) x 2-1/2" (l)] heating unit on top of a flat [7" (l) x 2-3/4" (w)] heating unit (Fisher Scientific). The furnace was placed inside a hood and positioned so that the air pulled through the furnace exhausted the fumes out of the back end of the furnace. The temperature of the furnace was controlled with a variable transformer and had a range of 0-700°C. When the ends were closed with insulation, the furnace had a temperature range of 0-1000°C. A 0-1200°C thermolyne pyrometer (Fisher Scientific) was used to calibrate the temperature of the open-ended furnace.

3. CO_2 LASERS. The laser ashing of the oil samples was accomplished with continuous wave 5, 30, and 250 watt CO_2 lasers. The 5 and 250 watt CO_2 lasers were attenuated to 3 and 52 watts, respectively. The beams from the 5, 30, and 250 watt CO_2 lasers were focused to spots of approximately 1, 4, and 10 mm in diameter, respectively.

4. RECIPROCATING SEMICYLINDRICAL ELECTRODE APPARATUS. The driving unit of the semicylindrical electrode was a reciprocating linear motion stirring device obtained from Sargent Welch, Chicago, Illinois. The stirring device produces a reciprocal motion through an amplitude of approximately 27 mm. A variable speed, rheostat controlled stirring motor, also obtained from Sargent Welch, was used to drive the reciprocating stirring device.

5. ATOMIZATION CHAMBERS.

a. The atomization chambers studied during this investigation were of two basic designs. The cylindrical design (Figure 7) was constructed from quartz glass tubing and was used with the graphite braid filament. The graphite ends of the chamber were used to support and supply power to the graphite braid. They were constructed from a graphite sheet (1.27 cm thick) obtained from Johnson Matthey, Inc.

b. Glass atomization chambers (Figure 8) were also constructed. The glass atomization chambers were constructed from Pyrex glass joints and tubing. The electrical leads (30 mil Ni wire) were sealed into the glass bottom of the atomization chamber. Various devices (alligator clips, tantalum foil, tungsten foil, and carbon rods) were fitted onto the ends of the electrical leads to support and supply power to the electrothermal atomizers. Graphite braid, graphite square-weave tape, and tungsten filaments were used with the glass atomization chamber.

c. The glass atomization chamber (Design C) was modified by incorporating a sample introduction port into the upper dome as shown in Figure 9.

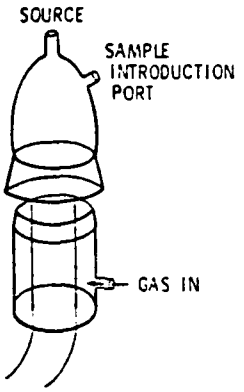

Figure 9. Design of Glass Atomization Chamber with Sample Introduction Port.

6. ELECTROTHERMAL ATOMIZER POWER SUPPLIES.

a. The current for the graphite braid and square-weave tape atomizers was supplied and controlled by a 115 volt, 22 amp variable transformer (Stayco Energy Products, Dayton, Ohio, Type SPN2210). The tungsten filament was controlled by two different power supplies. The first power supply employed two 115 volt, 10 amp variable transformers (Stayco Energy Products, Type 3PN1010) and is shown in Figure 10.

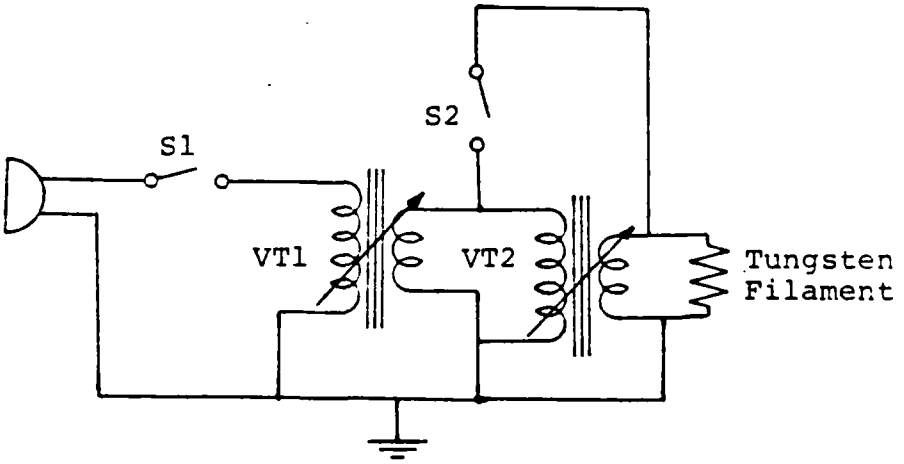

Figure 10. Circuit Diagram of Transformer Controlled Tungsten Filament Power Supply.

b. The second power supply used to control the tungsten filament employed three variable, wire-wound resistors (170, 85, and 20 ohms) obtained

from Sargent Welch placed in a parallel circuit and Potter and Brumfield time delay (CKB-38-70010) and interval on (CHB-38-70021) relays obtained from Graham Electronics, Cincinnati, Ohio. The power supply is shown in Figure 11.

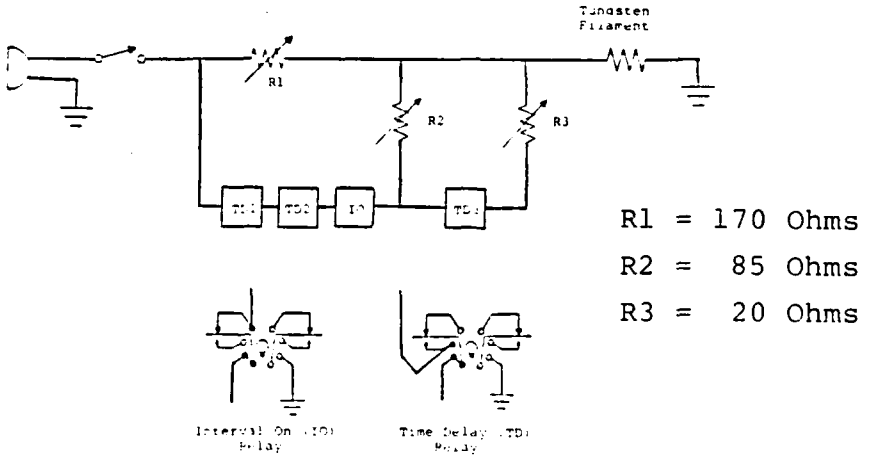

Figure 11. Circuit Diagram of Resistor Controlled Tungsten Filament Power Supply.

E. PREPARATION OF STANDARDS AND SAMPLES.

1. PREPARATION OF SINGLE ELEMENT STANDARDS. The concentrates were diluted with the appropriate amount of MIL-L-23699 lubricating oil containing 0.6 percent amine sulfonate stabilizer (Continental Oil Company) to yield standards containing 100 (C1-100), 50 (C1-50), 20 (C1-20), 10 (C1-10), and 5 (C1-5) ppm of metal. The MIL-L-23699 lubricating oil containing 0.6 percent amine sulfonate stabilizer was used as the blank.

2. PREPARATION OF MULTIELEMENT STANDARDS.

a. Appropriate amounts of the single element concentrates of Ag, Al, Cr, Cu, Fe, Mg, Mo, Na, Ni, Pb, Si, Sn, and Ti were combined to produce a 13-element standard containing 2641.5 ppm of each metal. The 13-element standard was then diluted with the appropriate amount of MIL-L-23699 lubricating oil containing 0.6 percent amine sulfonate stabilizer to yield standards containing 300 (C13-300), 100 (C13-100), 75 (C13-75), 50 (C13-50), 25 (C13-25), and 10 (C13-10) ppm of each metal present. The MIL-L-23699 lubricating oil containing 0.6 percent amine sulfonate stabilizer was used as the blank.

b. The 12-element oil calibration standards (contain no Na) used in this investigation were supplied by the JOAP-TSC, NAS, Pensacola, Florida in light hydrocarbon base oil and contained 300 (D12-300), 100 (D12-100), 50 (D12-50), 20 (D12-20), 10 (D12-10), and 5 (D12-5) ppm of each metal present. Two additional 12-element 50 ppm standards were prepared by diluting the D12-300 standard 1:5 with Mobil MIL-L-23699 ester base (C12) and Conostan 245 hydrocarbon base (D12) lubricating oils. The fresh 1100, MIL-L-23699, and 245 lubricating oils containing 0.6 percent amine sulfonate stabilizer were used as blanks.

3. PREPARATION OF SINGLE METAL POWDER SUSPENSIONS. The single element metal powder suspensions were prepared using sieved metal powders. The metal powders were passed through 45 μm, 30 μm, and 20 μm sieves to produce metal powders with particle sizes of +45, -45+30, -30+20, and -20 μm. Suspensions of 100 ppm were prepared for each particle size distribution by suspending 10.0 ± 0.5 mg of the selected powder in the appropriate amount of MIL-L-23699 lubricating oil.

4. PREPARATION OF CERAMIC AND FERRIC OXIDE POWDER SUSPENSIONS. The TiC, Fe_2O_3, and Si_3N_4 suspensions were prepared by weighing out 50.0 ± 0.5 mg of TiC and Fe_2O_3 powders and 60.0 ± 0.5 mg of Si_3N_4 powder and diluting to 500g with MIL-L-23699 lubricating oil to produce suspensions containing 100 ppm of TiC (79 ppm of Ti), 100 ppm of Fe_2O_3 (70 ppm of Fe) and 120 ppm of Si_3N_4 (72 ppm of Si).

5. PREPARATION OF 12-ELEMENT METAL POWDER SUSPENSIONS. A 12-element suspension containing 300 ± 6 ppm of each metal powder (M12-300) was prepared by weighing out 97.0 ± 2.0 mg of each metal powder and diluting to 323 g with MIL-L-23699 lubricating oil. The M12-300 suspension was thoroughly agitated and then diluted with the appropriate quantity of MIL-L-23699 lubricating oil to produce metal powder suspensions containing 100 ppm (M12-100), 50 ppm (M12-50), and 10 ppm (M12-10) of each metal present.

F. ANALYSIS OF SAMPLES.

1. ANALYSIS OF SUSPENSIONS. Each suspension was agitated on the Vortex mixer to resuspend any particles which had settled out and to reduce the number of agglomerated particles in suspension. Immediately before analysis, the samples were vigorously shaken by hand until the suspension was uniform. The suspension and a standard were then analyzed on the A/E35U-1 or A/E35U-3 spectrometer by the selected method. The analytical results were compared and the percent metal analyzed (A%) calculated as follows:

$$\text{Percent Metal Analyzed (A\%)} = \frac{\text{Emission Readout of Suspension}}{\text{Emission Readout of Standard}} \times 100$$

This procedure was repeated three to five times for each sample and standard. The average percent metal analyzed and accompanying percent error were then calculated for each developed method. In the figures where A% is plotted in bar graph format, X represents A% and the shaded region represents the standard deviation.

2. ANALYSIS OF AUTHENTIC USED LUBRICATING OILS. The authentic used lubricating oil samples analyzed during this investigation were MIL-L-23699 oils obtained from operational T56 Air Force jet turbine engines. These samples were thoroughly agitated on the Vortex mixer before analysis.

G. ANALYTICAL METHODS.

1. RDE-SSAE ACID DISSOLUTION METHOD-1. To 2 ml of oil, 0.4 ml of acid was added and heated to 65°C for 5 minutes. The reaction mixture was then

diluted with 2 ml of Neodol 91-8 to obtain a homogeneous solution for analysis on the RDE-SSAE spectrometers. The optimum acid mixture was found to be a 1:8.5:0.5 mixture of HNO_3, HCl and p-toluene sulfonic acid.

2. RDE-SSAE ACID DISSOLUTION METHOD-2. To 2 ml of oil sample, 2 ml of a Neodol 91-8 solution containing 6 percent of concentrated (70 percent) HNO_3 acid and 4.5 percent p-Toluene sulfonic acid (Conoco Chemicals Company, Hammond, Indiana) was added. The mixture was shaken by hand for 10 seconds, and then shaken for 3 minutes at 65°C in the preheated compartment of the modified Vortex mixer to provide a homogeneous solution for analysis on the A/E35U-3 spectrometer.

3. FURNACE ASHING METHOD. The oil sample (30 µl) was placed onto the rim of the rotating disk electrode or placed onto the surface of the rotating platform electrode or reciprocating semicylindrical electrode. The rotating disk electrode was suspended in the open-ended furnace by a glass rod inserted through the hole in its center. The rotating platform and reciprocating semicylindrical electrodes were placed directly on the lower heating element of the open-ended furnace. The rotating disk electrodes were ashed at 600°C and the rotating platform and reciprocating semicylindrical electrodes were ashed at 400°C for 1 minute and then analyzed by the appropriate method on the A/E35U-1 spectrometer. The A/E35U-1 was used without the hood to reduce the burn time. A burn time of 28 seconds resulted when the electrodes were prepared in this manner.

4. LASER ASHING METHOD. The oil sample (30 µl) was placed onto the surface of the rotating platform electrode. During laser irradiation the rotating platform electrode was held stationary while a steering mirror was used to move the laser beam across its surface. After the ashing was complete, the electrodes were analyzed on the A/E35U-1 spectrometer.

5. ACID DISSOLUTION/SPARK-TO-RESIDUE METHOD. The oil sample (2 ml) and acid solution (0.3 ml) of HF, HCl, and HNO_3 concentrated acids (1:8:1) were measured into a polyethylene 7 ml vial. The vial was closed, hand shaken for 10 seconds, placed into the preheated compartment of the modified Vortex mixer, and shaken for 3 minutes at 65°C. Neodol 91-8 (3.7 ml) was then added to the acid/oil mixture and shaken by hand to produce a homogeneous solution. The acid/oil/Neodol 91-8 solution was placed onto the rotating platform electrode, ashed in the open-ended furnace, and then analyzed on the A/E35U-1.

6. SPARK-IN-VAPOR METHODS.

a. Manual Spark-In-Vapor Method.

(1) The oil sample (7.5-50 µl) was dispensed onto the electrothermal atomizing device using a Eppendorf Digital Pippetter (10-100 µl). The top half of the atomizing chamber was then fitted onto the lower half and the chamber flushed with the selected gas at a preset gas flow (VT) rate. The manual spark-in-vapor method employed the variable transformer controlled power supply (Figure 10). The oil matrix was then ashed by closing switch S1 (Figure 10) causing the required current to pass through the electrothermal atomizer. The produced white smoke was carried out of the atomizing chamber into the exhaust system of the SSAE spectrometer by the gas flow. The

ashing step was accomplished in 5-15 seconds depending on the sample amount, as' 'ng temperature, and gas flow rate. After the ashing step was completed, ; .h S1 was opened. The boiler cap electrode was then fitted over the neck oi the atomizing chamber and the electrode gap set.

(2) After the preburn portion of the burn cycle ended (approximately 11 seconds), the electrothermal atomizer was reheated to the ashing temperature by closing switch S1. After a couple of seconds, switch (S2) (Figure 10) was closed causing the temperature of the electrothermal atomizer to instantaneously rise to the required temperature to atomize any remaining metal species. The atomizing step was continued for approximately three to five seconds depending upon the metal(s) being analyzed. At the end of the atomizing step, the switches S2 and S1 were opened, in that order, and the atomizer allowed to cool. By the time the data of the analyzed sample had been recorded, the electrothermal atomizer was cool enough for the deposition of the next sample.

b. In Situ Spark-In-Vapor Method.

(1) In contrast to the manual spark-in-vapor method, the in situ spark-in-vapor method was performed during the burn cycle of the SSAE spectrometer. As the atomization chamber was flushed with argon, the boiler cap electrode was fitted over the neck of the atomizing chamber and the electrode gap set. The oil sample (25 µl) was pipetted onto the tungsten filament atomizer through the sample introduction port (Figure 9) which was then closed off with a graphite cap.

(2) The ashing period of the spark-in-vapor method was started by closing the switch (Figure 11) as the burn cycle of the SSAE spectrometer was started. The ashing temperature was controlled by the 170 ohm rheostat, R1 (Figure 11) while the ashing time was controlled by the time delay relays, TD1 and TD2. When the TD1 and TD2 relays had completed their timing cycles, the interval delay relay, ID (Figure 11) was energized, resulting in the immediate incorporation of the 85 ohm rheostat R2 (Figure 11) into the power supply circuit. Since the resistors are in parallel, the total resistance in the circuit is 57 ohms (excluding the filament's resistance), which results in an increase in the tungsten filament's temperature and the start of the atomization period.

(3) With the activation of R2, the timing cycle of the time delay relay TD3 (Figure 11) started. At the end of the timing cycle of TD3, the 20 ohm rheostat R3 (Figure 11) was incorporated into the circuit reducing the total resistance in the circuit to 15 ohms causing the tungsten filament to reach its maximum atomization temperature. At the end of its timing cycle, the interval delay relay (ID) opened the circuit to R2 and R3, lowering the temperature of the filament back to the original ashing temperature. The switch was then opened de-energizing the power supply circuit. At the end of the SSAE spectrometer's burn cycle, the filament was cool enough for the deposition of the next sample.

c. Atmospheres for Atomization.

(1) The inert gases used in this study to protect the electrothermal atomizing device and transport the metal vapor to the spark source were obtained from Air Products and included welding grade argon (A/E35U-3) and ultrahigh purity (99.998%) argon, helium, and nitrogen (A/E35U-1). Carbon dioxide (Air Products, Anaerobe Grade, 99.99%) was also studied (A/E35U-1).

(2) The gas flows were controlled and measured by a Matheson Series 7600 150 mm flowmeter equipped with a high accuracy valve. The flowmeter was able to measure argon, carbon dioxide, and nitrogen flow rates of approximately 0.1-4.8 l/min. and helium flow rates of approximately 0.3-11 l/min.

III. RESULTS AND DISCUSSION

A. LITERATURE SEARCH.

1. INTRODUCTION.

a. In order to identify commercially available and state-of-the-art nonflame atomizers capable of eliminating the particle detection limitations of the A/E35U-3 spectrometer, a thorough literature search was conducted. Due to the extent of the information available on nonflame atomizers, the bibliography produced by the literature search presented herein lists only those references pertinent to this investigation.

b. According to the literature surveyed, a wide variety of nonflame atomizers have been used for atomic emission and atomic absorption spectrometric trace metal analyses. In atomic emission spectrometry the excitation source has been used to both atomize and excite the trace metals present in the sample. The excitation source has also been used to excite the metal vapor produced by thermal atomization. The thermal atomizers can be categorized into two general classes: (1) electrothermal atomizers and (2) laser probe atomizers.

2. ELECTROTHERMAL ATOMIZERS. The electrothermal atomizers are graphite or metal resistive heating elements in the form of tubes, rods, ribbons, filaments, and braids and have been used in the analysis of a wide range of samples, including lubricating oils. Of the various electrothermal atomizers described, the filament and braid type atomizers appear to be the most promising because they require the least electrical power to attain >2500°C atomizing temperatures, they are flexible, and they do not require a cooling system for the atomizer holder. Although very little work has been conducted using combinations of spark sources with the various electrothermal atomizers, the electrothermal atomizing apparatuses described in the literature should be applicable to the A/E35U-3 spectrometer.

3. LASER PROBE ATOMIZERS. The laser probe atomizers usually employ a microscope equipped with a special objective of uncemented glass to focus the radiation from conventional or Q-switched mode lasers onto a small area of the sample. In contrast to the electrothermal atomizers, laser probe analyzers have been used with spark excitation sources but have not been used for the analysis of trace metals in used lubricating oils. Although several researchers have performed quantitative trace metal analyses using the laser probe analyzer, the analyses were performed on micrometer areas of homogeneous, solid samples. For this work, millimeter areas of heterogeneous, liquid samples need to be analyzed. Therefore, the latent problems arising from these differences will have to be addressed before the full potential of the laser probe analyzer can be realized.

B. DEVELOPMENT OF AN IMPROVED ACID DISSOLUTION METHOD FOR THE RDE-SSAE SPECTROMETERS.

1. INTRODUCTION.

a. During the previous contract, an acid dissolution method was developed which dissolved wear metal particles by adding an acid/surfactant solution to the oil samples [reference (g)]. The acid dissolved any metal particles present and the surfactant, Neodol 91-8, provided a homogeneous sample suitable for analysis by the A/E35U-1 spectrometer. The developed acid method enabled the A/E35U-1 spectrometer to quantitatively analyze Al, Cu, Fe, Mg, Ni, and Sn wear metal particles in MIL-L-7808 lubricating oil. However, the developed A/E35U-1 acid method was ineffective for Ag and Cr wear metal particles (Mo and Ti were not studied since the A/E35U-1 is not designed for their analysis), and hydrofluoric acid is one of the acids used in the method. The presence of hydrofluoric acid is undesirable due to its detrimental effects on the glass windows protecting the optical systems of the A/E35U-1 and A/E35U-3 spectrometers. The presence of concentrated mineral acids is also undesirable due to their detrimental effects on metal components of the spectrometer.

b. During this project, research was conducted to develop acid dissolution methods applicable to the A/E35U-3 spectrometer and capable of quantitatively analyzing Ag, Al, Cr, Cu, Fe, Mg, Mo, Ni, Pb, Sn, and Ti wear metal particles in MIL-L-23699 lubricating oil without using hydrofluoric acid. The initial work was performed on the A/E35U-1 spectrometer, because it was readily accessible and modifications in the spectrometer could be made when necessary.

c. The first acid dissolution method (ADM-1) developed used a solution of concentrated acids and enabled the A/E35U-1 spectrometer to quantitatively analyze Ag, Al, Cr, Cu, Fe, Mg, Ni, and Sn wear metal particles in MIL-L-23699 oils. This acid dissolution method was used as the standard method in evaluating the particle detection capabilities of the various methods developed on the A/E35U-1.

d. The second acid dissolution method (ADM-2) was developed as a method to improve the particle detection capabilities of the RDE-SSAE spectrometers and to be usable by the Joint Oil Analysis Program. To increase the ease of operation, rapidness, and safety of the acid method, a dilute acid solution prepared in the Neodol 91-8 surfactant was used in place of the concentrated acids solution. The initial experiments to determine the effects of the reaction conditions on the percent metal recoveries were conducted on the A/E35U-1 spectrometer. Also, the corrosive effects of the acid/oil/surfactant solution on the A/E35U-1 spectrometer were reduced by using different electrodes, such as the vacuum cup and porous cup electrodes, in place of the rotating disk electrode and its acid susceptible rotation mechanism.

2. RDE-SSAE ACID DISSOLUTION METHOD-1.

a. Introduction. The first acid dissolution method (ADM-1) was developed for use as a standard method. The main effort in developing the

ADM-1 was to find an acid mixture which did not contain hydrofluoric acid but dissolved Mo and Ti metal particles, and to lower the amount of acid used to reduce the corrosive effects of the acid on the spectrometer. The effect of heating the standard prior to analysis was also studied as a method to improve the accuracy of the method.

b. Effect of Acid Type.

(1) Giering and Lukas have reported [reference (k)] that organic sulfonic acids dissolve Mo and Ti metal particles in the presence of an oxidizing agent. Of the organic sulfonic acids, p-toluene sulfonic acid appeared to be one of the best candidates, because it is soluble in both water and organic solvents and could help to homogenize the acid/oil mixture.

(2) To determine the effectiveness of various acids, mixtures of hydrochloric acid, nitric acid, acetic acid, and p-toluene sulfonic acid (PTS) were investigated and compared to the $HF/HCl/HNO_3$ (1:8:1) acid mixture which has previously been shown to give quantitative analyses of Al, Cr, Cu, Fe, Mg, Mo, Pb, Si, Sn, and Ti [reference (1)]. The presence of acetic acid was required to attain p-toluene sulfonic acid concentrations of greater than 5 percent in the HCl and HNO_3 acid solutions. The acid/oil ratio was 0.2/1.0, and the reaction time and temperature were 5 minutes and 65°C, as previously described [reference (1)]. After heating for 5 minutes the reaction mixture was diluted with Neodol 91-8 to obtain a homogeneous solution for analysis.

(3) As seen in Figure 12, the optimum $HNO_3/HCl/PTS$ ratio is 1.0/8.5/0.5 and gives approximately quantitative recoveries for all the metals studied except Si. To ensure that the 1.0/8.5/0.5 acid solution dissolves Mo and Ti metal particles, small amounts of Mo and Ti metal powders were added to the optimum acid solution and heated at 65°C. At the end of five minutes the Mo and Ti metal powders were completely dissolved.

c. Effect of Acid Amount. To reduce the corrosive effects of the acid on the A/E35U-1 spectrometer, the effectiveness of lower acid quantities were investigated. As the data in Figure 13 indicates, the acid/oil ratio of 0.05/1.0 is the lowest ratio which still produces quantitative results for all metals except Cu, and Si.

Ref: (k) Giering, L. P. and Lukas, M. "A Method for the Analysis of Lubricating Oils Containing Large Wear Metal Particles". Symposium No. 95a on Military Technology Oil Analysis 1978"; Materialpruefstelle der Bundeswehr und Bundesakademie fur Wehruerwaltung und Wehrtechnik: Erding, West Germany, July 1978.

(1) Kauffman, R. E.; Saba, C. S.; Rhine, W. E.; and Eisentraut, K. J. "Quantitative Multielement Determination of Metallic Wear Species in Lubricating Oils and Hydraulic Fluid". Anal. Chem., V. 54, P. 975, 1982.

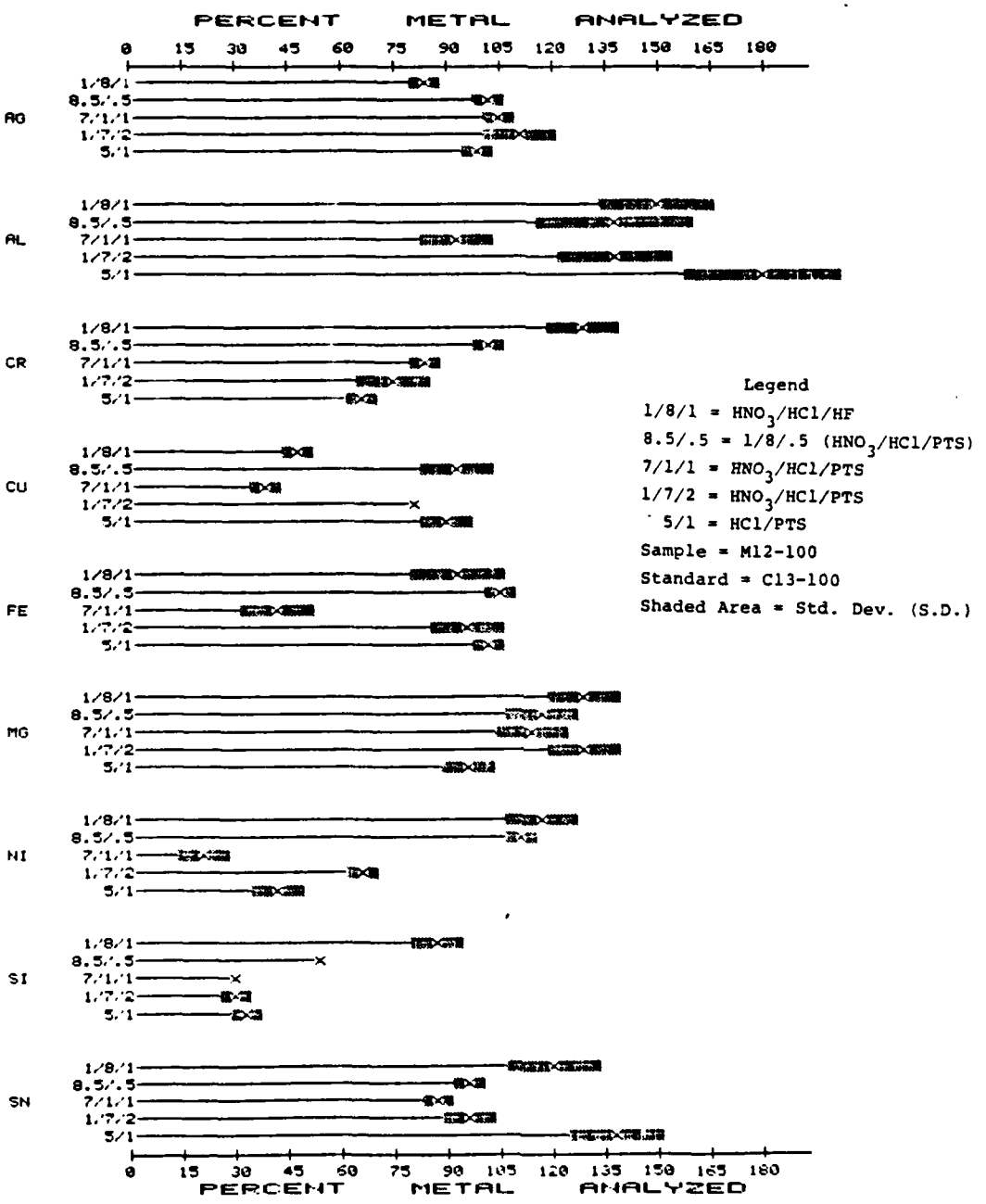

Figure 12. The Effects of Acid Type on the Percent Metal Analyzed by the ADM-1.

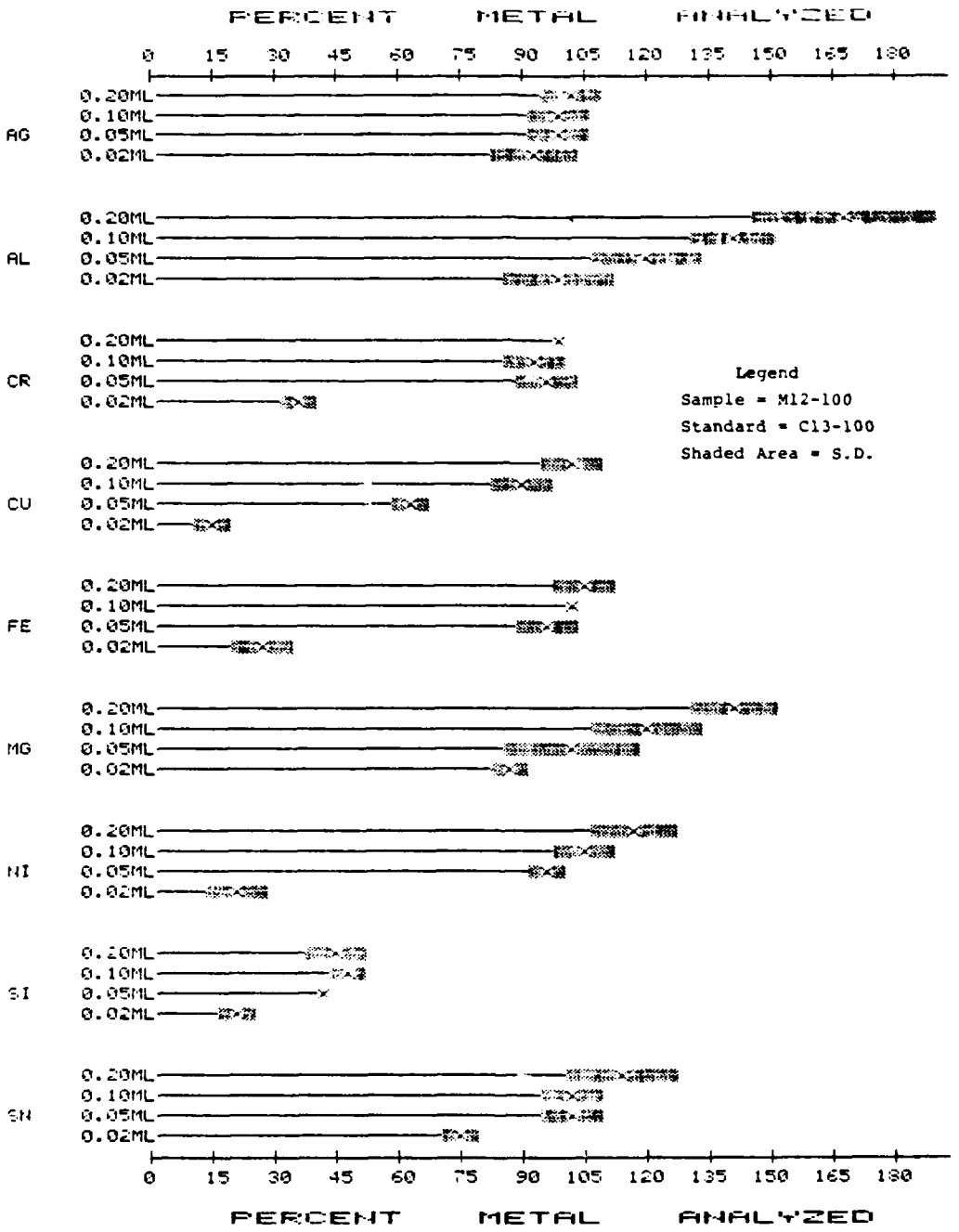

Figure 13. The Effects of Acid Amount (ml) on the Percent Metal Analyzed by the ADM-1.

d. Effect of Heating the Standard.

(1) One problem with the ADM-1 is the fact that the M12-100 suspension produces higher spectrometer readouts for Al than for the C13-100 standard. The differences are caused in part by the fact that the M12-100 suspension samples are heated at 65°C for 5 minutes, but the C13-100 standard is analyzed without prior heating.

(2) The effects of heating the standard on the analytical results are illustrated in Figure 14. As illustrated in Figure 14, the Al readouts for the C13-100 standard and the M12-100 suspension are in better agreement after the standard is heated, but the Ag and Mg readouts for the C13-100 standards and the M12-100 suspension are in worse agreement.

(3) Another possible reason for the observed differences in the spectrometer readouts is that the metals are present as alkyl aryl sulfonates in the C13-100 standard but are inorganic salts in the M12-100 acid treated samples. Also, sodium is present in the C13-100 standard but not in the M12-100 suspension.

3. RDE-SSAE ACID DISSOLUTION METHOD-2.

a. Introduction. The second acid dissolution method (ADM-2) used the ADM-1 as a starting point. Experiments were carried out to determine the effects of the acid mixture's strength, the reaction parameters, and the different solution transporting electrodes on the acid dissolution method's capability to quantitatively analyze metallic particles.

b. Effect of Acid Mixture Strength. In order to make the ADM-2 a one-step method and to eliminate the handling of concentrated acids, the effects of diluting the acid mixture with Neodol 91-8 prior to reaction with the oil sample were studied. As illustrated in Figure 15, the effectiveness of the acid is reduced by the presence of the surfactant during the reaction period.

c. Effect of Reaction Parameters.

(1) In an effort in increase the effectiveness of the diluted acid mixture, studies designed to optimize acid type, acid/oil ratio, reaction temperature, and reaction time were carried out. Figures 16 through 19 show that the best percent metal recoveries for the M12-100 suspensions are achieved by increasing the acid/oil ratio from 0.05/1.0 to 0.10/1.0 and by eliminating HCl from the acid mixture. The acid/oil ratio of 0.10/1.0 is achieved by using a solution of 10 percent acid in Neodol 91-8.

(2) As illustrated in Figures 18 and 19, no advantage is gained by reaction temperatures above 65°C and reaction times longer than 3 minutes. In fact, metal recoveries greater than 100 percent are obtained for Al and Sn at higher reaction temperatures and longer reaction times.

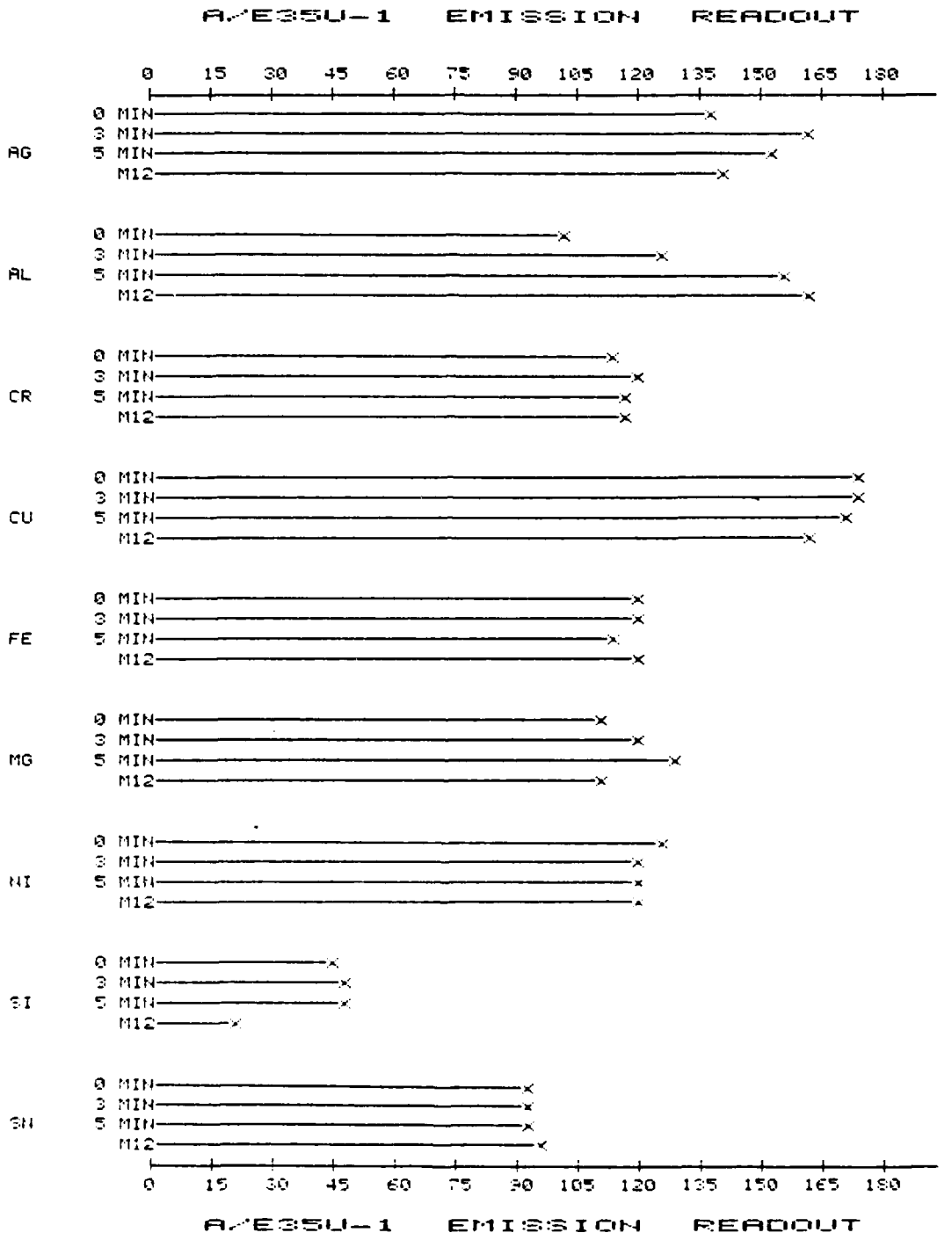

Figure 14. The Effects of Heating Time at 65°C on the A/E35U-1 Readouts of the C13-100 Standard.

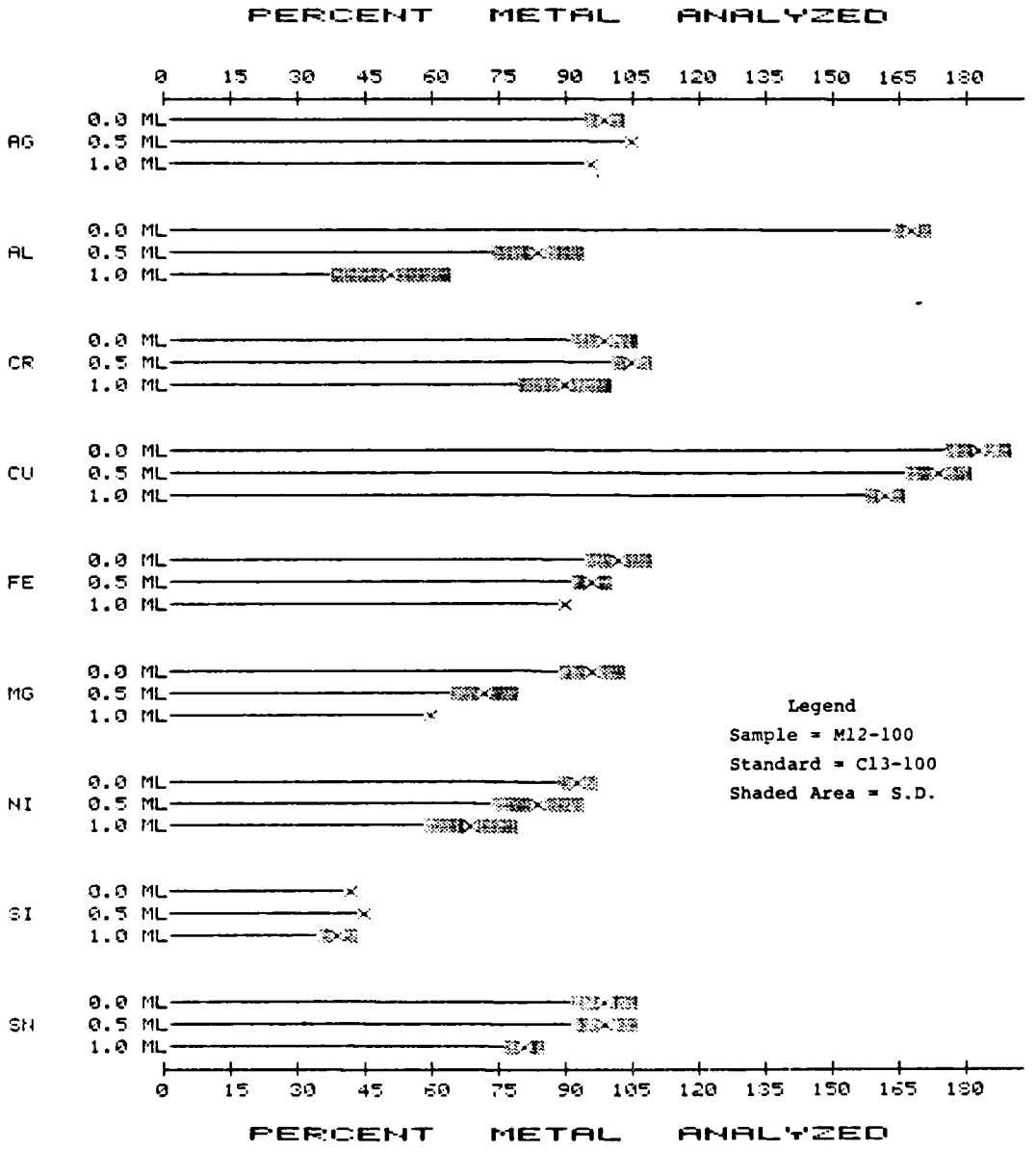

Figure 15. The Effects of Neodol 91-8 Amount on the Percent Metal Analyzed by the ADM-2.

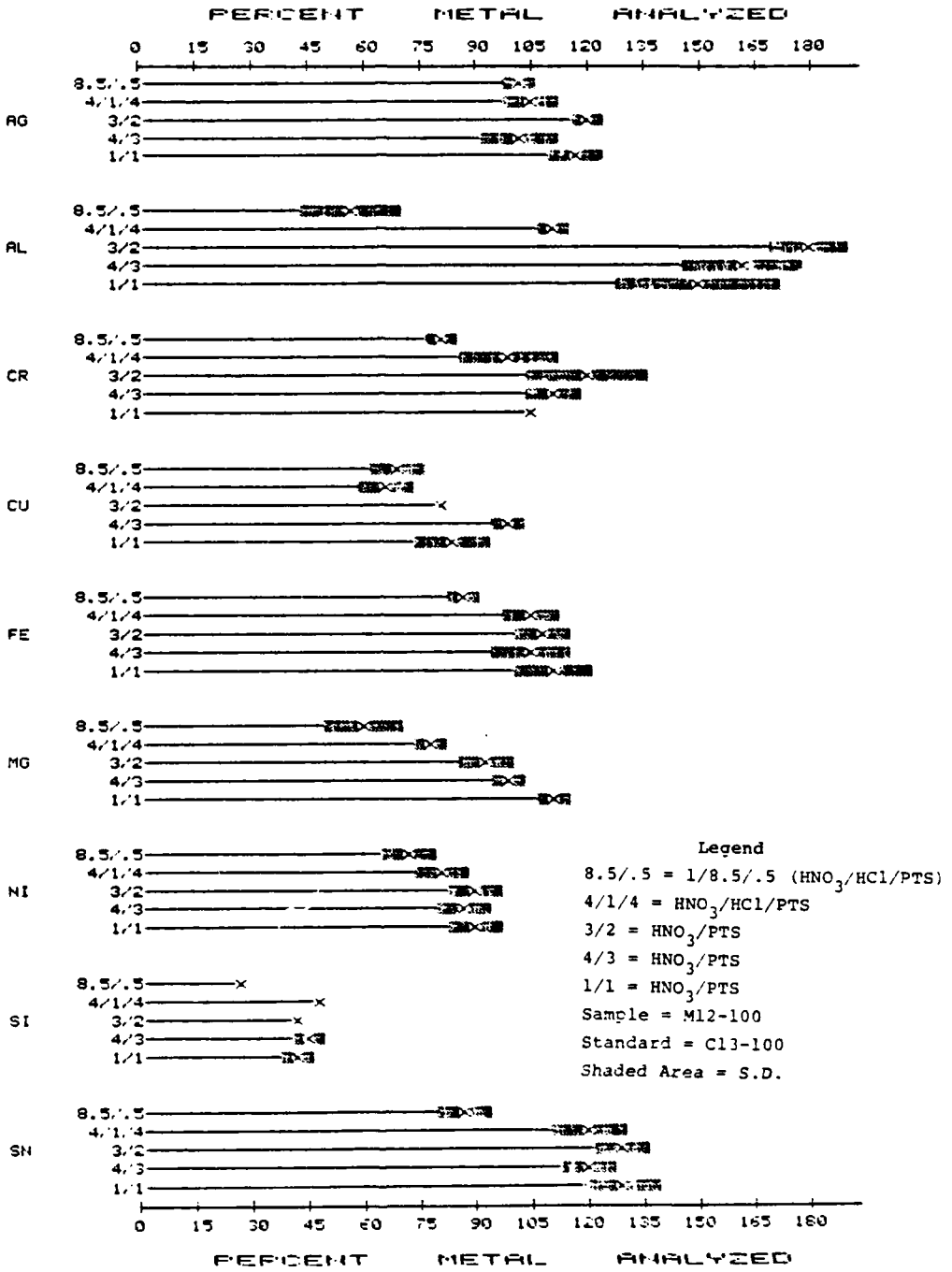

Figure 16. The Effects of Acid Type on the Percent Metal Analyzed by the ADM-2.

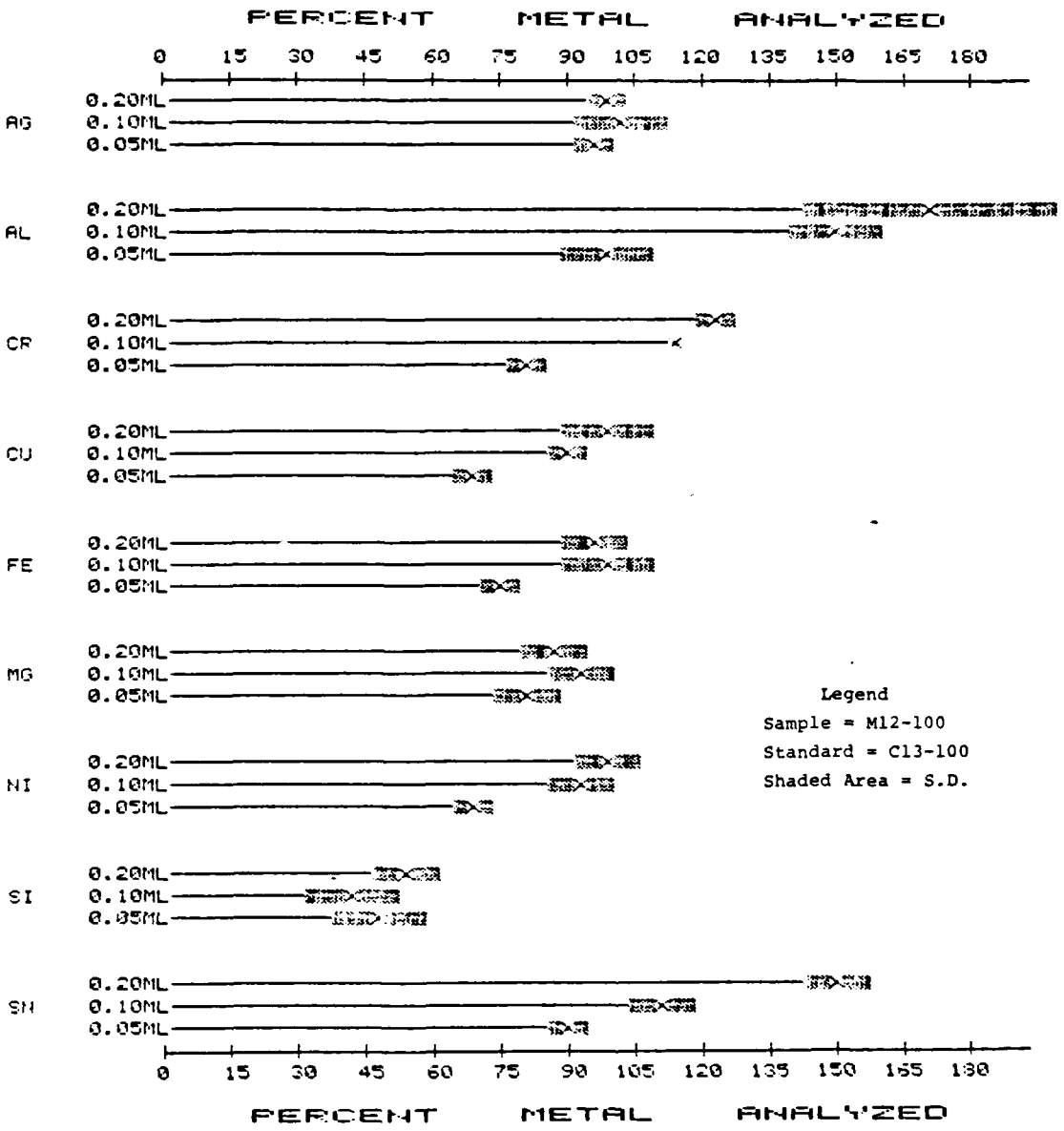

Figure 17. The Effects of Acid Amount on the Percent Metal Analyzed by the ADM-2.

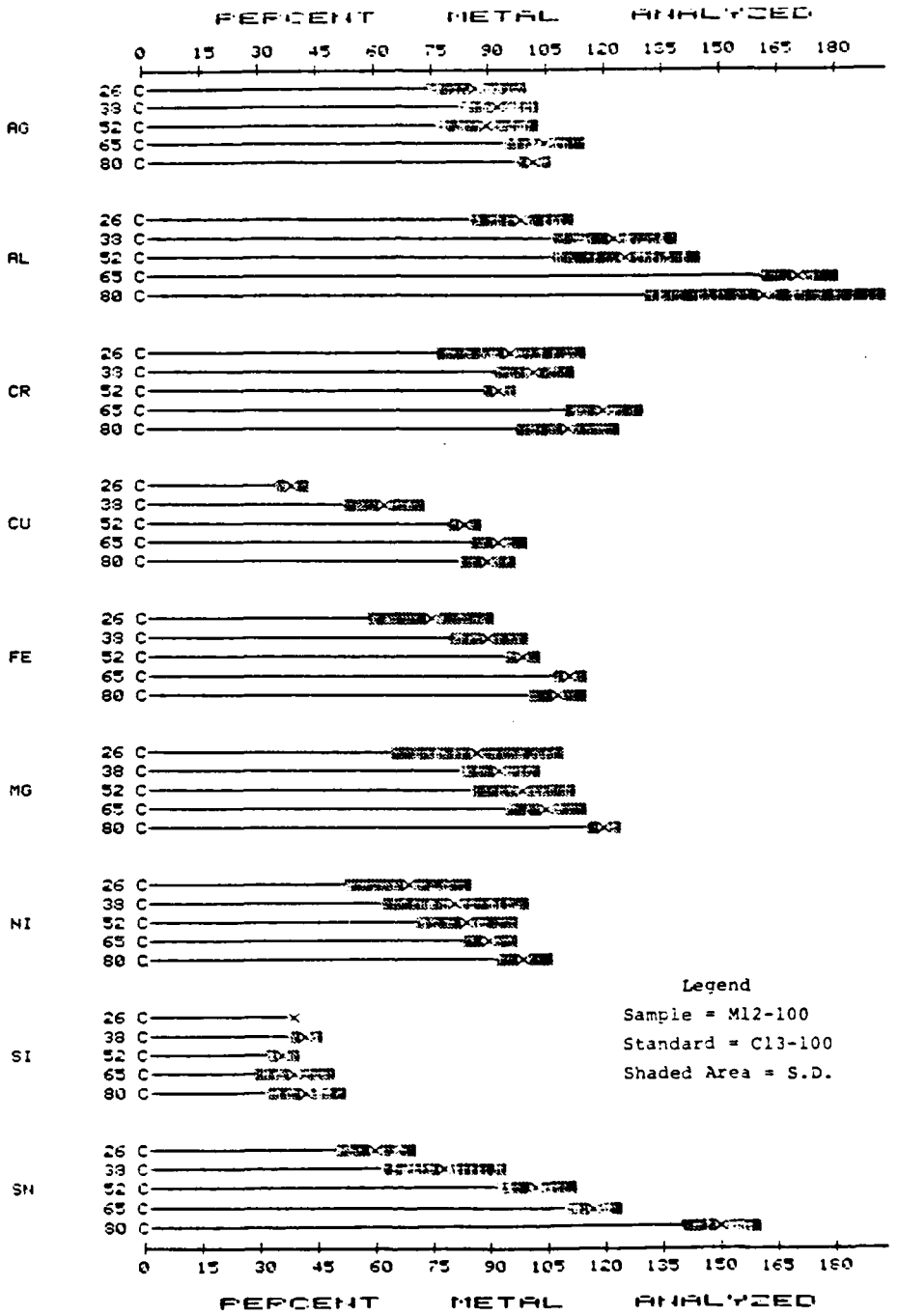

Figure 18. The Effects of Reaction Temperature (°C) on the Percent Metal Analyzed by the ADM-2.

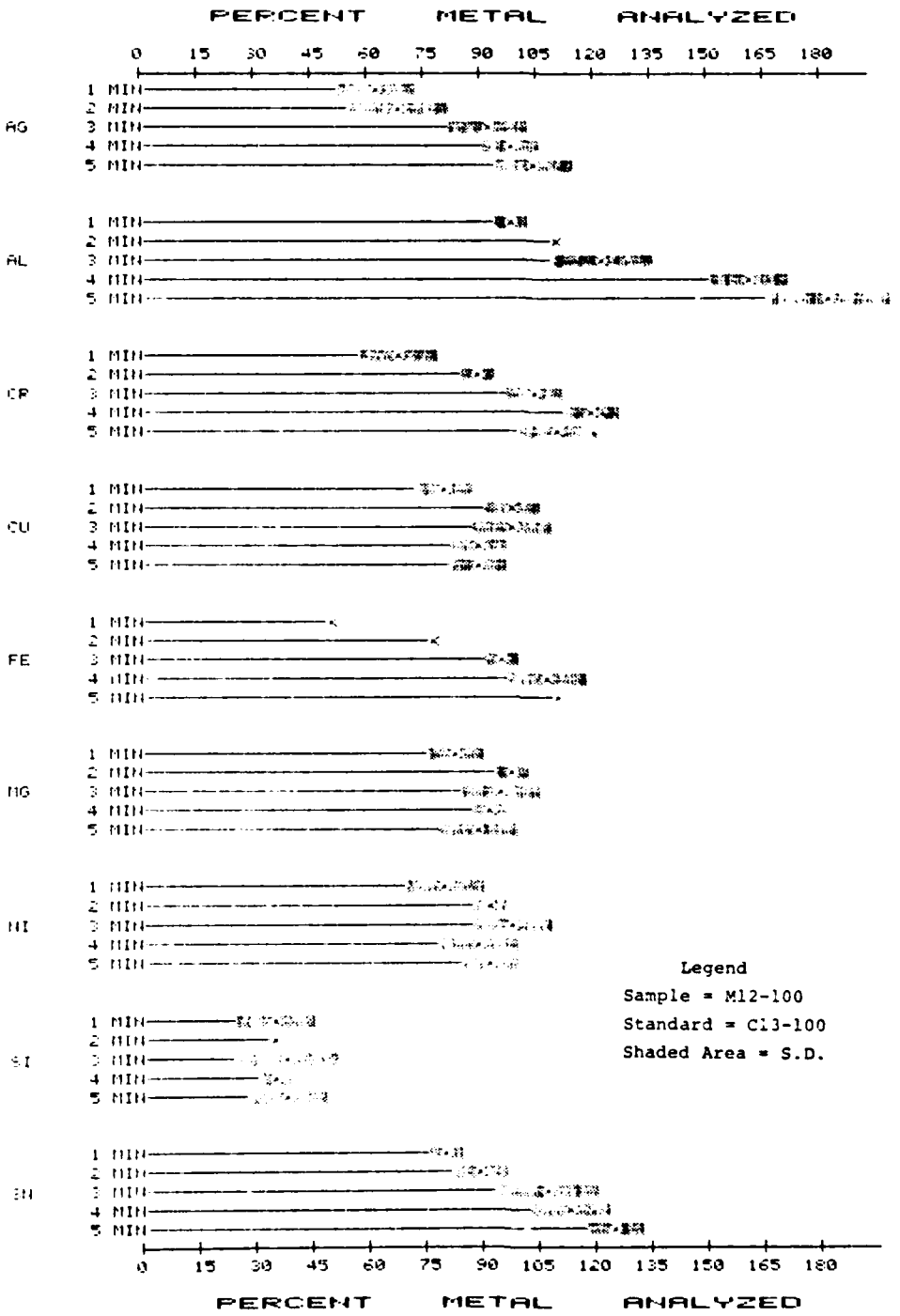

Figure 19. The Effects of Reaction Time on the Percent Metal Analyzed by the ADM-2.

d. Alternative Electrodes.

(1) Introduction. During the development of ADM-2, it was observed that the Cr, Fe, Ni, and Sn emission readouts for the blank were increasing from day to day as shown in Table 5, and that the metal spindle of the rotation mechanism was becoming corroded. Since it appeared that the acid/oil solution was reacting with the metal spindle of the rotation mechanism, different electrodes were tested as replacements for the rotating disk electrode and its acid susceptible rotating spindle. The alternative electrodes investigated during this work were the porous cup and vacuum cup electrodes.

(2) Porous Cup Electrode. The first electrode tested was a porous cup electrode [references (m) and (n)] with a 30^{o} chamber floor, PC-1 (Figure 5). However, this electrode was immediately rejected, because the acid/oil/surfactant solution boiled out the top of the electrode, even before the 10 second preburn cycle was complete. A solution of oil/surfactant without acid present did not boil even after the entire 35 seconds burn cycle. Therefore, the water present is causing the solution to boil. Another type of porous cup, PC-30 (Figure 5), which has a flat chamber floor, thicker electrode walls, and which holds more liquid was obtained, but suffered from the same limitations.

(3) Vacuum Cup Electrode.

(a) The second electrode tested was a vacuum cup electrode [references (o) and (p)]. The solution to be analyzed is poured into a teflon cup and is drawn into the spark by capillary action (Figure 5). The preliminary test with a C13-100 standard acid surfactant solution was favorable in that the solution stayed homogeneous and did not boil during the entire burn cycle. In fact, a second analysis of the same solution produced almost identical results. The results are listed in Table 6 and show that ADM-2 gives less quantitative results with the vacuum cup, but the standard deviations are better.

(b) These preliminary results indicate that if the accuracy of the analytical results can be improved, the vacuum cup electrode would be

---

Ref: (m) Gassman, A. and O'Neill, W. "The Use of a Porous-Cup Electrode in the Spectrographic Analyses of Lubricating Oils". Proceedings, Amer. Petrol. Inst., V. 29M, P. 79, 1949.

(n) Feldman, C. "Direct Spectrochemical Analysis of Solutions Using Spark Excitation and the Porous Cup Electrode". Anal. Chem., V. 21, P. 1041, 1949.

(o) MacGowan, R. J. "Spectrochemical Analysis of Oils Using Vacuum Cup Electrode". Appl. Spectrosc., V. 15, P. 179, 1961.

(p) Zink, T. "A Vacuum Cup Electrode for the Spectrochemical Analysis of Solutions". Appl. Spectrosc., V. 13, P. 94, 1959.

TABLE 5. THE EFFECTS OF TIME ON THE A/E35U-1 READOUTS OF THE BLANK

Date	Ag	Al	Cr	Cu	Fe	Mg	Ni	Si	Sn
5/2/83	1	1	3	2	1	1	2	1	1
5/16/83	2	3	10	0	15	0	5	0	3
5/31/83	1	2	22	1	115	1	10	2	7

TABLE 6. THE PERCENT METAL ANALYZED BY THE ADM-2 USING THE D-2 AND VC-2 ELECTRODES

Electrode	Ag	Al	Cr	Cu	Fe	Mg	Ni	Si	Sn
D-2[a]	92±9	122±12	105±6	99±8	95±4	95±8	98±10	41±12	108±12
VC-2[b]	94±2	100±2	81±2	50±3	62±1	103±4	55±3	33±2	100±2

[a]Rotating Disk Electrode
[b]Vacuum Cup Electrode
Reaction Conditions - Reaction Time: 3 minutes
Reaction Temperature: 65°C
Acid Type: 10% HNO_3/PTS (4:3) in Neodol 91-8
Acid Amount: 1 ml of 10%/1 ml of oil (0.1 ml acid/1 ml of oil)
Standard: C13-100 (Not heated)

better suited for the ADM-2 than the rotating disk electrode due to the higher precision of the analytical results. The vacuum cup electrode also reduces the acid susceptibility of the A/E35U-1 spectrometer by eliminating the need for the rotating mechanism.

C. DEVELOPMENT OF A SPARK-TO-RESIDUE METHOD FOR THE A/E35U-3 SPECTROMETER.

1. INTRODUCTION.

a. During the previous contract, the preliminary results of a spark-to-residue method were obtained on the A/E35U-1 spectrometer [reference (g)]. The spark-to-residue method (STRM) eliminates the particle transport inefficiency of the rotating disk electrode because the oil sample is directly deposited onto the sample electrode. Also, the particle detection capabilities of the RDE-SSAE spectrometers are improved, because the oil matrix is vaporized (ashed) prior to analysis. The spark-to-residue method employing the rotating disk electrode (RDE), produced quantitative results for Cu, Fe, and Mg metal particles (<20 μm) on the A/E35U-1 spectrometer, but did not detect Al particles. When the rotating platform electrode (RPE) was used in place of the RDE, the spark-to-residue method produced nonquantitative results for all the metal particles studied [reference (g)].

b. During this project, research was conducted to develop a spark-to-residue method for the A/E35U-3 spectrometer which was capable of producing quantitative analyses for Ag, Al, Cr, Cu, Fe, Mg, Mo, Ni, Pb, Sn, and Ti wear metal particles in used MIL-L-23699 lubricating oil samples. To optimize the spark-to-residue method, the effects of ashing conditions, electrode configuration and porosity, speed and direction of electrode movement, number and length of analyses, acid dissolution of the metal particles prior to ashing, and spark atmosphere on the percent metal recoveries of the A/E35U-1 spectrometer were studied. The developmental research was performed on the A/E35U-1 spectrometer due to the numerous modifications in the source stand required to analyze the ashed electrodes.

2. ROTATING PLATFORM ELECTRODE.

a. Introduction. The rotating platform electrode (RPE) was evaluated for use in the spark-to-residue method. The RPE was specifically designed for spark-to-residue methods (STRM) and has been studied by Baer and Hodge [reference (q)] and Hodge [reference (r)] as an alternative to the rotating disk electrode (RDE). They reported that the RPE was more sensitive than the RDE and was effective for the analysis of suspended matter. However, during our previous research [reference (g)], the RPE produced nonquantitative

---

Ref: (q) Baer, W. and Hodge, E. "The Spectrochemical Analysis of Solutions, A Comparison of Five Techniques". J. Appl. Spectry., V. 14, P. 141, 1960.

(r) Hodge, E. "Spectrographic Tricks". J. Appl. Spectry., V.15, P. 21, 1961.

results on the A/E35U-1 spectrometer for all the metals tested. Therefore, a thorough investigation was conducted into the factors which affect the analytical results produced by the RPE-STRM for the A/E35U-1 spectrometer. The effects of the RPE's position and porosity, counter-electrode configuration, furnace ashing conditions, laser ashing, length and number of analyses, and spark atmospheres on the analytical results of the A/E35U-1 were determined.

b. Effect of Rotating Platform Electrode's Position.

(1) The effect of the position of the RPE on the analytical results was investigated by studying five different positions of the RPE. The positions are illustrated in Figure 20 and show the position of the RPE with respect to the counter-electrode and the window of the optical system of the A/E35U-1 spectrometer. The RPE was positioned so that the point A, B, C, D, or E was directly below the center of the counter-electrode. Alignment of the counter-electrode with position A, B, C, or D affects the direction that the sample enters the spark relative to the spectrometer window.

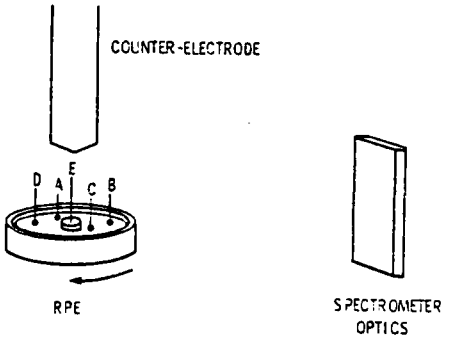

Figure 20. Different Positions of Rotating Platform Electrode.

As shown in Figure 21, positions A-D produce similar emission readouts for the C13-50 standard while position E, as expected, produces much lower emission readouts. Previous research [reference (g)] showed that during the preburn cycle (11 seconds) most of the metal on the surface of the RPE is vaporized before the integration cycle begins. For this reason the RPE was held stationary during the preburn cycle and then rotated during the integration cycle. In positions A-D, unexposed surfaces of the RPE are rotated into the spark for analysis. In position E, the same region of the RPE exposed to the spark during the preburn cycle is analyzed, since rotation does not effect the center region of the RPE. Also, position E is elevated and has less sample deposited on it than positions A-D.

(2) The position of the rotating platform has a larger effect on the percent metal recoveries obtained for the M12-50 suspension. As shown in Figure 22, positions B, C, and D produced the highest percent metal recoveries, followed by positions A and E. For consistency, all further research was conducted using position D.

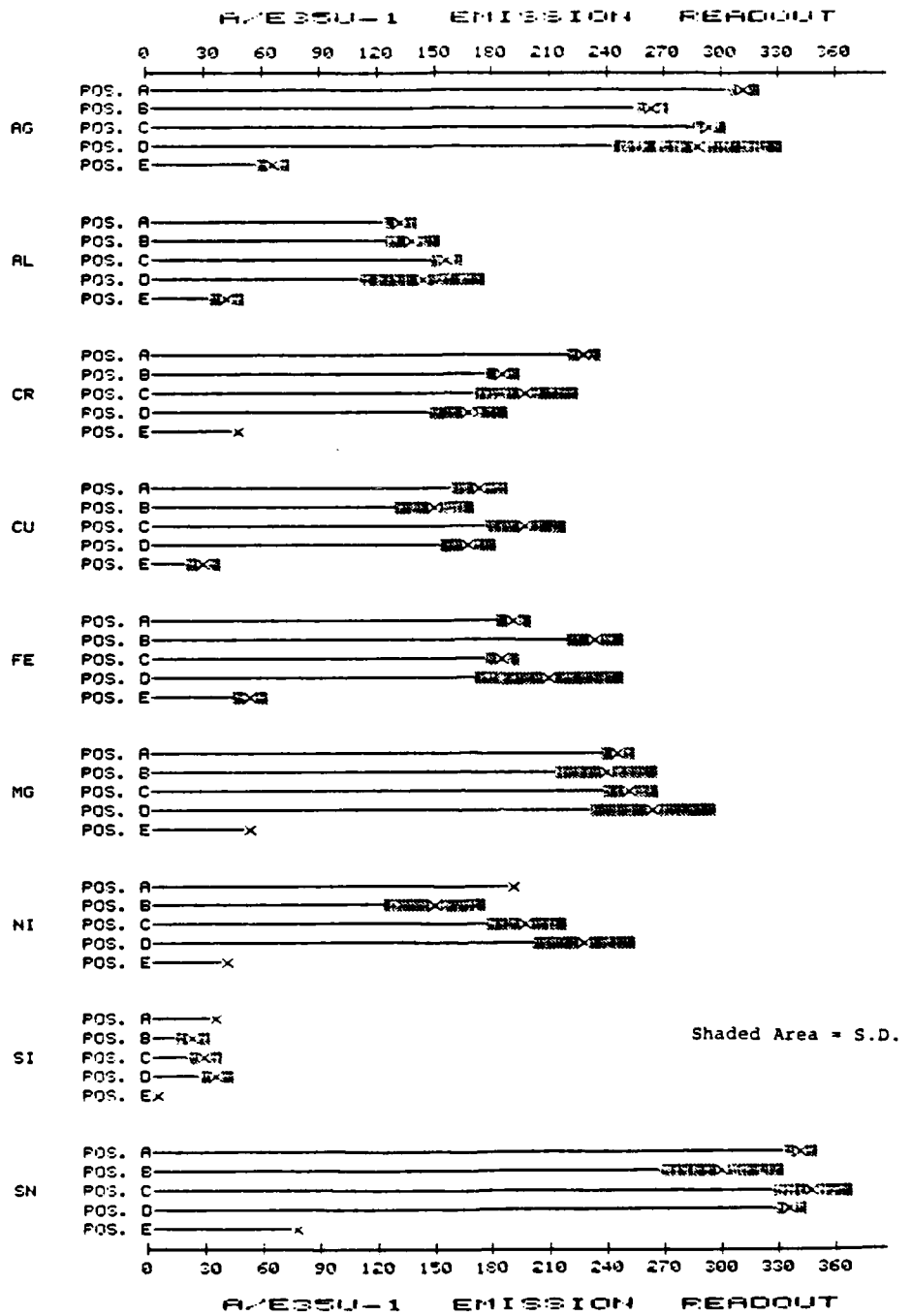

Figure 21. The Effects of the RPE Position on the A/E35U-1 Readouts for the C13-50 Standard.

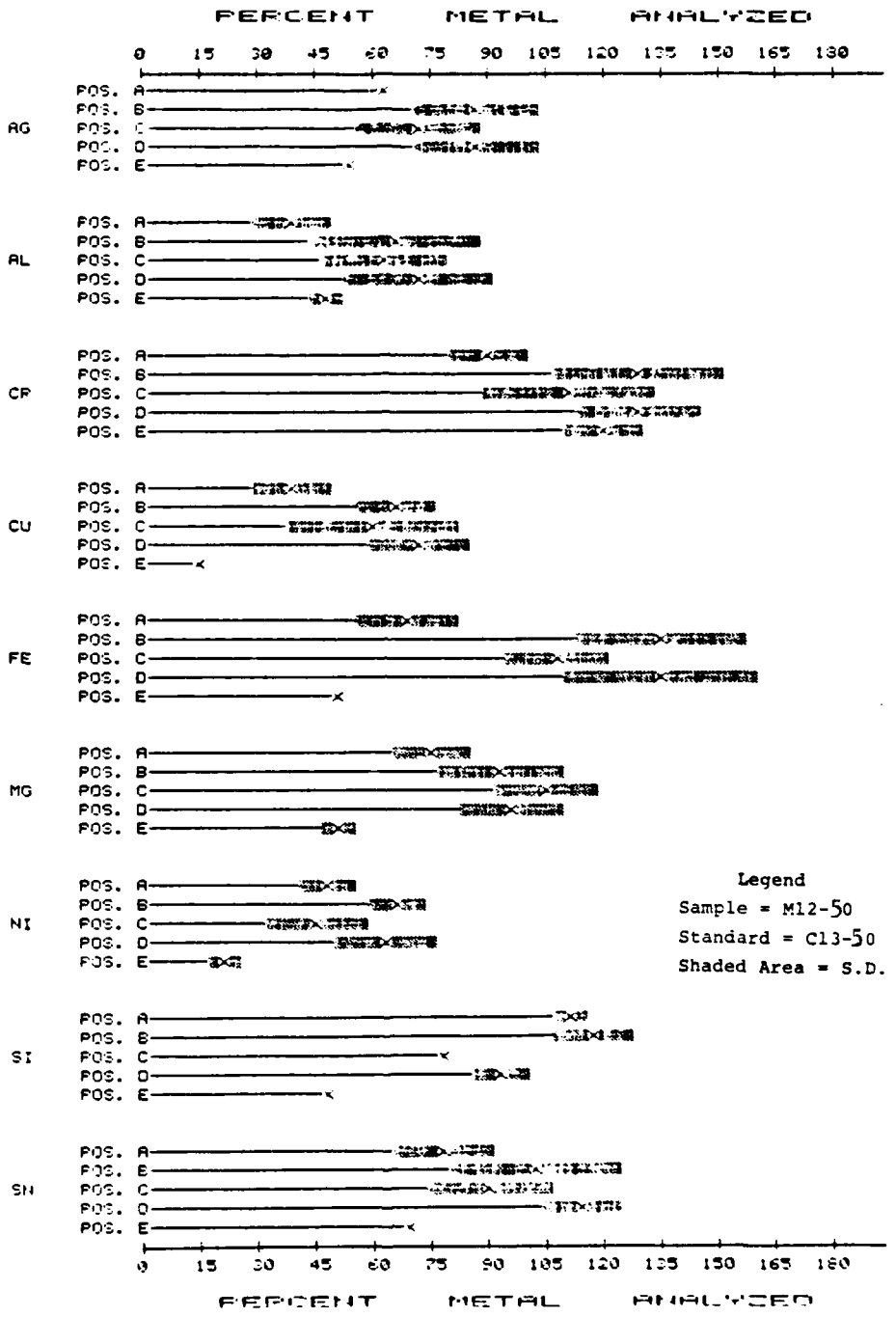

Figure 22. The Effects of the RPE Position on the Percent Metal Analyzed by the RPE-STRM.

c. Effect of Counter-Electrode's Configuration.

(1) Two different configurations (tip angle) of the counter-electrode were studied. The configurations will be referred to as the 160° and 15° electrodes (Figure 6), where the angles refer to the tip angles of the electrodes. The 160° electrode is the one recommended for the A/E35U-3 spectrometer, and the 15° taper electrode is the one recommended for the A/E35U-1.

(2) The results listed in Table 7 indicate that the counter-electrode's configuration has little effect on the emission readouts for the C13-50 standard, but has a significant effect on the percent metal analyzed (%A) for the M12-50 suspension. The 160° electrode produces higher percent metal analyzed than the 15° electrode for all the metals studied. The 160° electrode was used for further research.

d. Effect of Porosity.

(1) Two different grades of graphite, BCI 100 HD and BCI 100 MD-X, were studied. The BCI 100 HD has an apparent density of 1.85 and should be less porous than the BCI 100 MD-X graphite grade which has an apparent density of 1.64.

(2) As seen in Table 8, the RPE's porosity has a small effect on the emission readouts of the C13-50 standard. The more dense BCI 100 HD grade RPE produces slightly higher readouts than the less dense BCI 100 MD-X grade. However, the BCI 100 MD-X grade RPE produces higher percent metal analyzed, especially for Al and Ni particles, than the BCI 100 HD grade.

e. Effects of Furnace Ashing Conditions.

(1) Introduction. The two ashing conditions studied in this investigation were the effects of ashing temperature and ashing time. Ashing temperatures of 400°C and 600°C were chosen for this work. Above 600°C the oil sample ignited and below 400°C the ashing was not complete after 5 minutes.

(2) Effect of Ashing Temperature. The RPE was heated at the desired temperature until the vapors evolving from the surface ceased (1.0 minute at 400°C and 0.5 minutes at 600°C). The data listed in Table 9 shows that the emission readouts of the C13-50 standard are essentially unaffected by the ashing temperature, but the ashing temperature does affect the percent metal analyzed of the M12-50 suspension. The 400°C ashing temperature produces higher percent metal analyzed than the 600°C temperature. Recoveries for Cr, Mg, and Si metal particles are especially enhanced by the 400°C ashing temperature.

(3) Effect of Ashing Time. The effects of ashing time on the analytical results of the RPE were studied at 400°C. The data in Table 10 indicates that increased ashing times decrease the emission readouts of the C13-50 standard. The effect of ashing time on the metal particle recoveries depends upon the metal being analyzed. Increased ashing time decreases the

TABLE 7. THE EFFECTS OF THE COUNTER-ELECTRODE'S CONFIGURATION ON THE ANALYTICAL RESULTS OF THE RPE-STRM

	Tip Angle	Ag	Al	Cr	Cu	Fe	Mg	Ni	Si	Sn
Readout (C13-50)	160°	303±3	171±5	163±7	196±10	271±9	270±5	180±7	65±4	347±11
	15°	299±16	167±8	148±12	231±9	241±10	245±10	185±10	61±5	334±15
A%* (M12-50)	160°	79±4	33±3	70±7	102±10	171±5	47±8	52±6	55±3	116±10
	15°	66±8	23±4	47±10	42±5	101±8	35±7	25±7	33±3	69±11

Ashing Conditions - Time: 1 minute

Temperature: 400°C

*Percent Metal Analyzed

TABLE 8. THE EFFECTS OF POROSITY ON THE ANALYTICAL RESULTS OF THE RPE-STRM

	Graphite Grade	Ag	Al	Cr	Cu	Fe	Mg	Ni	Si	Sn
Readout (C13-50)	BCI 100 HD	343±7	201±10	185±9	248±6	320±8	297±10	221±16	60±3	391±75
	BCI 100 MDX	303±3	171±5	163±7	196±10	271±9	270±5	180±7	65±4	347±71
A%* (M12-50)	BCI 100 HD	74±5	12±7	55±11	87±8	144±8	43±11	25±12	45±4	108±79
	BCI 100 MDX	79±4	33±3	70±5	102±11	171±6	47±6	52±8	55±5	116±12

Ashing Conditions - Time: 1 minute
Temperature: 400°C

*Percent Metal Analyzed

TABLE 9. THE EFFECTS OF ASHING TEMPERATURE ON THE ANALYTICAL RESULTS OF THE RPE-STRM

	Temperature	Ag	Al	Cr	Cu	Fe	Mg	Ni	Si	Sn
Readout (C13-50)	400°C	173±4	90±4	68±3	103±7	91±6	115±2	81±4	28±9	133±1
	600°C	133±4	85±10	72±7	100±4	89±13	108±15	94±11	20±7	114±20
A%* (M12-50)	400°C	96±5	62±6	277±10	69±8	169±10	111±4	90±6	96±10	185±6
	600°C	83±4	41±6	86±8	58±5	145±18	37±12	104±15	35±6	145±10

Ashing Time: 400°C - 1 minute
600°C - 0.5 minute
*Percent Metal Analyzed

TABLE 10. THE EFFECTS OF ASHING TIME ON THE ANALYTICAL RESULTS OF THE RPE-STRM

	Time	Ag	Al	Cr	Cu	Fe	Mg	Ni	Si	Sn
Readout (C13-50)	1 minute	341±9	171±3	187±10	233±15	329±19	289±20	191±5	49±2	304±10
	10 minutes	222±8	138±9	141±9	142±3	227±15	229±12	139±8	50±1	272±11
A%* (M12-50)	1 minute	63±4	34±2	70±11	74±16	140±16	53±6	50±6	59±2	141±9
	10 minutes	99±8	16±8	101±8	173±5	198±14	35±10	129±9	68±4	172±10

Ashing Temperature: 400°C
*Percent Metal Analyzed

percent metal analyzed for Al and Mg particles, but increases the recoveries for the other metal particles.

f. Effect of Laser Ashing.

(1) To evaluate lasers as an alternative to the furnace, three continuous wave CO_2 lasers with power levels of 5, 30, and 250 watts were tested. The beams from the 5 and 250 watt lasers were attenuated to 3 and 52 watts, respectively, for this work. The initial attempt was made with the 3 watt CO_2 beam having a diameter of 1 mm. A steering mirror was used to move the beam across the surface of the RPE. The RPE was irradiated with the 3 watt laser until the oil was completely vaporized which required 15 minutes. In contrast to the 1 mm beam obtained with the 3 watt laser, the 10 mm beam obtained with the 52 watt CO_2 laser required only 1 minute to ash the oil. To determine the effect of increased ashing time, an oil sample was ashed for 4 minutes with the 52 watt CO_2 laser beam. The results of these experiments are shown in Figures 23 and 24.

(2) As seen in Figure 23 the emission readouts of the C13 standard ashed by the 3 watt CO_2 laser were greatly reduced compared to the results obtained with the 52 watt CO_2 laser beam at 1 minute. Also, the 4-minute ashing time with the 52 watt CO_2 laser beam produced a substantial decrease in the emission readouts of the C13 standard.

(3) The percent metal analyzed for the M12-50 suspension were less affected by the power of the laser beam (Figure 24). The percent metal analyzed for Al, Mg, and Ni are greater for the 3 watt laser while the percent metal analyzed for the other metals are greater with the 52 watt laser beam. The percent metal analyzed for all the metals are significantly reduced by the increased ashing time with the 52 watt beam.

g. Comparison of Furnace Ashing and Laser Ashing Results.

(1) Research on laser ashing methods was discontinued for the following reasons. First, as shown in Figure 23, the emission readouts of the C13 standard are significantly lower for the laser ashing method than for the furnace ashing method. Secondly, and more important, several problems were encountered during the ashing of the oil sample with the laser beam. When the RPE was irradiated with the various CO_2 laser beams, the oil sample moved from a positive meniscus on the graphite to a negative central portion with the major portion of the oil moving toward the edges. For all samples analyzed with the 30 and 52 watt laser beams, portions of the oil sample were pushed over the edge of the RPE.

(2) The third disadvantage of the laser ashing method was that when a blank RPE was irradiated, vapors were evolved from the surface. Therefore, near the end of the ashing period it was impossible to determine if the vapors originating from the surface of the RPE were being produced by the remaining oil or by the electrode. This is important since extended ashing times lower the sensitivity as well as the percent metal analyzed of the STRM. All of these factors combine to decrease the repeatability of the laser ashing method and make lasers an impractical heat source for ashing oil samples in comparison to the furnace.

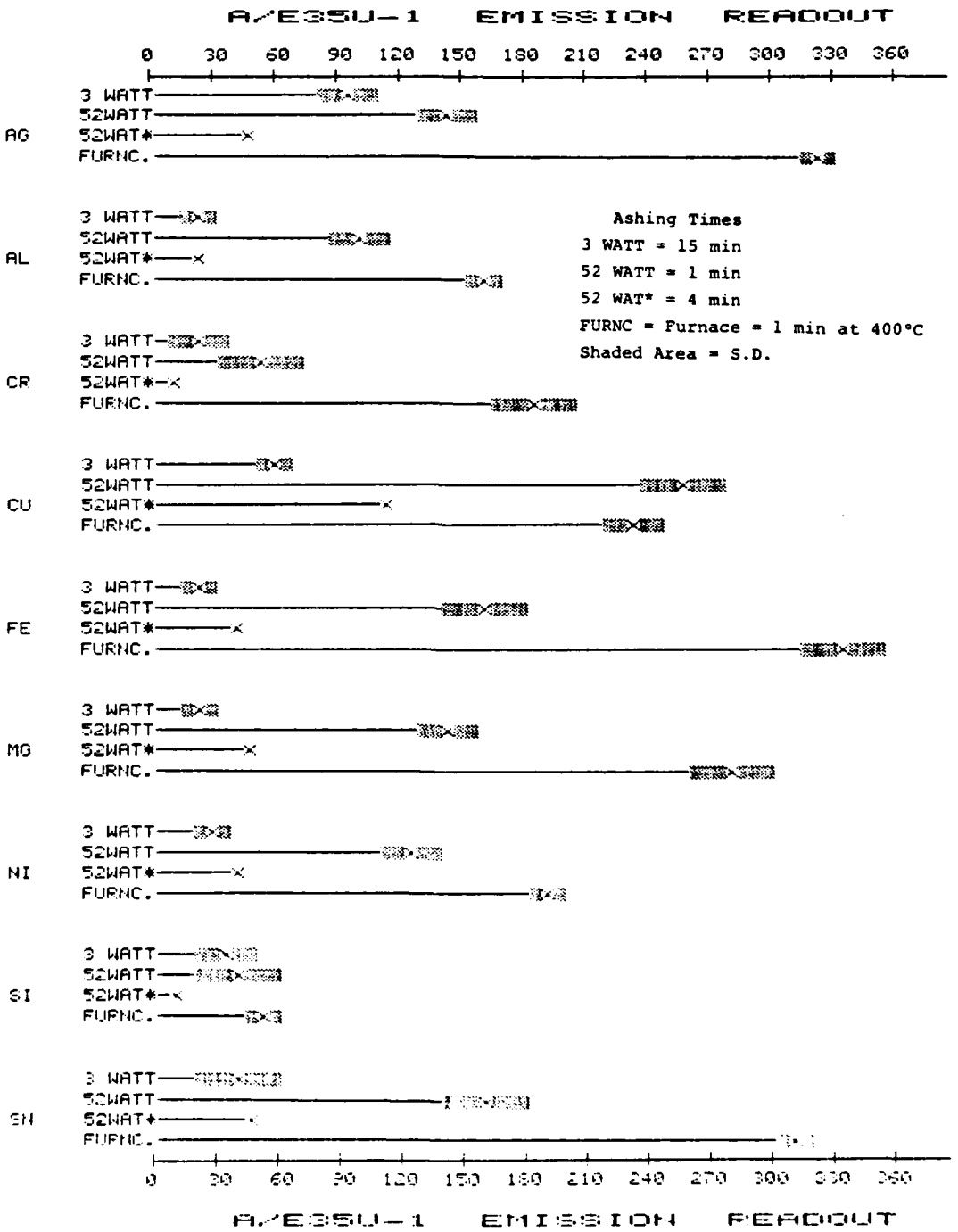

Figure 23. The Effects of Laser Ashing on the A/E35U-1 Readouts for the C13-50 Standard.

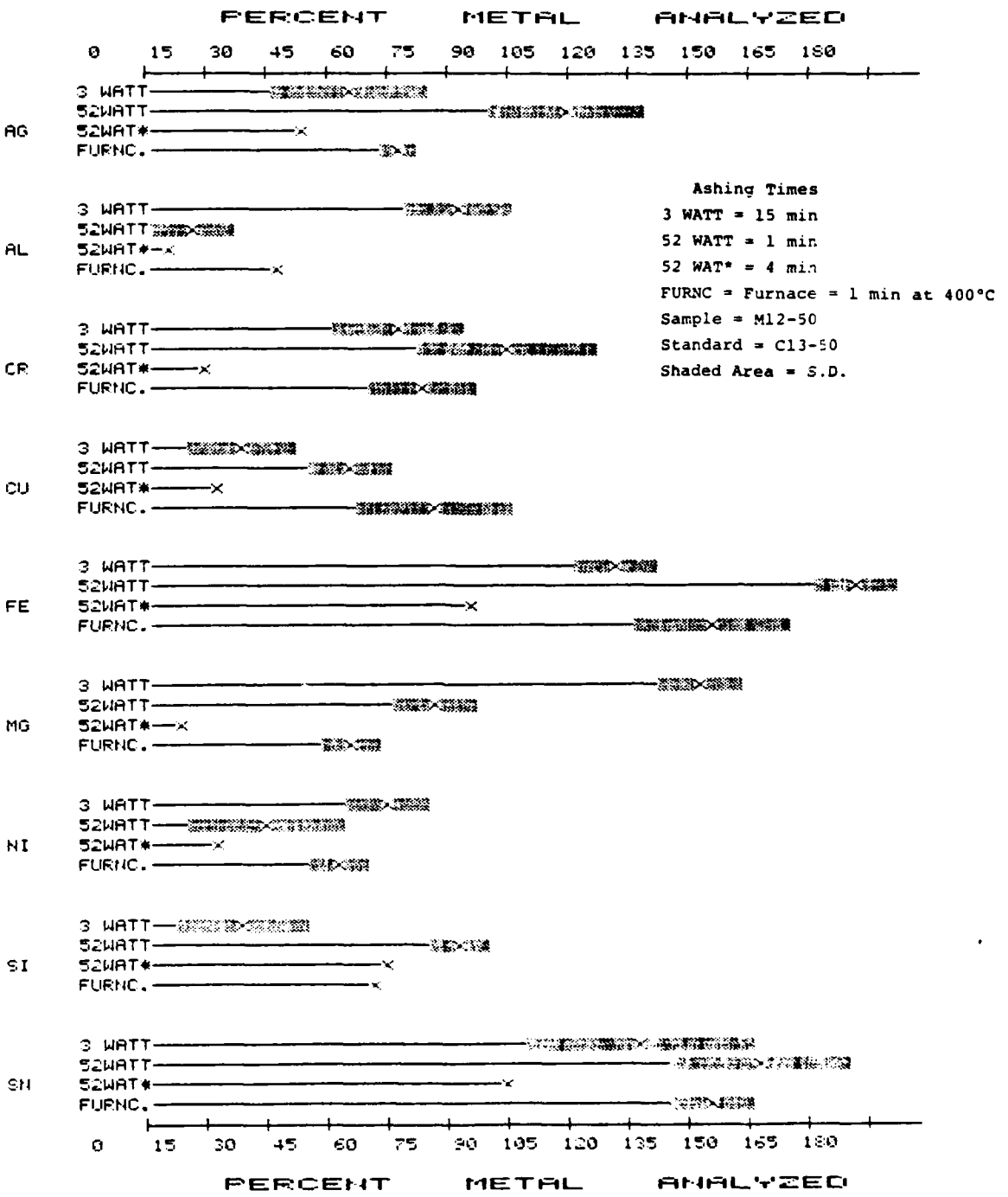

Figure 24. The Effects of Laser Ashing on the Percent Metal Analyzed by the RPE-STRM.

h. Effect of Multiple Analyses.

(1) As seen by the data presented thus far, there is very poor agreement between the emission readouts for the M12-50 suspension and C13-50 standard. To gain some insight into the factors producing these differences, samples of the M12-50 suspension and C13-50 standard were deposited on the RPE and analyzed twice.

(2) As shown in Table 11, the emission readouts for the C13-50 standard decrease with the second analysis. If the emission readouts for the metal particles and dissolved, metallo-organic standard compounds were decreasing at similar rates the percent metal analyzed should remain constant. The data in Table 11 shows that this is not the case. The percent metal analyzed for each metal decreases sharply from the first analysis to the second analysis indicating that the metal particles are vaporized faster from the surface of the RPE than the metallo-organic compounds. Since the metal particles are vaporized at a faster rate, they should produce higher emission readouts during the first burn than the metallo-organic standard. However, except for Fe and Sn, the metal particles produce lower emission readouts. Therefore, additional factors must be responsible for the differences observed between the emission readouts for the metal particles and metallo-organic standard compounds.

i. Effect of Number of Rotations.

(1) Since the metal particles appear to be vaporizing from the surface of the RPE at a faster rate than the metallo-organic standard compounds, increasing the period of time the RPE is held stationary should increase the emission readouts of the metal particles relative to those of the standard and increase the percent metal analyzed for the M12-50 suspension.

(2) The RPE makes one rotation every 6 seconds (10 rpm) so that during the 18 second integration period the RPE makes three complete rotations. By holding the RPE stationary for 6 and 12 seconds the RPE will make 2 and 1 rotations, respectively, during the integration period. If the metal particles are vaporizing at a faster rate than the metallo-organic compounds, the percent metal analyzed should be directly proportional to the time the RPE is held stationary.

(3) As indicated by the data listed in Table 12, the percent metal analyzed for Ag, Al, Fe, Mg, and Sn increase significantly as the time the RPE is held stationary increases. However, the other metals' percent metal analyzed are essentially unaffected. Therefore, factors other than the vaporization rate are contributing to the differences between the emission readouts of the M12-50 suspension and C13-50 standard.

j. Effect of Spark Atmosphere.

(1) Introduction. The final factor studied was the effect of gases on the analytical results of the RPE on the A/E35U-1 spectrometer. It is well known that the spark sources can be stabilized by gases such as argon. The argon stabilized spark may analyze metal particles more efficiently than

TABLE 11. THE EFFECTS OF MULTIPLE ANALYSES ON THE ANALYTICAL RESULTS OF THE RPE-STRM

	Analysis	Ag	Al	Cr	Cu	Fe	Mg	Ni	Si	Sn
Readout (C13-50)	1st	341±9	171±3	187±18	238±15	329±19	289±20	191±5	49±2	384±10
	2nd	130±9	85±10	85±10	92±25	138±4	150±10	70±8	35±2	180±10
A% (M12-50)	1st	63±8	43±1	70±9	73±6	141±5	53±18	50±6	59±1	141±6
	2nd	52±9	7±1	41±8	41±4	67±5	28±10	24±6	28±2	55±10

Ashing Conditions - Time: 1 minute
Temperature: 400°C

TABLE 12. THE EFFECTS OF THE NUMBER OF ROTATIONS ON THE ANALYTICAL RESULTS OF THE RPE-STRM

	Number of Rotations	Ag	Al	Cr	Cu	Fe	Mg	Ni	Si	Sn
Readout (C13-50)	1	205±5	124±4	115±5	146±8	201±1	184±2	136±1	39±1	254±7
	2	299±10	169±6	168±5	230±3	259±9	250±5	189±4	53±1	357±8
A% (M12-50)	1	82±7	78±3	76±5	89±7	233±4	78±8	56±3	66±2	208±3
	2	65±6	61±4	77±2	85±2	177±5	60±6	55±1	66±1	175±4

Ashing Conditions - Time: 1 minute
Temperature: 400°C

the unstabilized spark. For this study, holes with diameters of 1/8 and 1/16 inch were drilled lengthwise through the counter-electrode. Argon or nitrogen was then passed at flow rates between 2.5-0.2 1/min. through the counter-electrode into the spark source. Nitrogen did not visibly change the spark, but the argon visibly decreased its diameter.

(2) Effect of Nitrogen. The effects of nitrogen on the emission readouts of the C13 standard and the percent metal recoveries of the M12 suspension were studied. As Figures 25 and 26 show, increasing nitrogen flow rates decreased both the sensitivity and percent metal analyzed of the STRM. These effects decreased as the bore of the counter-electrode was decreased (Figures 27 and 28). In addition, the presence of nitrogen did not significantly increase the reproducibility of the analytical results.

(3) Effect of Argon. The effects of argon on the sensitivity and percent metal analyzed of the STRM were also studied. As with nitrogen, the emission readouts of the C13-50 standard decrease as the argon flow increases (Figure 29). However, the percent metal recoveries of the M12-50 suspension increased (Figure 30). Although the argon decreased the diameter of the spark, the reproducibility of the A/E35U-1 analyses did not increase significantly. Since a 100 percent recovery was obtained only for Fe at argon flow rates below 2.1 1/min. (Figure 30), it appears that higher percent metal analyzed might be attained by argon flow rates faster than those used in this study.

3. ROTATING DISK ELECTRODE (RDE).

a. Introduction. The next electrode evaluated for use in a spark-to-residue method was the rotating disk electrode (RDE). Although the RDE was specifically designed as a solution transporting electrode, previously reported analyses of the residue on the RDE produced higher results on the A/E35U-1 spectrometer than the RPE [reference (g)]. In order to optimize the STRM for the RDE, the effects of ashing conditions, RDE porosity, counter-electrode configuration, speed and direction of rotation, and the length and number of analyses on the analytical results of the A/E35U-1 spectrometer were determined for the M12-50 suspension and C13-50 standard. The RDE was usually not rotated during the preburn cycle so that the metals would not be exposed to the spark before the integration cycle began.

b. Effect of Furnace Ashing Conditions.

(1) Introduction.

(a) The two ashing conditions studied in this investigation were the effects of rotating the RDE during the ashing period and the effect of ashing time. The effect of furnace ashing temperature was not studied, because above 600°C the oil sample on the RDE ignited and below 600°C the oil sample dripped off the bottom of the RDE before vaporizing, whether the RDE was rotated or held stationary. At 600°C a droplet formed at the bottom of the RDE but stayed intact until completely vaporized.

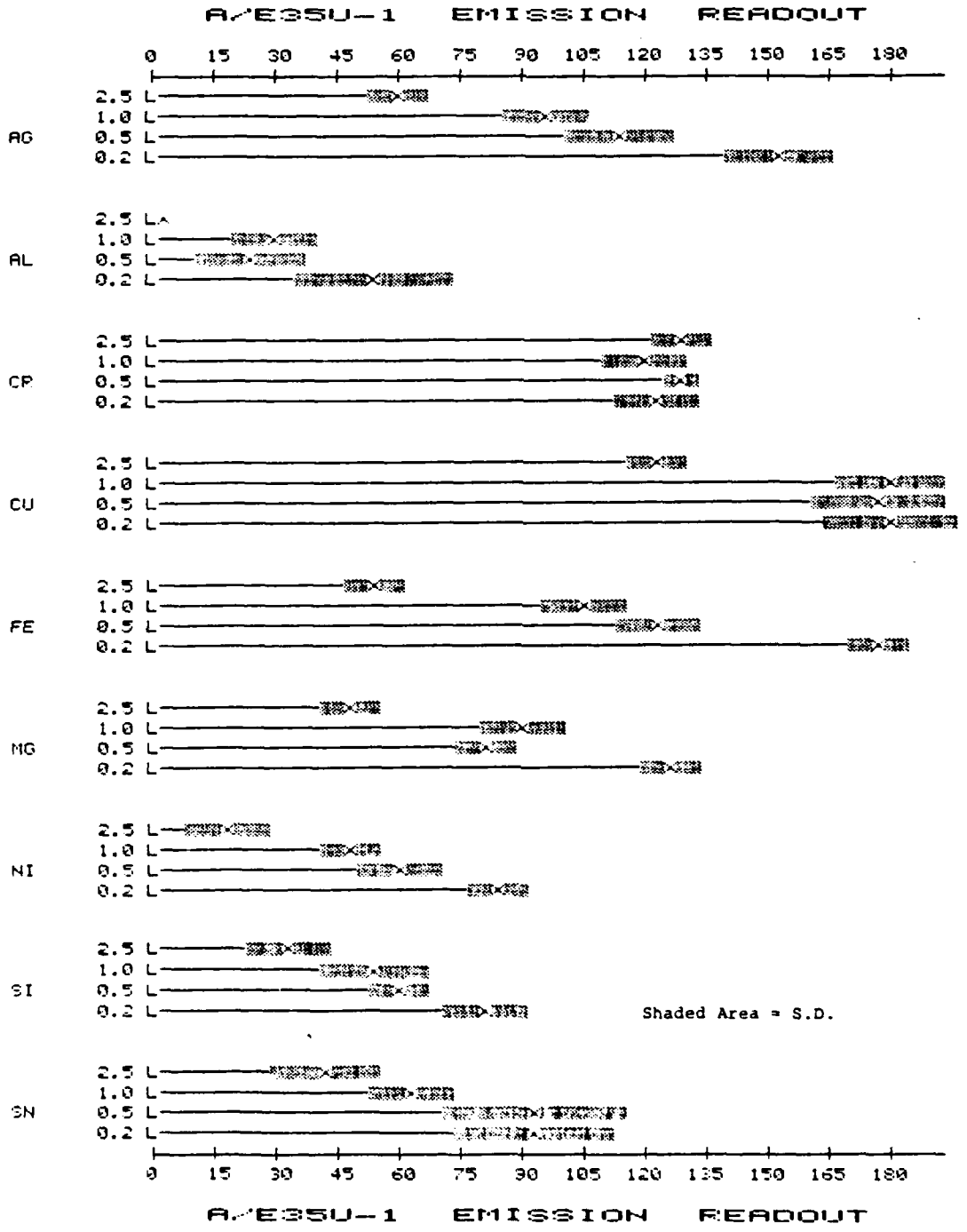

Figure 25. The Effects of Nitrogen Flow Rates (l/min.) on the A/E35U-1 Readouts for the C13-50 Standard with a 1/8" Diameter Bored Counter-Electrode.

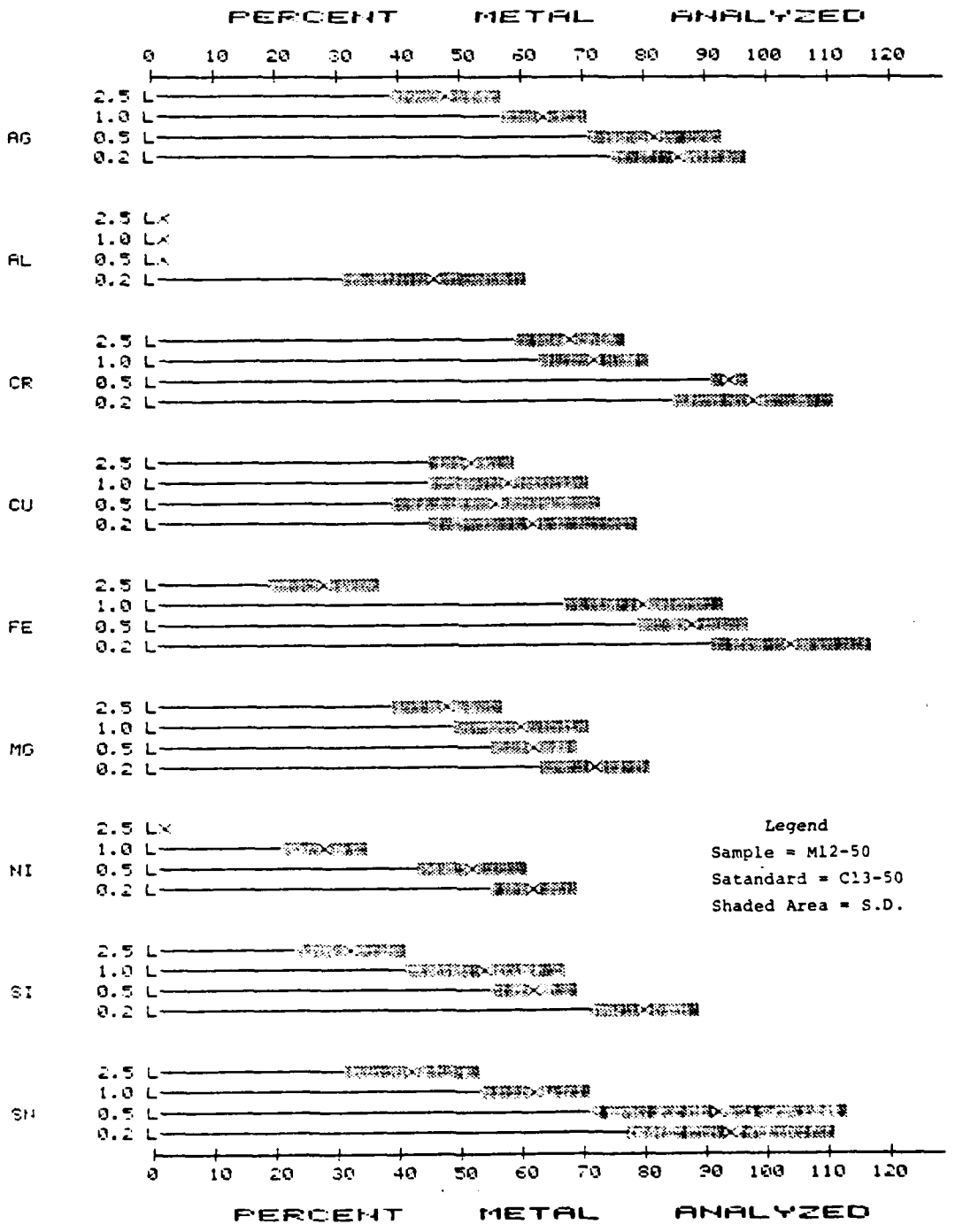

Figure 26. The Effect of Nitrogen Flow Rates (l/min.) on the Percent Metal Analyzed by the RPE-STRM with a 1/8" Diameter Bored Counter-Electrode.

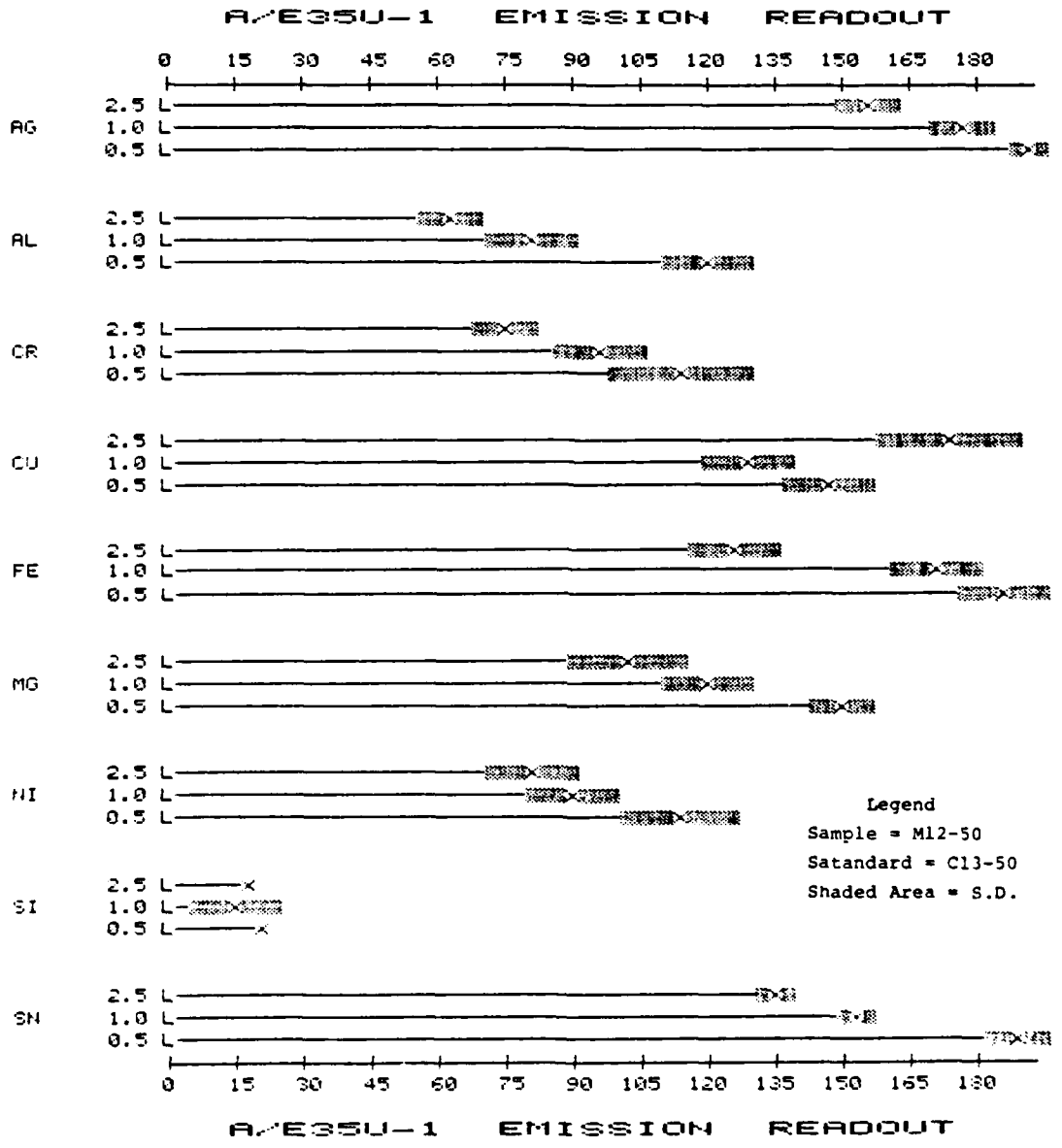

Figure 27. The Effects of Nitrogen Flow Rates (1/min.) on the A/E35U-1 Readouts for the C13-50 Standard with a 1/16" Bored Counter-Electrode.

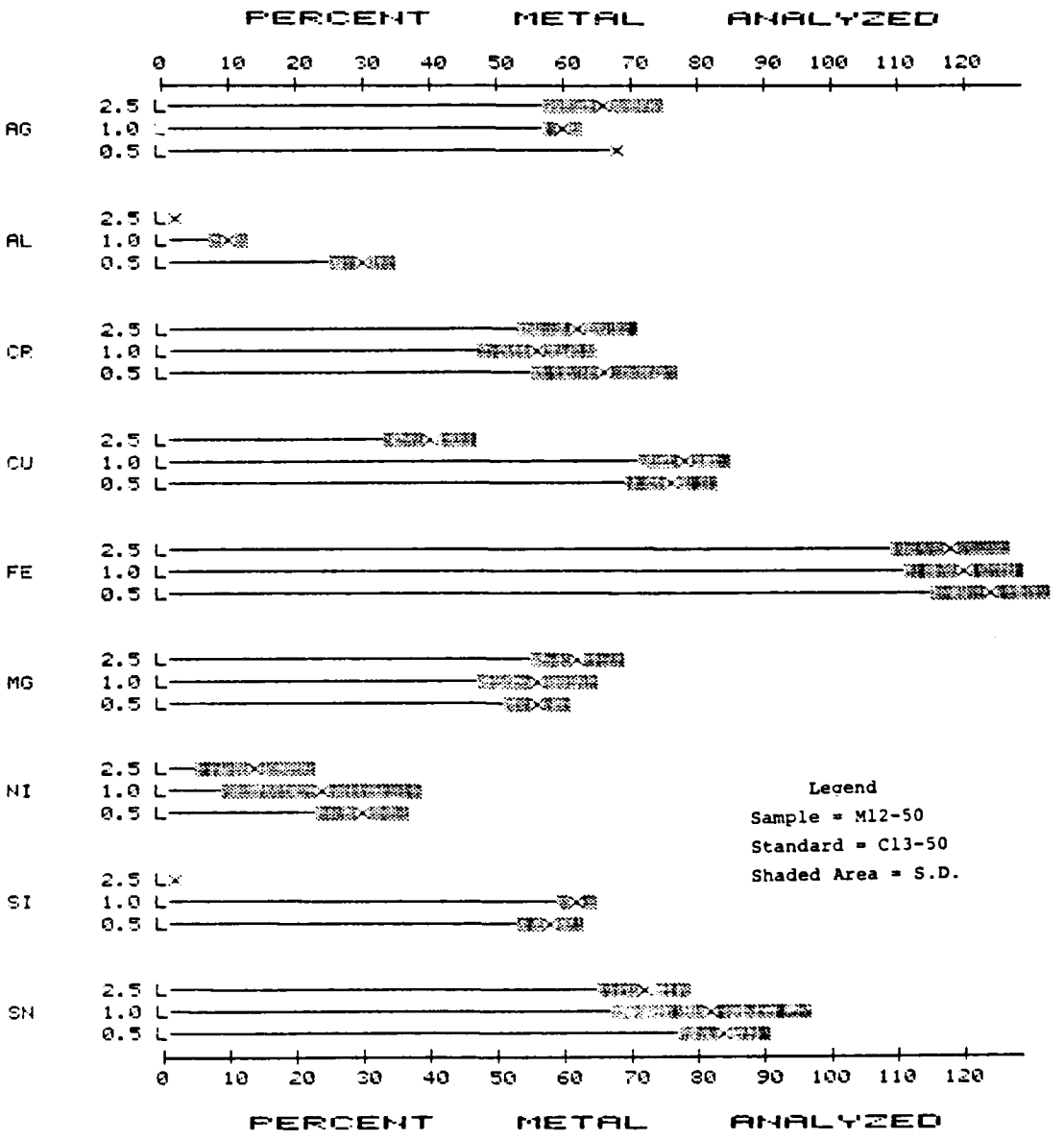

Figure 28. The Effects of Nitrogen Flow Rates (1/min.) on the Percent Metal Analyzed by the RPE-STRM with a 1/16" Diameter Bored Counter-Electrode.

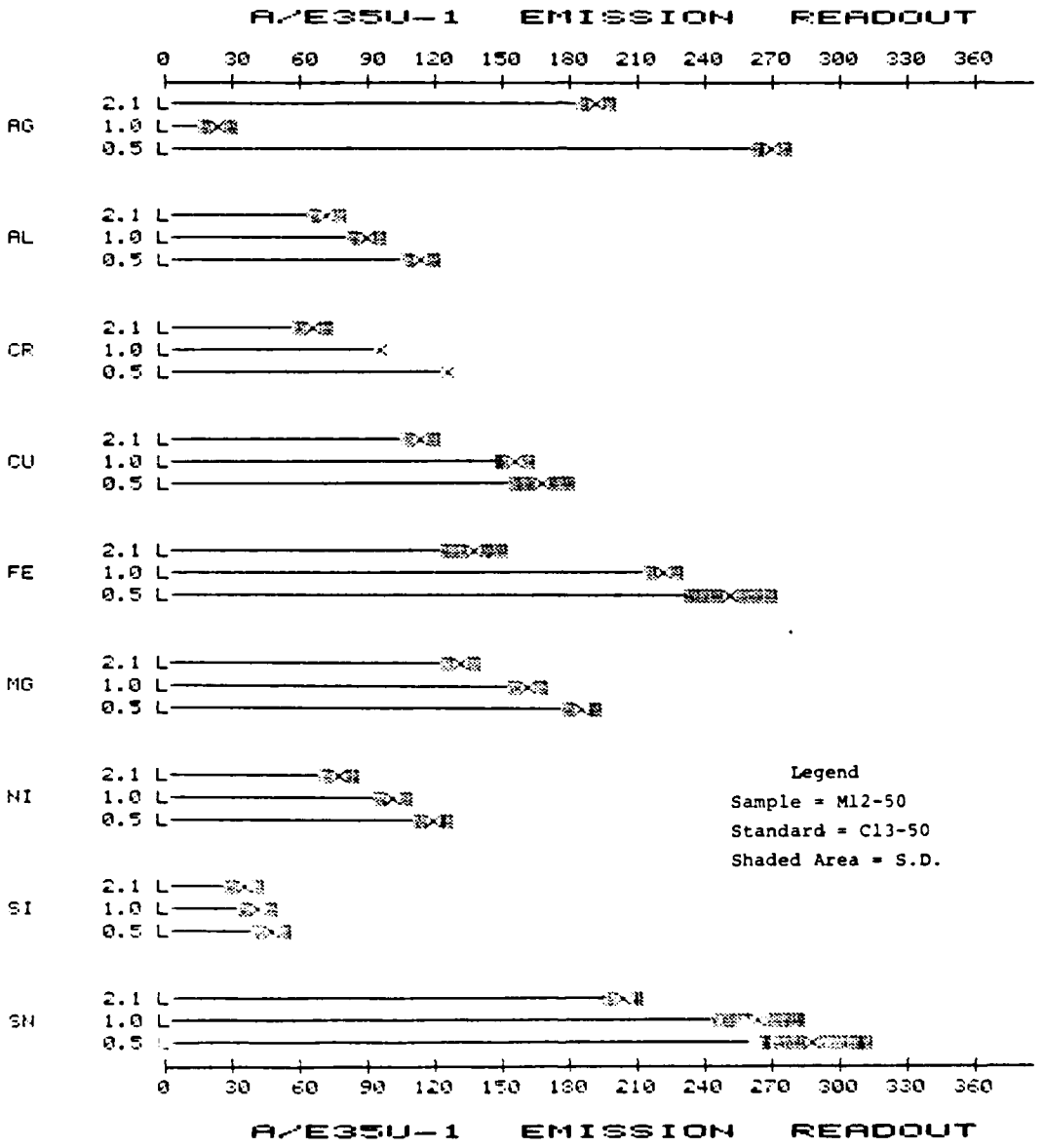

Figure 29. The Effects of Argon Flow Rates (l/min.) on the A/E35U-1 Readouts for the C13-50 Standard with a 1/8" Diameter Bored Counter-Electrode.

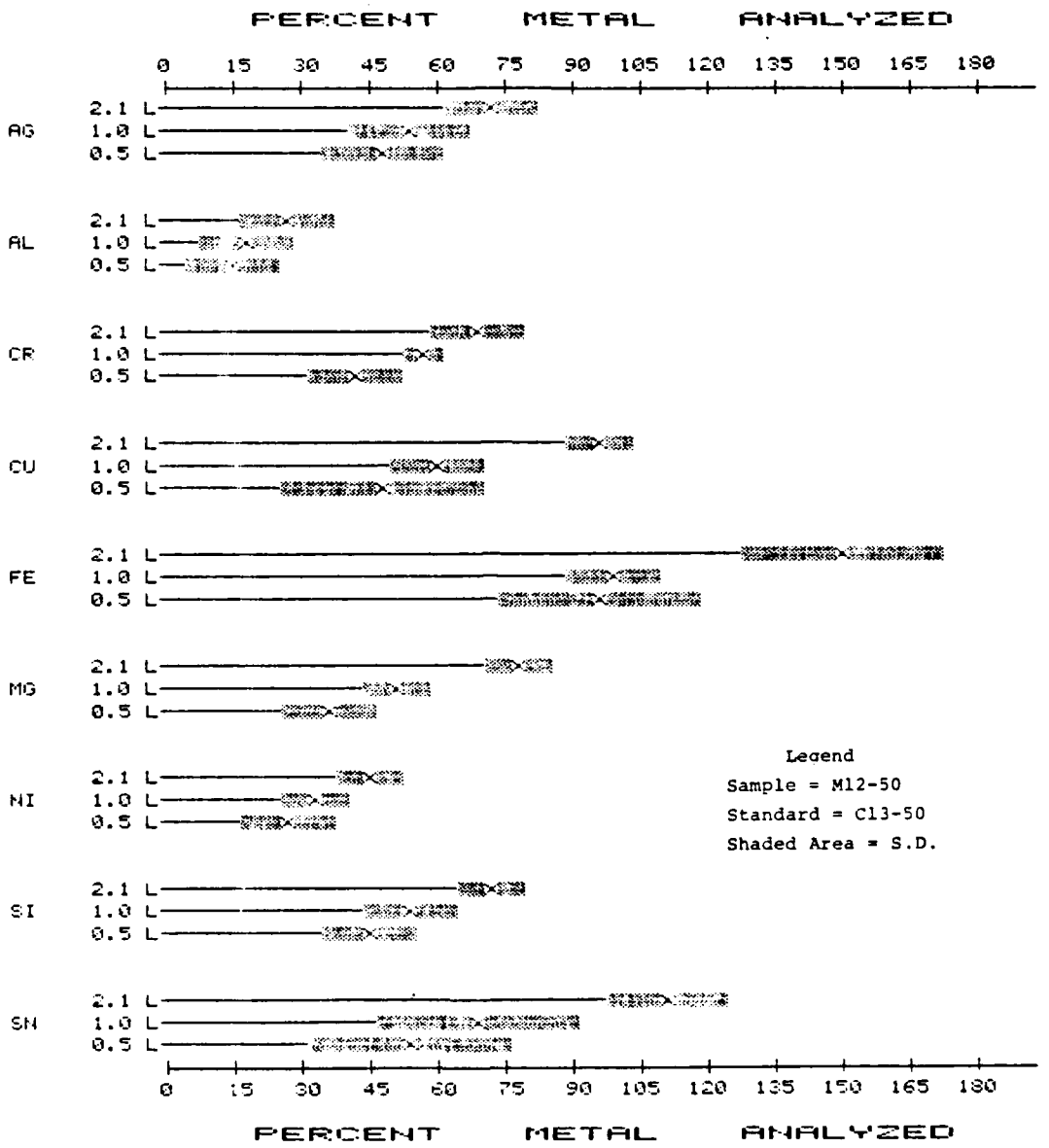

Figure 30. The Effects of Argon Flow Rates (1/min.) on the Percent Metal Analyzed by the RPE-STRM with a 1/8" Diameter Bored Counter-Electrode.

(b) By holding the RDE stationary during the ashing period, the oil sample was concentrated on one side of the RDE. The RDE could then be placed on the rotation spindle of the A/E35U-1, so that during the preburn cycle the spark was directed to the side of the RDE opposite to where the oil sample was concentrated. During analysis on the spectrometer, the RDE was turned off during the preburn cycle and started after the preburn cycle was completed.

(c) By allowing the RDE to rotate during the ashing period, the oil sample was distributed evenly over the entire rim of the RDE. Regardless of the positioning of the RDE on the spindle of the A/E35U-1 spectrometer, some of the sample is vaporized by the source during the preburn cycle. Therefore, holding the RDE stationary during the ashing period should increase the emission readouts of the A/E35U-1 relative to rotating the RDE during the ashing period.

(2) Effect of Rotating the RDE During Ashing. The effect of rotating the RDE on the results of the STRM was studied by holding the RDE stationary and by rotating the RDE during the ashing period. As shown by the data in Table 13, holding the RDE stationary while ashing increases the emission readouts of the C13 standard relative to allowing the RDE to rotate while ashing. However, holding the RDE stationary or allowing it to rotate while ashing, does not affect the percent metal analyzed for the M12-50 suspension.

(3) Effect of Ashing Time. The effect of ashing time on the analytical results of the STRM was studied next and the results are presented in Table 14. Increasing the ashing time from 1 minute to 10 minutes decreased the emission readouts of the C13 standard, which caused the percent metal analyzed for all the metals to increase significantly. In fact, after 10 minutes of ashing, every metal has over 100 percent recovery with Ag, Cr, Cu, Fe, and Sn metal particles producing over 200 percent recoveries.

c. Effect of RDE's Porosity.

(1) The same grades of graphite used in the RPE study, BCI 100 HD and BCI 100 MD-X, were also used for the RDE investigation. As seen in Table 15, the RDE's porosity has only a small effect on the emission readouts for the C13 standard. The more dense grade BCI 100 HD produces higher results than the BCI 100 MD-X grade as was the case with the RPE.

(2) The percent metal analyzed is also affected by the RDE's porosity with the BCI 100 HD grade producing higher recoveries than the BCI 100 MD-X grade. This is opposite to the porosity effect seen for the RPE in which the BCI 100 MD-X grade produced higher percent metal recoveries than the BCI 100 HD grade.

d. Effect of Counter-Electrode's Configuration. The same two configurations of the counter-electrode used for the RPE investigation were used for the RDE study and are illustrated in Figure 6. As listed in Table 16, the 160^{o} counter-electrode produced higher emission readouts for the C13 standard and higher percent metal recoveries for every metal studied.
The 160^{o} counter-electrode was used for further analyses with the RDE-STRM.

TABLE 13. THE EFFECTS OF ROTATING THE RDE DURING ASHING ON THE ANALYTICAL RESULTS OF THE RDE-STRM

		Ag	Al	Cr	Cu	Fe	Mg	Ni	Si	Sn
Readout (C13-50)	Rotating	77±8	34±12	33±19	67±10	66±19	71±7	34±10	34±9	77±9
	Stationary	108±6	36±2	40±6	77±11	70±3	102±5	63±7	26±9	134±10
A% (M12-50)	Rotating	106±8	6±3	130±15	42±6	100±12	30±5	59±11	26±7	139±11
	Stationary	108±6	3±1	115±7	42±7	109±6	54±6	27±4	38±3	90±12

Ashing Conditions - Time: 1.5 minutes
Temperature: 600°C in a Furnace

TABLE 14. THE EFFECTS OF ASHING TIME ON THE ANALYTICAL RESULTS OF THE RDE-STRM

		Ag	Al	Cr	Cu	Fe	Mg	Ni	Si	Sn
Readout (C13-50)	1 minute	122±9	51±6	49±8	85±7	112±6	129±9	71±8	28±3	147±12
	10 minutes	72±2	25±3	35±3	60±3	60±4	87±3	49±2	15±1	89±3
A% (M12-50)	1 minute	134±10	20±4	194±9	103±8	159±8	71±10	56±6	82±4	140±10
	10 minutes	283±11	108±4	380±20	265±16	420±10	105±8	186±4	186±4	258±4

Ashing Temperature: 600°C in a Furnace

TABLE 15. THE EFFECTS OF POROSITY ON THE ANALYTICAL RESULTS OF THE RDE-STRM

		Ag	Al	Cr	Cu	Fe	Mg	Ni	Si	Sn
Readout (C13-50)	BCI 100 HD	227±6	107±3	94±1	179±15	206±7	185±3	140±8	28±4	255±6
	BCI 100 MD-X	216±13	103±14	95±12	176±3	165±13	148±4	131±6	26±3	230±6
A% (M12-50)	BCI 100 HD	85±4	47±4	208±9	43±8	127±6	70±6	79±4	126±3	123±9
	BCI 100 MD-X	68±14	38±12	160±8	25±9	121±8	69±7	63±5	100±5	88±10

Ashing Conditions - Time: 1 minute
Temperature: 600°C in a Furnace

TABLE 16. THE EFFECTS OF THE COUNTER-ELECTRODE'S CONFIGURATION ON THE ANALYTICAL RESULTS OF THE RDE-STRM

	Tip Angle	Ag	Al	Cr	Cu	Fe	Mg	Ni	Si	Sn
Readout (C13-50)	160^{o}	122±9	51±6	49±8	85±7	112±6	129±9	71±8	28±3	147±12
	15^{o}	109±6	37±4	40±6	74±13	75±3	102±5	63±7	23±9	133±10
A% (M12-50)	160^{o}	133±7	19±6	193±9	103±11	158±12	72±10	56±7	82±6	140±11
	15^{o}	116±7	5±2	120±11	48±7	128±9	56±6	46±8	47±5	95±6

Ashing Conditions - Time: 1 minute
Temperature: $600^{o}C$ in a Furnace

e. Effect of the Rotating Electrode's Rotation Direction and Speed.

(1) To determine the effect of rotation direction and speed, the RDE was placed on a steel shaft driven through a pulley system by a reversible, variable speed stirring motor. The effect of rotation direction was studied at 30 rpm using the 160^{o} and 15^{o} counter-electrodes.

(2) In normal operating procedures the RDE is rotated at 30 rpm in a clockwise direction. For this study the RDE was studied using clockwise and counterclockwise rotations at 30 rpm. For the emission readouts of the C13-50 standard, the rotation direction has essentially no effect regardless of the counter-electrode configuration (Figure 31). With the 15^{o} electrode the direction also has no effect on the percent metal recoveries of the M12-50 suspension (Figure 32). However, when the 160^{o} electrode is used, the counterclockwise direction produced higher percent metal recoveries for the M12-50 suspension than the normal clockwise direction (Figure 32).

(3) The effect of speed of rotation was studied in both clockwise and counterclockwise directions between 5-60 rpm. The speed of rotation had no effect on the emission readouts of the C13-50 standard or on the percent metal recoveries of the M12-50 suspension regardless of the counter-electrode or direction of rotation used.

f. Effect of Multiple Analyses.

(1) As was the case for the RPE, the emission readouts for the C13 standard and M12-50 suspension obtained using the RDE on the A/E35U-1 spectrometer are in very poor agreement. To gain insight into the factors producing the differences between the M12-50 and C13-50 emission readouts, the samples of the M12-50 suspension and the C13-50 standards were deposited on the RDE, ashed, and then analyzed twice.

(2) As listed in Table 17, the emission readouts of the C13-50 standard decrease with the second analysis. If the emission readouts of the suspension and standard decrease at similar rates, the percent metal recoveries should remain constant, but the percent metal recoveries decrease sharply from the first analysis to the second (Table 17). Thus, the metal particles are vaporized from the surface of the RDE at a faster rate than the standard.

g. Effect of Number of Rotations.

(1) Since the percent metal recoveries of the M12-50 suspension appear to decrease with time, increasing the length of time the RDE is held stationary should increase the percent metal recoveries of the M12-50 suspension. The RDE makes one rotation every 2 seconds (30 rpm) so that during the 18 second analysis period, the RDE makes nine complete rotations. Therefore, by holding the RDE stationary for 6 and 12 seconds the RDE will make 6 and 3 rotations, respectively, and the percent metal recoveries should increase.

(2) As illustrated in Table 18, the percent recoveries for all the metals, except Cr, increase as the time the RDE is held stationary increases.

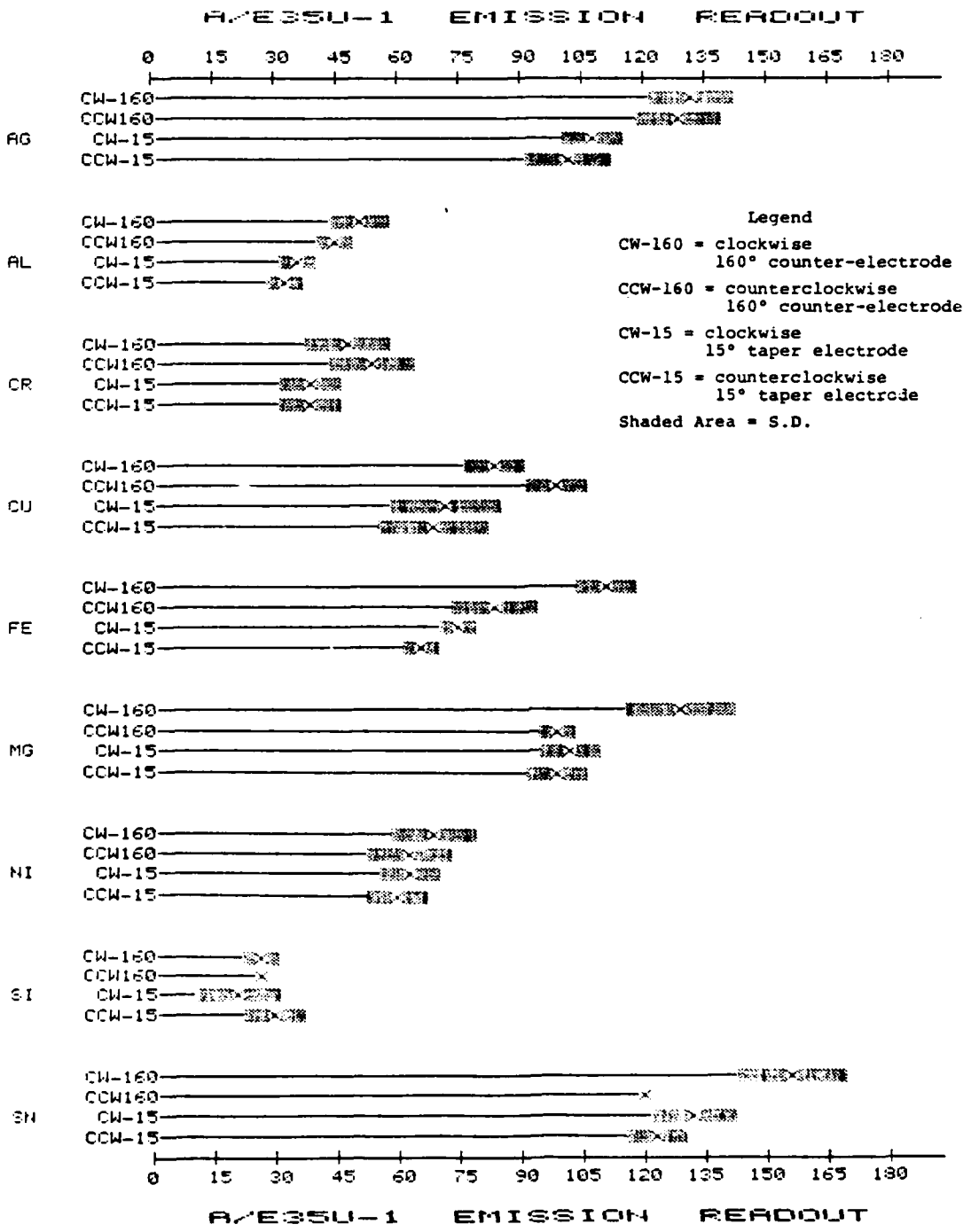

Figure 31. The Effects of the RDE's Direction of Rotation on the A/E35U-1 Readouts for the C13-50 Standard.

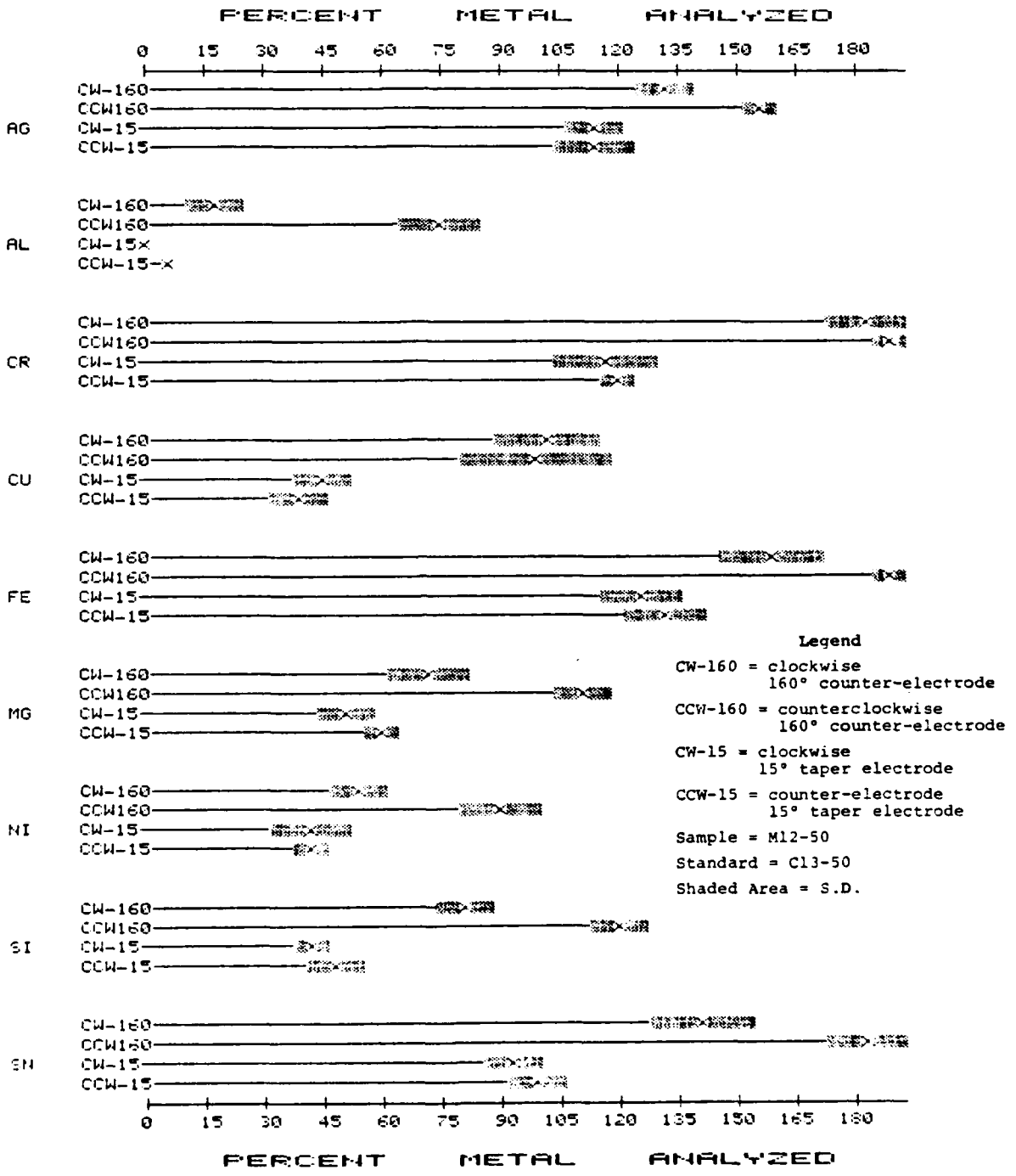

Figure 32. The Effects of the RDE's Direction of Rotation on the Percent Metal Analyzed by the RDE-STRM.

TABLE 17. THE EFFECTS OF MULTIPLE ANALYSES ON THE ANALYTICAL RESULTS OF THE RDE-STRM

	Analysis	Ag	Al	Cr	Cu	Fe	Mg	Ni	Si	Sn
Readout (C13-50)	1st	123±7	62±7	61±3	81±6	101±4	121±8	74±8	29±2	149±20
	2nd	61±2	21±4	52±1	27±4	33±6	59±11	37±4	14±1	115±16
A% (M12-50)	1st	139±6	29±7	161±4	100±10	130±11	72±11	56±8	83±1	110±12
	2nd	62±3	5±1	140±5	39±6	62±9	30±6	14±9	46±10	69±6

Ashing Conditions - Time: 1 minute
Temperature: 600°C in a Furnace

TABLE 18. THE EFFECTS OF THE NUMBER OF ROTATIONS ON THE ANALYTICAL RESULTS OF THE RDE-STRM

	Number of Rotations	Ag	Al	Cr	Cu	Fe	Mg	Ni	Si	Sn
Readout (C13-50)	3	121±10	35±3	60±7	96±10	58±6	67±6	72±6	10±2	113±8
	6	226±4	88±4	90±5	176±4	78±6	175±6	135±6	30±4	261±7
A% (M12-50)	3	101±6	120±7	203±6	47±9	286±9	130±4	125±4	211±4	211±8
	6	67±4	51±4	222±9	44±6	257±7	67±9	54±5	150±7	117±6

Ashing Conditions - Time: 1 minute
Temperature: 600°C in a Furnace

In contrast to the results for the RPE (Table 12), the emission readouts obtained for 3 rotations of the RDE are higher for the metal particles than those for the standard, except for Cu and Ag. The higher readouts for the metal powder suspension are expected since the metal particles are vaporized at a faster rate which results in a higher initial concentration of metal in the spark.

4. RECIPROCATING SEMICYLINDRICAL ELECTRODE.

a. Introduction.

(1) Due to the limitations of the RDE and RPE, a third type of electrode, the reciprocating semicylindrical electrode (RSE), was designed for use in the spark-to-residue method. The RSE was designed so that the sample was not exposed to the spark source during the preburn cycle. Shallow craters [1.0(l) x 0.20(w) x 0.012"(d)] were ground into the flat surface of the RSE to retain the samples.

(2) A preliminary investigation into the factors which affect the analytical results produced by the RSE on the A/E35U-1 spectrometer was conducted. The effects of the direction of linear motion and multiple analyses on the analytical results of the RSE-STRM were determined.

b. Effect of Linear Motion Direction.

(1) To determine the effect of direction on the analytical results, the stirring motor was set at a speed which caused the RSE to make one pass of the spark per integration period. When the RSE was moved toward the window of the optics system, as illustrated in Figure 33, the emission readouts for the C13-50 standard were lower for Ag, Fe, Mg, Ni, and Sn than when the RSE was moved away from the window (Table 19). The other metals' emissions were essentially unaffected by the direction of the linear motion.

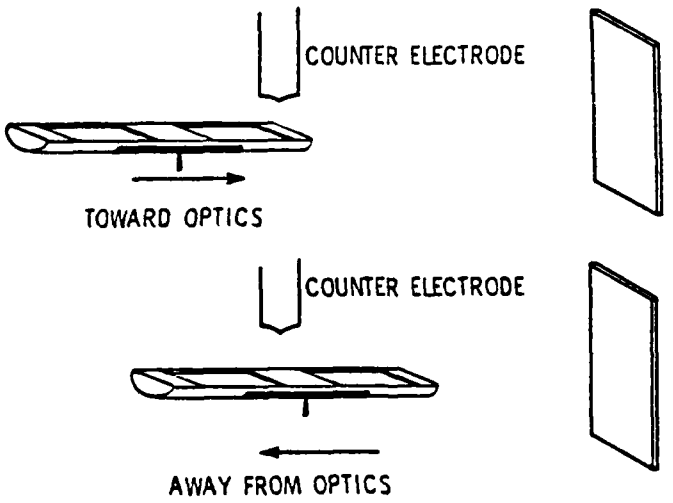

Figure 33. Horizontal Motion of the Reciprocating Semicylindrical Electrode.

TABLE 19. THE EFFECTS OF THE RSE'S DIRECTION OF MOTION ON THE ANALYTICAL RESULTS OF THE RSE-STRM

	Direction	Ag	Al	Cr	Cu	Fe	Mg	Ni	Si	Sn
Readout (C13-50)	A. W.[a]	135±2	63±6	28±2	91±6	186±6	140±4	68±6	8±2	135±9
	T. W.[b]	92±7	58±5	29±1	88±10	120±8	110±8	45±6	9±1	102±10
A% (M12-50)	A. W.	152±5	44±5	317±8	76±10	225±5	108±6	90±8	150±4	165±8
	T. W.	272±6	67±6	750±12	47±11	241±6	181±16	212±4	450±2	207±6

[a]Away from the window of the optics system.
[b]Toward the window of the optics system.
Ashing Conditions - Time: 1 minute
Temperature: 400°C in a Furnace

(2) Except for Cu, the percent metal recoveries for the metals studied are higher when the RSE is moved toward the window (Table 19). However, better agreement between the emission readouts of the M12-50 suspension and C13-50 standard is obtained when the RSE is moved away from the window.

c. Effect of Multiple Analyses. Of the three types of electrodes studied thus far, the emission readouts obtained by analyzing M12-50 suspensions and C13-50 standards on the RSE are in the least agreement. Samples of the M12-50 suspension and C13-50 standards were deposited on the RSE, ashed, and analyzed twice. As with the RDE and RPE, the emission readouts of the C13-50 standard and the percent metal recoveries of the M12-50 suspension (Table 20) decrease significantly from the first analysis to the second. Since, the percent metal recoveries decrease from the first analysis to the second, the metal particles are being vaporized from the surface of the RSE at a faster rate than the standard as was the case for the RPE and RDE.

5. ACID DISSOLUTION/SPARK-TO-RESIDUE ASHING METHOD.

a. Introduction. Due to the large differences between the emission readouts of the M12-50 metal powder suspension and C13-50 Conostan standard, acid dissolution of the particles prior to ashing was studied and is referred to as the acid dissolution/spark-to-residue method (AD-STRM). Since the acid/oil/surfactant solution is ashed prior to analysis, the detrimental effects of the acid on the spectrometer are nullified and the original acid mixture (1:8:1 = HNO_3/HCl/HF) containing HF was used. The strong matrix effects which reduced the reproducibility of the A/E35U-3 acid dissolution method should be greatly reduced since the matrix is removed by ashing prior to analysis. The effects of acid dissolution time, acid type, and the presence of amine sulfonate stabilizer on the analytical results of the A/E35U-1 were determined.

b. Effect of Acid Dissolution Time. To determine the effect of the acid dissolution time, the acid/oil sample mixture was reacted for 1, 3, and 5 minutes at 65°C in the modified Vortex mixer. As seen in Figure 34, the percent metal recoveries do not improve with longer dissolution times, in fact, the recoveries of Al, Cr, and Mg decrease with dissolution times greater than three minutes. Except for Cu, the emission readouts of the M12-50 suspension and C13-50 standard are in better agreement than any of the spark-to-residue methods developed thus far.

c. Effect of Acid Type. Because the metals in the Conostan standards are present as alkyl aryl sulfonates, dodecylbenzene sulfonic acid was added to the acid solution in differing amounts in an attempt to improve the agreement between the emission readouts of the M12-50 suspension and C13-50 standard. As seen in Figure 35, the additions of dodecylbenzene sulfonic acid, improved the agreement between the emission readouts of the M12-50 suspension and C13-50 standard for Ag, Cu, Fe, Mg, Ni, and Sn. However, the presence of dodecylbenzene sulfonic acid decreased the percent metal recoveries of Al, Cr, and Si metal particles.

d. Effect of Amine Sulfonate Stabilizer. Another difference between the M12-50 suspension and C13-50 standard is that the oil matrix of the C13-50 standard is prepared with amine sulfonate stabilizer to help keep the metallo-organic

TABLE 20. THE EFFECTS OF MULTIPLE ANALYSES ON THE ANAYTICAL RESULTS OF THE RSE-STRM

	Analysis	Ag	Al	Cr	Cu	Fe	Mg	Ni	Si	Sn
Readout (C13-50)	1st	92±7	53±5	24±1	83±10	120±8	110±8	49±6	4±1	102±10
	2nd	47±2	28±2	13±3	23±3	70±6	53±1	22±1	0	49±1
A% (M12-50)	1st	272±6	67±5	750±12	47±11	241±7	181±20	212±4	450±6	287±12
	2nd	172±3	21±3	185±4	13±3	131±4	36±2	77±4	0	124±4

Ashing Conditions - Time: 1 minute
Temperature: 400^{o}C in a Furnace
Direction - Toward the window of the optics system.

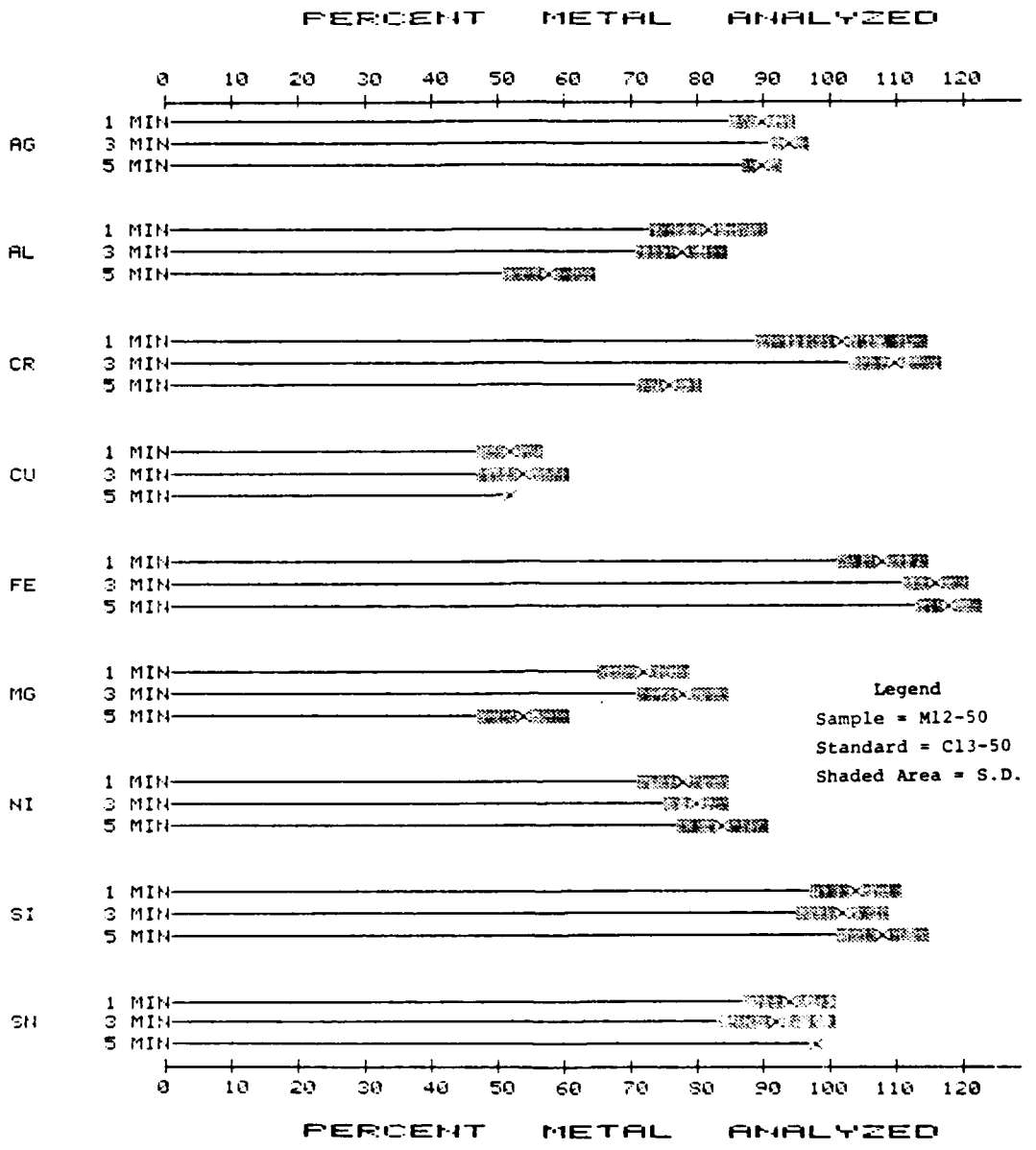

Figure 34. The Effects of Acid Dissolution Time (Minutes) on the Percent Metal Analyzed by the AD-STRM.

AD-A150 139 SAMPLE INTRODUCTION METHODS FOR IMPROVING THE PARTICLE 2/2
DETECTION CAPABILI..(U) DAYTON UNIV OH RESEARCH INST
W E RHINE ET AL. 04 JAN 85 UDR-TR-84-37 NAEC-92-185
UNCLASSIFIED N68335-83-C-0625 F/G 20/6 NL

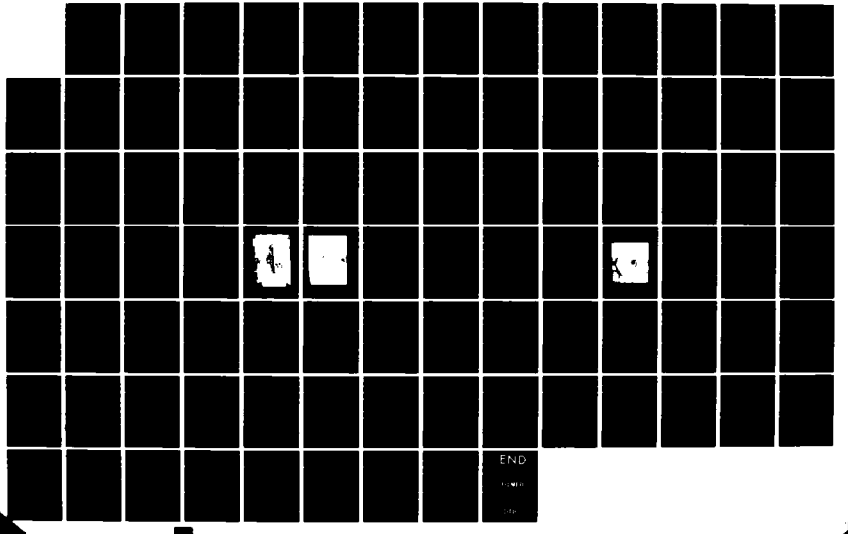

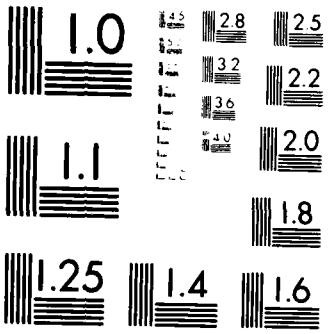

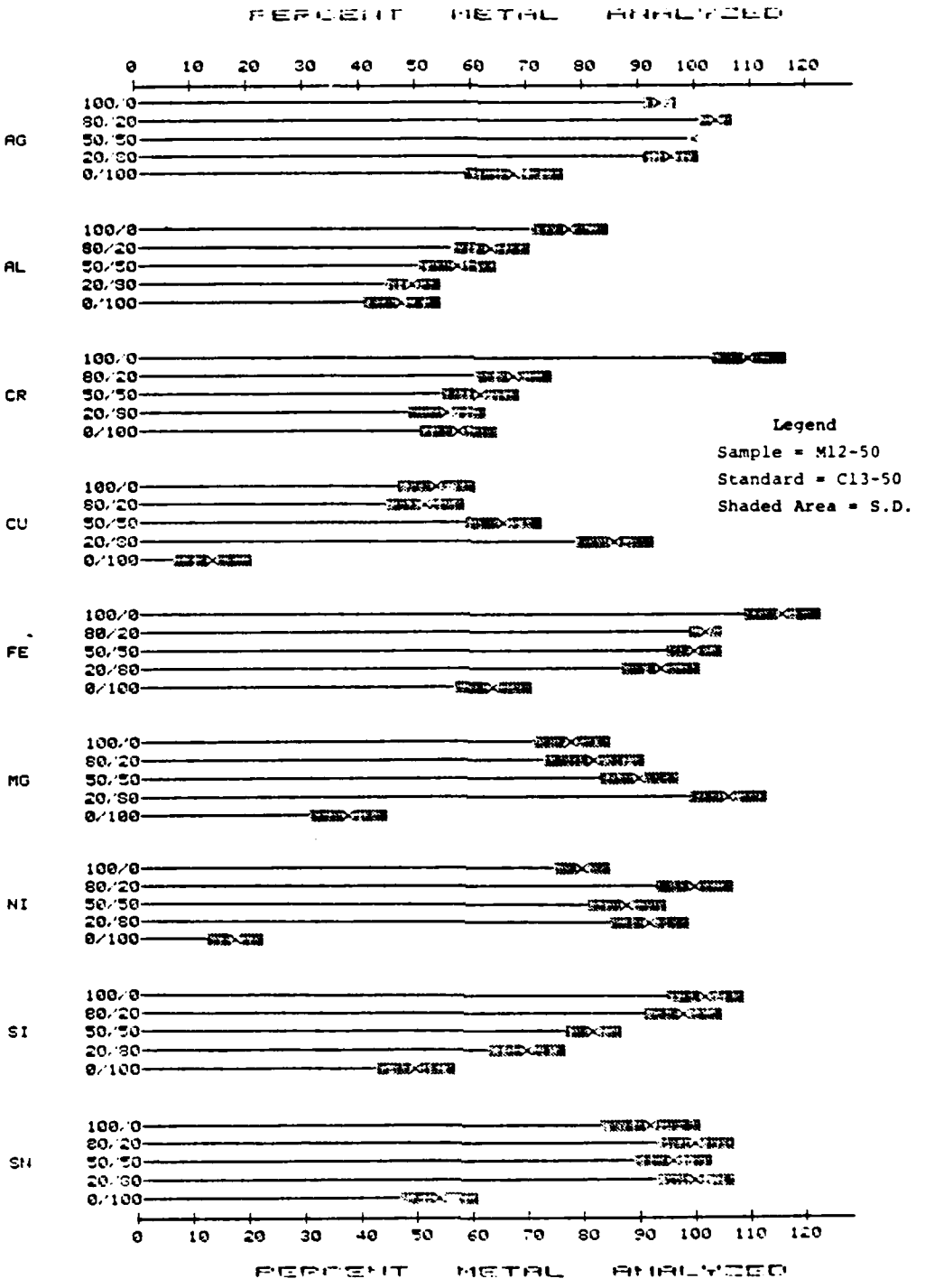

Figure 35. The Effects of the 1:8:1/Dodecylbenzene Sulfonic Acid Ratio on the Percent Metal Analyzed by the AD-STRM.

compounds soluble. To determine the effects of the amine sulfonate stabilizer on the analytical results of the AD-STRM a 10 percent solution of amine sulfonate stabilizer in Neodol 91-8 was used to solubilize the acid/oil mixture prior to ashing. As seen in Table 21, the presence of amine sulfonate increases the emission readouts for all the metals in the C13-50 standard, except for Cu. The addition of the amine sulfonate improved the agreement between the emission readouts for the M12-50 suspension and C13-50 standard for every metal tested, except for Al.

6. COMPARISON OF THE DEVELOPED STRM AND AD-STRM RESULTS.

a. The ultimate goal of this investigation is to develop methods capable of making the wear metal analyses of the A/E35U-3 spectrometer particle size independent. For this reason, a multielement MIL-L-23699 oil suspension containing Ag, Al, Cr, Cu, Fe, Mg, Mo, Ni, Pb, Si, Sn, and Ti metal powders with maximum sized particles of approximately 44 μm was used to optimize and evaluate the capabilities of the different spark-to-residue methods.

b. The percents metal analyzed for the optimized spark-to-residue ashing methods (STRM) are listed in Table 22. Although the percents metal analyzed by the STRM are much better than those obtained by direct RDE analysis on the A/E35U-1 spectrometer, the STRMs are dependent on sample differences and give superficially high values for most of the metal particles suspended in MIL-L-23699 oils.

c. The enhanced analyses for particles are caused by the fact that the metal particles and Conostan standards behave differently in the spark source. Although the percent metal recoveries are enhanced by shorter burn times and by the 160° electrode, the effects of the other factors studied depended on the type of lower electrode used and the metal being analyzed. Of the electrodes tested the highest percent metal recoveries for all the metals studied were produced by the RDE, followed by the RSE, and then the RPE. In previous research, the RDE was also found to produce higher percent metal recoveries than the RPE [reference (g)].

d. To eliminate the particle size dependence of the STRM analyses, acid dissolution of the particles prior to ashing was used and is referred to as the acid dissolution/spark-to-residue method (AD-STRM). The 1:8:1 acid solution was used because previous research has shown that the 1:8:1 acid solution completely dissolved all of the metal particles present in the multielement suspension. As the data in Table 22 indicates the AD-STRM produced superficially high metal recoveries for many of the metals analyzed which resulted from poor agreement between the emission readouts for the M12-50 suspension and the C13-50 standard. Addition of the amine sulfonate stabilizer prior to analysis was found to improve the agreement between the C13-50 standard and M12-50 suspension for the AD-STRM and 100±5 percent metal recoveries were obtained for all metals except Al and Sn.

TABLE 21. THE EFFECTS OF AMINE SULFONATE STABILIZER ON THE ANALYTICAL RESULTS OF THE AD-STRM

	Solubilizer	Ag	Al	Cr	Cu	Fe	Mg	Ni	Si	Sn
Readout (C13-50)	Neodol 91-8	100±8	42±1	82±12	134±14	97±10	88±4	76±6	39±9	150±25
	Neodol 91-8+AS*	142±2	78±10	114±10	109±3	130±8	125±73	100±8	58±10	190±10
A% (M12-50)	Neodol 91-8	112±4	112±1	124±8	67±14	124±12	124±4	134±6	120±7	134±16
	Neodol 91-8+AS*	102±2	74±10	103±8	105±2	95±9	98±6	101±5	102±5	119±8

*AS - Amine Sulfonate
Reaction Conditions - Acid Type: 1:8:1
Time: 3 minutes
Ashing Conditions - Time: 1 minute
Temperature: 400°C in a Furnace

TABLE 22. SUMMARY OF METHODS USED TO ANALYZE M12-50 SUSPENSIONS ON THE A/E35U-1 SPECTROMETER

	Percent Metal Analyzed								
Method	Ag	Al	Cr	Cu	Fe	Mg	Ni	Si	Sn
RDE-Direct	50	35	50	2	40	55	9	10	40
RPE-STRM[a]	82	71	76	89	233	76	46	66	208
RDE-STRM[b]	191	52	240	115	240	112	130	150	290
RSE-STRM[c]	152	44	317	76	225	108	90	150	165
AD-STRM[d]	112	112	154	67	142	114	134	120	134
AD-STRM[e]	102	74	103	105	95	98	101	102	119

[a] 160^{o} Counter-electrode - BCI 100 MD-X (RPE) - Position D - One rotation - Ashed at $400^{o}C$ for 1 minute.
[b] 160^{o} Counter-electrode - BCI 100 HD (RDE) - Rotated counterclockwise 3 times - Ashed at $600^{o}C$ for 1 minute.
[c] 160^{o} Counter-electrode - Moved away from optics window into spark - Ashed at $400^{o}C$ for 1 minute.
[d] Dissolution with 1:8:1 acid method for 3 minutes at $65^{o}C$ - 160^{o} Counter-electrode - RPE - Ashed at $400^{o}C$ for 1 minute.
[e] Same as (d) except amine sulfonate stabilizer added before ashing.

D. DEVELOPMENT OF A SPARK-IN-VAPOR METHOD.

1. INTRODUCTION.

a. A technique with the potential of eliminating the particle detection limitations of the RDE-SSAE spectrometers is termed the spark-in-vapor method (SIVM). The SIVM involves the direct deposition of the oil sample onto an electrothermal atomization device (eliminating particle transport limitations), followed by sequential vaporization of the oil and metal species. As the metal vapor is produced, it is carried by a gas stream into the source for analysis. By vaporizing the oil prior to analysis of the metal species, the efficiency of spark source should be increased. Vaporizing the metal species from the atomization device into the spark source, should also increase the efficiency of the spark source, since the spark is required only for excitation of the vaporized metal species.

b. Electrothermal atomization devices which have been used for the atomic absorption and atomic fluorescence spectrometric analyses of trace metals in lubricating oils include tantalum ribbons [reference (s)], carbon rods [references (t)-(x)], and furnaces [reference (f)]. All of the reported combinations of electrothermal atomizer-emission spectrometric analytical

---

Ref: (s) Wynn, T. F.; et al. "Wavelength-Modulated, Continuum-Source Excited Atomic Fluorescence Spectrometric System for Wear Metals in Jet-Engine Lubricating Oils Using Electrothermal Atomization". Anal. Chim. Acta, V. 124, P. 155, 1981.

(t) Chuang, F.S. and Winefordner, J. P. "Jet Engine Oil Analysis by Atomic Absorption Spectrometry with Graphite Filament". Appl. Spectrosc., V. 28, P. 215, 1974.

(u) Hall, G.; Bratzel, M. P.; and Chakrabarti, C. L. "Evaluation of a Carbon-Rod Atomizer for Routine Determination of Trace Metals by Atomic-Absorption Spectroscopy: Applications to Analysis of Lubricating Oil and Crude Oil". Talanta, V. 20, P. 755, 1973.

(v) Patel, B. M. and Winefordner, J. D. "Graphite Rod Atomization and Atomic Fluorescence for the Simultaneous Determination of Silver and Copper in Jet Engine Oils". Anal. Chim. Acta, V. 64, P. 135, 1973.

(w) Reeves, R. D.; et al. "Determination of Wear Metals in Engine Oils by Atomic Absorption Spectrometry With a Graphite Rod Atomizer". Anal. Chem., V. 44, P. 2205, 1972.

(x) Reeves, R. D.; Molnar, C. J.; and Winefordner, J. D. "Rapid Atomic Absorption Determination of Silver and Copper by Sequential Atomization From a Graphite Rod". Anal. Chem., V. 44, P. 1913, 1982.

techniques used to analyze trace metals in liquid samples employed either an inductively coupled plasma or a microwave induced plasma source and none of these techniques have been used to analyze trace metals in lubricants.

c. Therefore, research was conducted to develop a SIVM applicable to the spark source spectrometers and capable of producing quantitative analyses for Ag, Al, Cr, Cu, Fe, Mg, Mo, Ni, Pb, Sn, and Ti wear metal particles in used MIL-L-23699 lubricating oil samples. To develop the optimum SIVM, the effects of the composition and configuration of the electrothermal atomizing device, ashing and atomizing conditions, composition and flow rate of the inert gas atmosphere, atomizing chamber configuration, sample size, electrode configuration, and particle size distribution of the metal powder on the percent metal recoveries of the A/E35U-1 spectrometer were studied. Initial investigations of interelement and matrix effects on the analytical results of the SIVM were also carried out. The developmental research of the SIVM was performed on the A/E35U-1 spectrometer due to the numerous modifications in the source stand required by the research.

2. EFFECT OF ELECTROTHERMAL ATOMIZER TYPE.

a. Introduction.

(1) The most common of the electrothermal atomizers include furnaces, rods, and metal strips (see Bibliography). However, these types of electrothermal devices require up to several kilowatts of power to achieve temperatures in the range of 2,500°-3,000°C. Due to the inefficient transfer of electrical energy into thermal energy, shielding or precise circuit designs are required to minimize the electromagnetic radiation produced by the dissipated electrical energy. Also the bulk and electrical requirements of the atomizer power supplies as well as the cooling requirements of the atomizer holders reduce the potential of electrothermal devices as techniques which could be easily incorporated into the A/E35U-3 spectrometer.

(2) In contrast to the furnaces, rods, and metal strips, atomizers constructed from graphite braids [references (y) and (z)], graphite square

---

Ref: (y) Alder, J. F. and West, T. S. "Atomic Absorption and Fluorescence Spectrophotometry with a Carbon Filament Atom Reservior: Part IX. The Direct Determination of Silver and Copper in Lubricating Oils". Anal. Chim. Acta, V. 58, P. 331, 1972.

(z) Everett, G. L.; West T. S.; and Williams, R. W. "The Determination of Manganese in Lubricating Oils by Carbon Filament Atomic Absorption Spectrometry". Anal. Chim. Acta, V. 70, P. 204, 1974.

weave tapes, and tungsten filaments [references (aa) and (bb)] require much lower electrical power (less than 500 watts) to reach >2,500°C temperatures and their holders do not require cooling systems. Therefore, this investigation was limited to the study of these low power, electrothermal atomizing devices.

b. Graphite Braid Atomizer.

(1) The graphite braid atomizer was first studied inside the atomization chamber illustrated in Figure 7. A 4-inch portion of the graphite braid was threaded through the hole in the center of each graphite plug which was then fitted over the ends of the atomization chamber. A 20 µl blank oil sample was then deposited onto the braid through the reduced neck of the atomizer chamber. A flow rate of 2.0 l/min. of argon was established through the atomization chamber and the 10 amp variable transformer was set to 10 percent. Upon turning the variable transformer on, the oil began to ash immediately without a change in the appearance of the braid. After approximately eight seconds the evolution of the white smoke ceased and the braid emitted a slight, reddish glow. However, when this system was placed inside the analysis chamber of the A/E35U-1 spectrometer, the electronics of the A/E35U-1 spectrometer were effected to the extent that the preburn period of the burn cycle became greater than 20 seconds and had to be terminated by pressing the reset button.

(2) Therefore, the graphite braid was studied inside the atomization chamber of design a (Figure 8). The graphite braid was cut to a 1 1/4 inch length. The ends of the braid were positioned between two 1/4 inch squares of 1 mil tantalum foil which were spot welded to hold the braid in place. The opposite side of the welded tantalum foil was then spot welded to the 30 mil Ni wire electrical leads. A 20 µl blank oil sample was then deposited onto the braid. The top portion of the chamber was fitted onto the lower portion and a flow rate of 2.0 l/min. of argon established through the system. Again, a 10 percent setting was used to ash the oil in approximately 8 seconds.

(3) The atomization system was then placed inside the analysis chamber of the A/E35U-1 spectrometer and the electrode gap set. With the hood removed from the optics system window, the spectrometer functioned correctly and produced a total burn cycle of 25 seconds. The diameter of the spark source was decreased by the flow of argon into a well-defined column between the tip of the boiler cap electrode and the center of the 160° upper electrode. When the flow of argon was stopped the spark scattered and covered the entire surfaces of both electrodes.

Ref: (aa) Dodge, W. B. and Allen, R. O. "Trace Analysis by Metastable Energy Transfer for Atomic Luminescence". Anal. Chem., V. 53, P. 1279, 1981.

(bb) Williams, M. and Piepmeir, E. H. "Commercial Tungsten Filament Atomizer for Analytical Atomic Spectrometry". Anal. Chem., V. 44, P. 1342, 1972.

(4) When the 10 amp variable transformer was turned up to approximately 20 percent, the current of the circuit exceeded 12 amps blowing the fuse of the 10 amp variable transformer. The 10 amp variable transformer was replaced by a 22 amp variable transformer. Upon turning the 20 amp transformer to 20 percent, the braid became white hot and Al, Fe, and Si were detected by the A/E35U-1 spectrometer. After three to five cleaning cycles (turning the transformer up to 20 percent for 5 seconds), the Al, Fe, and Si signals fell below the detection limits of the A/E35U-1 spectrometer.

(5) Samples (20 µl) of the C12-50 multielement standard and M12-50 multielement suspension were then analyzed using the same ashing procedure. As seen in Table 23, the temperature of the graphite braid atomizer is sufficient to atomize all of metals of interest and the emission signals of the dissolved metallo-organic standard and metal particle suspension are similar except for Cr, Ni, and Si. However, after a sample was analyzed, a second and third analysis of the graphite braid produced emission signals for Cr, Fe, and Ni. When a higher setting of the variable transformer was used, the current of the circuit exceeded 25 amps and blew the fuse of the 22 amp transformer.

(6) Although a power supply capable of currents over 25 amps would be expected to enable the carbon braid atomizer to completely atomize any metal species present, the previously discussed problems of using high power electrothermal atomizers would be of increasing concern. Also, increasing the temperature of the braid atomizer would substantially reduce its life. It has been reported [reference (cc)] that increasing the operating temperature of the braid atomizer from 1,500° to 2,000°C decreases its life from 228 to 60 analyses. The braid atomizer's life was less than 30 analyses at the 20 percent setting. Therefore, other low power atomizers were investigated.

c. Graphite Square-Weave Tape Atomizer.

(1) The graphite square-weave tape atomizer was studied inside the atomizer chamber of design a (Figure 8). The graphite square-weave tape was cut lengthwise and widthwise to produce atomizers of 1/2 inch width and 1 1/4 inch length. The tape was folded lengthwise and the ends placed between two 1/4 inch x 1/4 inch tantalum (1 mil) squares which were then spot welded together to hold the tape in place. The tantalum foil was then spot welded to the 30 mil Ni electrical leads. The atomizer produced in this manner is shown in Figure 36 and produced a furnace-like environment for the atomization process.

Ref: (cc) Montaser, A.; Goode, S. R.; and Crouch, S. R. "Graphite Braid Atomizer for Atomic Absorption and Atomic Fluoresence Spectrometry". Anal. Chem., V. 46, P. 599, 1974.

TABLE 23. THE A/E35U-1 EMISSION READOUTS OF THE SIVM WITH THE GRAPHITE BRAID ATOMIZER

	Repetitive Analysis	Ag	Al	Cr	Cu	Fe	Mg	Ni	Si	Sn
C12-50	1	159±6	60±5	46±15	125±9	135±10	145±1	81±10	90±15	170±7
	2	--*	2±1	10±3	--	41±6	--	15±4	--	--
	3	--	--	5±3	--	10±5	--	4±3	--	--
M12-50	1	180±10	88±10	20±8	138±8	109±15	137±7	44±9	50±8	186±9
	2	--	--	8±4	--	33±5	--	10±3	--	--
	3	--	--	2±1	--	8±3	--	8±2	--	--

*Below A/E35U-1 Detection Limits
Ashing Conditions - Time: 8 seconds
Voltage Setting: 10% of 115V (22 amp, 115V transformer)
Atomizing Conditions - Time: 5 seconds
Voltage Setting: 20% of 115V (22 amp, 115V transformer)
Argon Flow Rate - 2.0 l/min.

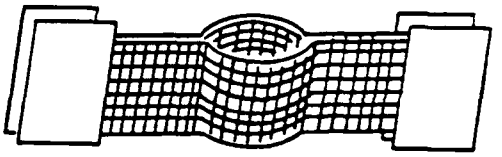

Figure 36. Graphite Square-Weave Tape Atomizer.

(2) A 20 µl sample of blank oil was deposited into the center of the atomizer. The top portion of the atomizer chamber was then fitted onto the bottom half, and a flow rate of 2.0 l/min. of argon was established through the system. The 22 amp variable transformer was set to 10 percent. Upon turning the transformer on, the oil began to ash immediately without a change in the appearance of the tape. After approximately 10 seconds the evolution of the white smoke ceased and the tape emitted a slight, reddish glow which was not as uniform as the glow from the graphite braid atomizer. The glow from the intersections of the graphite threads was less intense than the threads themselves.

(3) The system was then placed inside the analysis chamber for the A/E35U-1 spectrometer. The appearance of the spark source and the burn time (25 seconds) were the same as with the carbon braid atomizer. Upon turning the variable transformer to 20 percent the tape atomizer became uniformally white hot and Al, Fe, and Si were detected by the A/E35U-1 spectrometer. After two to three cycles (turning the transformer up to 20 percent for 5 seconds), the Al, Fe, and Si signals fell below the detection limits of the A/E35U-1 spectrometer.

(4) Samples (20 µl) of the C12-50 multielement standard and M12-50 multielement suspension were then analyzed using the same procedure. The results listed in Table 24 show that the graphite square-weave tape atomizer's temperature is adequate to atomize all of the metals of interest. However, the emission signals of the metallo-organic standard and metal particle suspension are lower in value and in less agreement than those produced by the graphite braid atomizer. For each metal the particles produced higher emission readouts than the metallo-organic standard.

(5) As with the graphite braid atomizer, a second and third analysis of the same sample using the tape atomizer produced emission signals for Cr, Fe, and Ni. The variable transformer was turned up to 24 percent, but Cr and Fe emission signals were still present for the second and third analyses. Turning the setting of the variable transformer past 24 percent

TABLE 24. THE A/E35U-1 EMISSION READOUTS OF THE SIVM WITH THE GRAPHITE SQUARE-WEAVE TAPE ATOMIZER

	Repetitive Analysis	Ag	Al	Cr	Cu	Fe	Mg	Ni	Si	Sn
C12-50	1	78±11	32±6	28±2	27±1	80±9	58±7	28±7	15±1	47±1
	2	--*	--	10±5	--	18±8	--	7±3	--	--
	3	--	--	7±4	--	2±1	--	4±1	--	--
M12-50	1	84±10	76±9	34±3	62±4	124±8	106±7	42±8	41±5	107±6
	2	--	--	8±4	--	19±8	--	1±1	--	--
	3	--	--	5±6	--	8±5	--	--	--	--

*Below A/E35U-1 Detection Limits
Ashing Conditions - Time: 10 seconds
Voltage Setting; 10% of 115V (22 amp, 115V transformer)
Atomizing Conditions - Time: 5 seconds
Voltage Setting: 20% of 115V (22 amp, 115V transformer)
Argon Flow Rate - 2.0 l/min.

blew the fuse of the transformer. Also, the life of the graphite square-weave tape atomizer was shortened from 20 analyses (20 percent) to less than 10 analyses when the setting of the variable transformer was increased to 24 percent. Therefore, increasing the temperature of the atomizer to eliminate the residual metal species would shorten the graphite square-weave tape atomizer's life to the point that its use would be impractical for routine analysis.

d. Tungsten Filament Atomizer.

(1) The last electrothermal atomizers to be studied were prepared using the tungsten filaments obtained from 115V-100, 200, and 300 watt incandescent light bulbs. A package of the 200 watt filaments was also obtained separately. The tungsten filaments were tested in the atomization chamber of design a (Figure 8). The filaments were supported by clamping their ends with mini-alligator clips which were attached to the 30 mil Ni electrical leads.

(2) A 20 µl blank oil sample was then deposited onto the tungsten atomizer, the top portion of the chamber was fitted onto the lower half, and a flow rate of 2.0 l/min. of argon established through the closed atomization chamber. The oil sample distributed itself inside the coil of the tungsten filament enabling the 100, 200, and 300 watt tungsten filaments to support up to approximately 15, 30, and 50 µl of oil, respectively.

(3) The 10 amp variable transformer was set to 10 percent. Upon turning the transformer on, the portion of the filament not covered with oil began to emit a slight, reddish glow and the oil started to ash without a change in appearance of the rest of the oil-coated filament. After approximately eight seconds the evolution of the white smoke ceased and the entire filament emitted a slight reddish glow.

(4) The atomization system was placed inside the analysis chamber of the A/E35U-1 spectrometer. When the 10 amp variable transformer was turned up to approximately 60 percent, the filament became white hot and Fe was detected by the A/E35U-1 spectrometer. It is assumed that the atomized impurity was tungsten oxide which has a spectral line at 2598.7Å which interferes with the Fe line at 2599.4Å used by the A/E35U-1 spectrometer. Only one cleaning cycle at a transformer setting of 60 percent for 2 seconds is needed to reduce the emission signal of Fe below the detection limit of the A/E35U-1 spectrometer.

(5) Samples (20 µl) of the C12-50 multielement standard and M12-50 multielement suspension were then analyzed by the same procedure using the 200 watt filament. The data listed in Table 25 indicates that the temperature of the tungsten filament atomizer is adequate to atomize all of the metals of interest. Also, except for Cu, Fe, Si, and Sn, the emission signals of the dissolved metallo-organic standard and metal particle suspension are similar. In contrast to the graphite braid and square-weave tape atomizers, a second analysis of the tungsten filament produced emission signals below the detection limits of the A/E35U-1 spectrometer for all the metals analyzed.

TABLE 25. THE A/E35U-1 EMISSION READOUTS OF THE SIVM WITH THE 200 WATT TUNGSTEN FILAMENT ATOMIZER

	Ag	Al	Cr	Cu	Fe	Mg	Ni	Si	Sn
C12-50	70±4	110±4	80±1	52±4	104±7	67±8	105±8	42±3	156±8
M12-50	78±3	111±1	75±9	89±4	139±9	70±5	90±5	79±1	225±10

Ashing Conditions - Time: 8 seconds
Voltage Setting: 10% of 115V (10 amp, 115V transformer)
Atomizing Conditions - Time: 3 seconds
Voltage Setting: 60% of 115V (10 amp, 115V transformer)
Argon Flow Rate - 2.0 l/min.

The 200 watt tungsten filament atomizer could atomize approximately 20 samples at the 60 percent setting before disintegrating. Similar results were obtained for the 100 and 300 watt filament atomizers.

e. Comparison of Electrothermal Atomizer Types.

(1) Of the three atomizers studied, the tungsten filaments have the best potential for development into a SIVM suitable for the A/E35U-3 spectrometer. They require only one cleaning cycle, provide complete atomization of the metals studied, can be controlled by a 115V-10A variable transformer, and have lives of approximately 20 analyses at 60 percent power. Since a transformer setting of 60 percent is sufficient to atomize all of the metals of interest and the filaments can be used up to 100 percent power (2900°C), they should be capable of completely atomizing titanium and molybdenum.

(2) The graphite braid and square-weave tape atomizers are incapable of atomizing titanium or molybdenum unless used with high (>25 amp) current power supplies. Another advantage of the tungsten filaments is that due to their low mass and low current requirements, they heat the atomizer support system to a much lesser degree than the graphite atomizers. For these reasons, the tungsten filament atomizers were used for the rest of the study.

3. EFFECTS OF THE ASHING CONDITIONS.

a. Introduction. The ashing conditions studied in this investigation were ashing temperature, ashing time, gas flow rate, sample size, and atomizing chamber configuration. Unless stated otherwise, the investigations were carried out using the 200 watt filament in an argon atmosphere and the atomizing chamber design a (Figure 8). The 200 watt filament was used for this study because it held more sample than the 100 watt filament, was less rigid (easier to use), and required less current than the 300 watt filament. The larger sample capability of the 300 watt filament was not needed due to the good sensitivity of the SIVM.

b. Effect of Ashing Temperature.

(1) Due to the size of the filament and the lack of temperature measuring equipment, a temperature calibration could not be performed at the time of the study. The settings of the variable transformer were used as reference points for comparing the results. The ashing conditions were studied for transformer settings between 3 and 20 percent.

(2) The lowest setting at which the ashing could be accomplished was 5 percent. At this setting the ashing step required 30 seconds to complete. At a setting of 15 percent, the temperature of the filament rose too quickly and caused the oil to "explode" off the filament without ashing. At settings above 8 percent, the subsequent Si analyses for the metallo-organic standard were reduced and less reproducible in comparison to the Si analyses performed after the oil was ashed at settings between 5 to 8 percent. The subsequent analyses of the Si metallic particles were not affected by the

ashing temperature. At a setting of 8 percent the ashing step required approximately 8 seconds as compared to 30 seconds at 5 percent. Therefore, a setting of 8 percent was used for the ashing step in the subsequent studies.

c. Effect of Ashing Time. The effect of ashing time on the subsequent analytical results were studied for ashing times of 8-30 seconds. Again only the analytical results of the Si metallo-organic standard were affected by extended ashing times. The emission readouts of the Si standard decreased for ashing times greater than 12 seconds. An ashing time of eight seconds was used during the development of the SIVM in order to keep the total time required as short as possible.

d. Effect of Argon Gas Flow Rate. The effect of argon flow rate on the ashing time of the SIVM was studied between argon flow rates of 0.2-3.4 l/min. At an argon flow of 0.2 l/min., the ashing time increased to approximately 30 seconds, because the oil ashed faster than the argon could flush it out of the atomizing chamber allowing the chamber to fill up with the white smoke. Also, the ashed oil began to condense on the chamber's walls at the 0.2 l/min. argon flow rate. At flow rates above 1.5 l/min., the ashing time remained at approximately 8 seconds. In order to conserve argon, all further ashing studies were conducted using a flow rate of 1.5 l/min.

e. Effect of Sample Size. The effect of sample size on the ashing time of the SIVM was studied using sample sizes between 7.5 and 30 µl. Although the sample ashed smoothly regardless of the sample amount, the ashing time increased with sample size. The ashing time increased from approximately 8 to 20 seconds when the sample size was increased from 7.5 to 30 µl. At sample sizes above 25 µl, the ashed oil began to condense on the chamber walls. Since the SIVM is being developed for the analysis of particles, larger samples will be more representative of the oil being analyzed. Therefore, the sample size used was 20 µl, even though the ashing time was slightly longer than that obtained with the 7.5 µl sample.

f. Effect of Atomizing Chamber Configuration.

(1) To study the effect of atomizing chamber configuration, different chamber sizes of designs a, b, and c in Figure 8 were studied. At an argon flow rate of 1.5 l/min., the oil sample was completely ashed in approximately 8 seconds regardless of the atomizing chamber size. However, at a flow rate of 0.5 l/min. only the smallest chamber size, design c, allowed the sample to be ashed in approximately 15 seconds.

(2) Therefore, the study on the effects of the experimental parameters on the ashing step of the SIVM have shown that the optimum ashing conditions are achieved by decreasing the sample size and atomization chamber while increasing the gas flow rate.

4. EFFECT OF ATOMIZING CONDITIONS.

a. Introduction. The atomizing conditions studied in this investigation were the atomizing temperature, rate of atomizing temperature rise, atomizing time, gas flow rate, sample size, atomizing chamber configuration, composition of chamber atmosphere, and electrode configuration. The initial experimental parameters used in the investigations into the effects of atomizing conditions on the analytical results of the SIVM included an argon flow rate of 1.5 l/min., 200 watt tungsten filament atomizers, and the design a (Figure 8) atomization chamber.

b. Effect of Atomizing Temperature.

(1) Voltage Settings Required for Complete Atomization.

(a) As stated before the settings of the variable transformer were used as reference points for comparing the results. A 20 µl sample was deposited onto the filament and ashed at an 8 percent setting on the variable transformer and 1.5 l/min. argon flow rate. The emission readouts of the different metals were obtained by setting the percent voltage of the variable transformer, starting the spectrometer's burn cycle, turning the transformer on for three seconds after the preburn cycle was completed, then turning the transformer off. This procedure was repeated for percent voltage settings of 8-50 percent for each sample. By a voltage setting of 46 percent all of the metals had been completely atomized.

(b) The results of the C12-50 standard and M12-50 suspension are given in Table 26. As the data in Table 26 indicates, the various metals atomize in basically three groups: Ag then Cu, Mg and Sn followed by Al, Cr, Fe, Ni, and Si.

(c) The separation of the three groups is not precise since Cr begins to atomize at the same temperature as Cu but is the last metal to be completely atomized. Also, the metallo-organic Si emission readout is affected by the temperature and time of the ashing step, as previously discussed, even though it requires one of the highest atomization temperatures. The analysis of metallic Si is not affected by the ashing temperature or time. Other than the results for Si, the temperature requirements of each metal is independent of its chemical form, i.e., the metallo-organic standard compounds and metal particles atomize in the same temperature range for each metal studied.

(2) Effect of Ramped Temperature Increase.

(a) Since the metals atomize at different temperatures, interelement effects should be minimized by increasing the filament's temperature from that required to atomize Ag to the required to atomize Fe during the 5-second atomizing step. The technique of increasing the filament's temperature during the atomizing step is termed "ramping". To determine the effect of "ramping", samples of the C12-50 standard and M12-50

TABLE 26. THE EFFECTS OF THE ATOMIZING TEMPERATURE ON THE A/E35U-1 READOUTS FOR THE SIVM

% Voltage Setting	Sample	Ag	Al	Cr	Cu	Fe	Mg	Ni	Si	Sn
8%*	C[a]	--[c]	--	--	--	--	--	--	--	--
	M[b]	--	--	--	--	--	--	--	--	--
10%	C	3	--	--	--	--	---	--	--	--
	M	5	--	--	--	--	--	--	--	--
16%	C	60	--	3	7	--	--	--	--	3
	M	54	--	6	12	--	4	--	--	6
22%	C	10	--	6	38	--	43	--	--	20
	M	4	12	8	68	8	28	--	--	36
28%	C	--	15	26	2	31	18	24	10	5
	M	--	16	26	4	29	15	28	15	7
34%	C	--	32	62	--	24	--	32	4	--
	M	--	10	26	--	10	--	10	3	--
40%	C	--	--	8	--	7	--	6	2	--
	M	--	--	6	--	--	--	2	1	--
46%	C	--	--	--	--	--	--	--	--	--
	M	--	--	--	--	--	--	--	--	--

*Transformer Setting for Ashing
[a]C12-50
[b]M12-50
[c]Below A/E35U-1 Detection Limit

suspension were analyzed. The "ramped" atomizing temperature was attained by turning the transformer on at the ashing temperature (8 percent setting) and then smoothly turning the dial by hand to the 50 percent setting during the 5 second atomizing period. The "instantaneous" atomizing temperature was attained by setting the variable transformer to 50 percent, turning the transformer on for 5 seconds, and then turning if off.

(b) The effects of the ramped and instantaneous temperature atomizing procedures on the emission readouts of the C12-50 standard and the percent metals analyzed of the M12-50 suspension are shown in Figures 37 and 38, respectively. As seen in Figure 37, ramping the atomization temperature increased the emission readouts of the C12-50 standard for all of the metals except for Cr and Si.

(c) Ramping the atomization temperature enhanced (>100 percent) the percent metals analyzed for the M12-50 suspension for Cr, Cu, Ni, Si, and Sn but decreased the percent metal analyzed for Ag, Al, Fe, and Mg (Figure 38). Ramping the atomization temperature also dramatically increased the life of the tungsten filament from 20 analyses up to >60 analyses. A negative aspect of ramping the atomization temperature was that ramping decreased the repeatibility of the SIVM (Figure 37). Whether this is due to human error or other factors cannot be determined at this time.

(3) Effect of a Two Step Temperature Increase.

(a) The main reason that ramping extended the filament's life is thought to be that gradually increasing the voltage greatly reduces the current surge caused by "instantaneously" turning the transformer on at the 50 percent setting. Although the resistance of the filament when white hot is approximately 44 ohms, the filament's resistance is only approximately 2.5 ohms at room temperature causing an initial surge of approximately 24 amps when the variable transformer is first turned on.

(b) Therefore, a two step atomization temperature increase was studied. In order to accomplish a two step temperature increase the circuit in Figure 10 was constructed. This circuit allows the filament to be heated to a preset temperature controlled by variable transformers VT1 and VT2. By closing switch S2, the filament is heated to a higher temperature controlled only by variable transformer VT1. Using this method, the current surge is minimized since the full potential is applied to a heated filament.

(c) The variable transformer (VT2) was set so that the initial atomizing step was varied from 8 percent (ashing setting) to 20 percent (Ag, Cu, Mg, and Sn atomizing temperature). After approximately three seconds, the switch (S2) was closed, which instantaneously increases the filament's temperature to above the atomizing temperature of Cr. The second step of the atomization procedure was ended after three seconds by opening switch S1.

(d) The results in Figure 39 show that the initial atomizing temperature affects the percent metal analyzed of the M12-50 suspension.

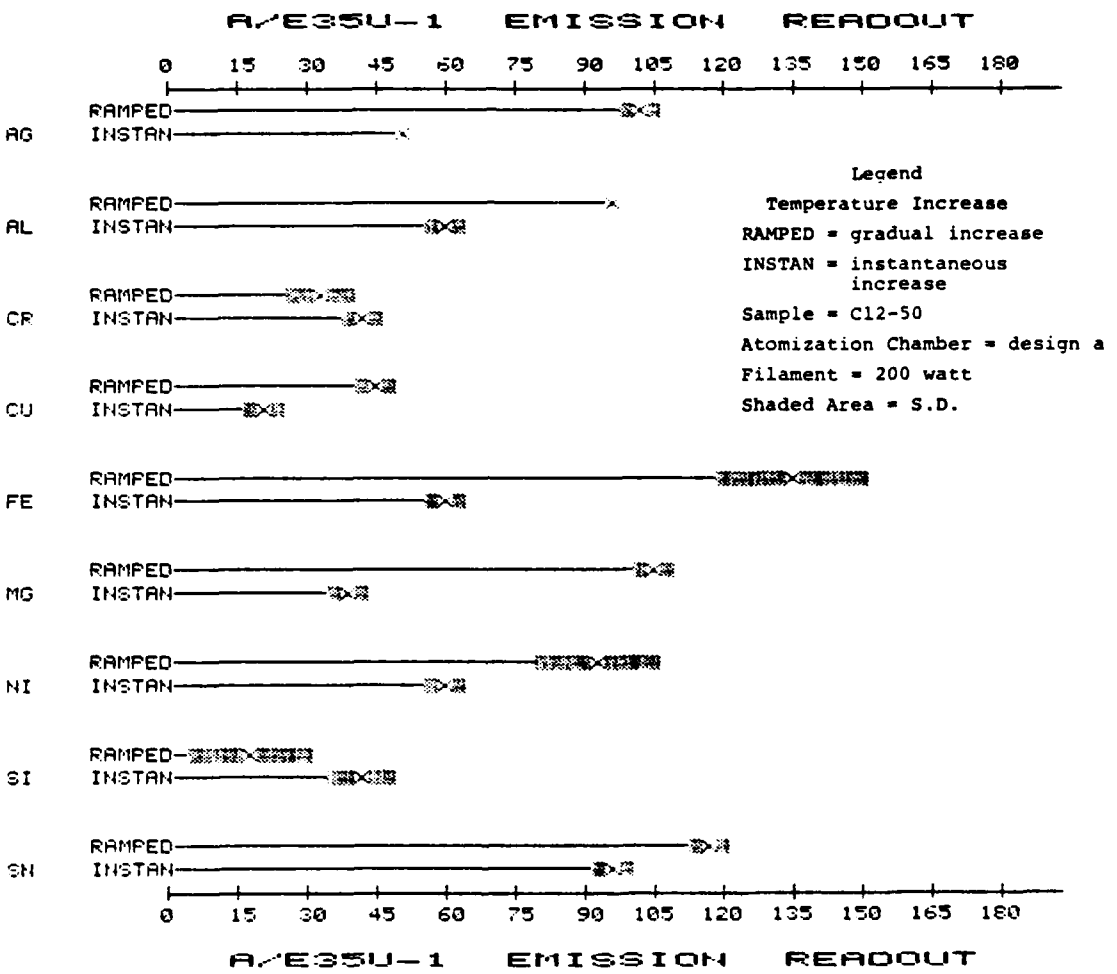

Figure 37. The Effects of Ramping the Atomization Temperature on the A/E35U-1 Readouts of the SIVM.

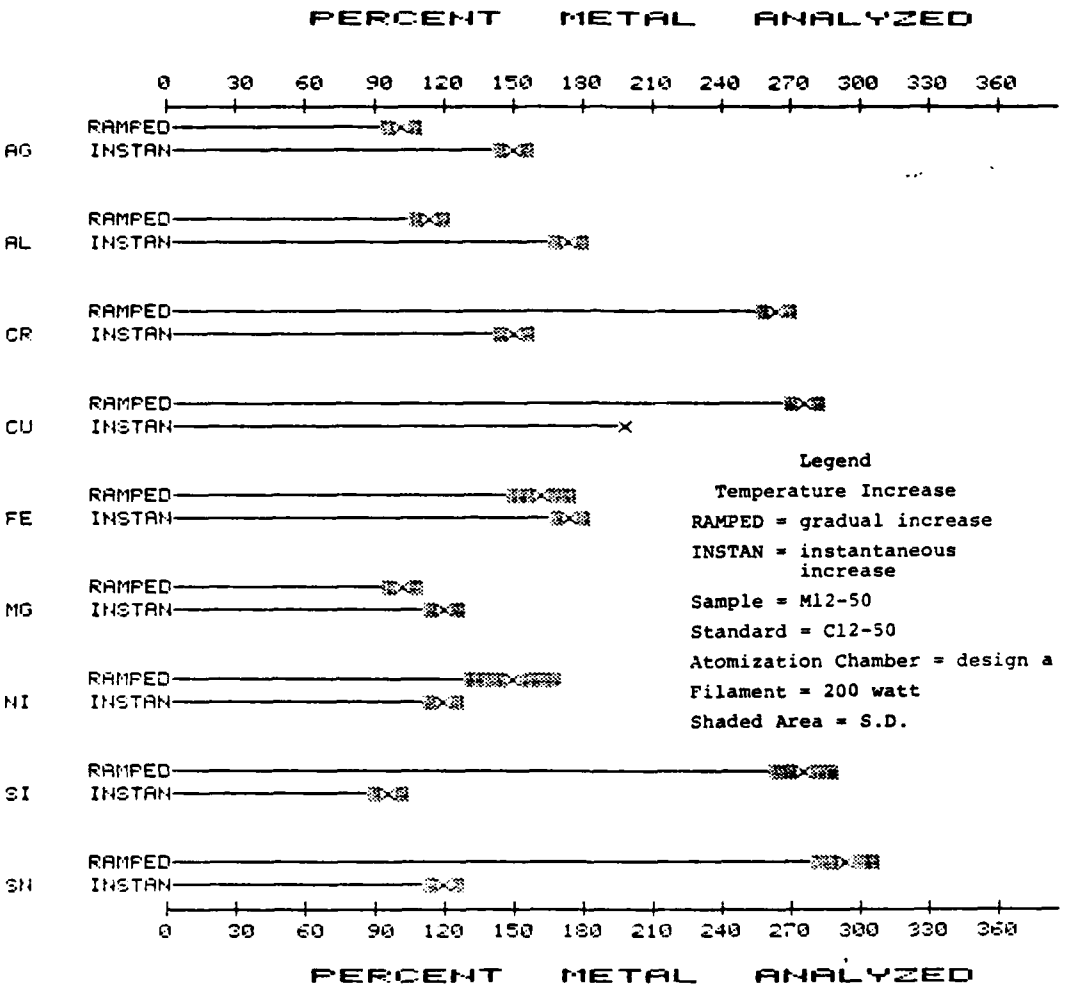

Figure 38. The Effects of Ramping the Atomization Temperature on the Percent Metal Analyzed by the SIVM.

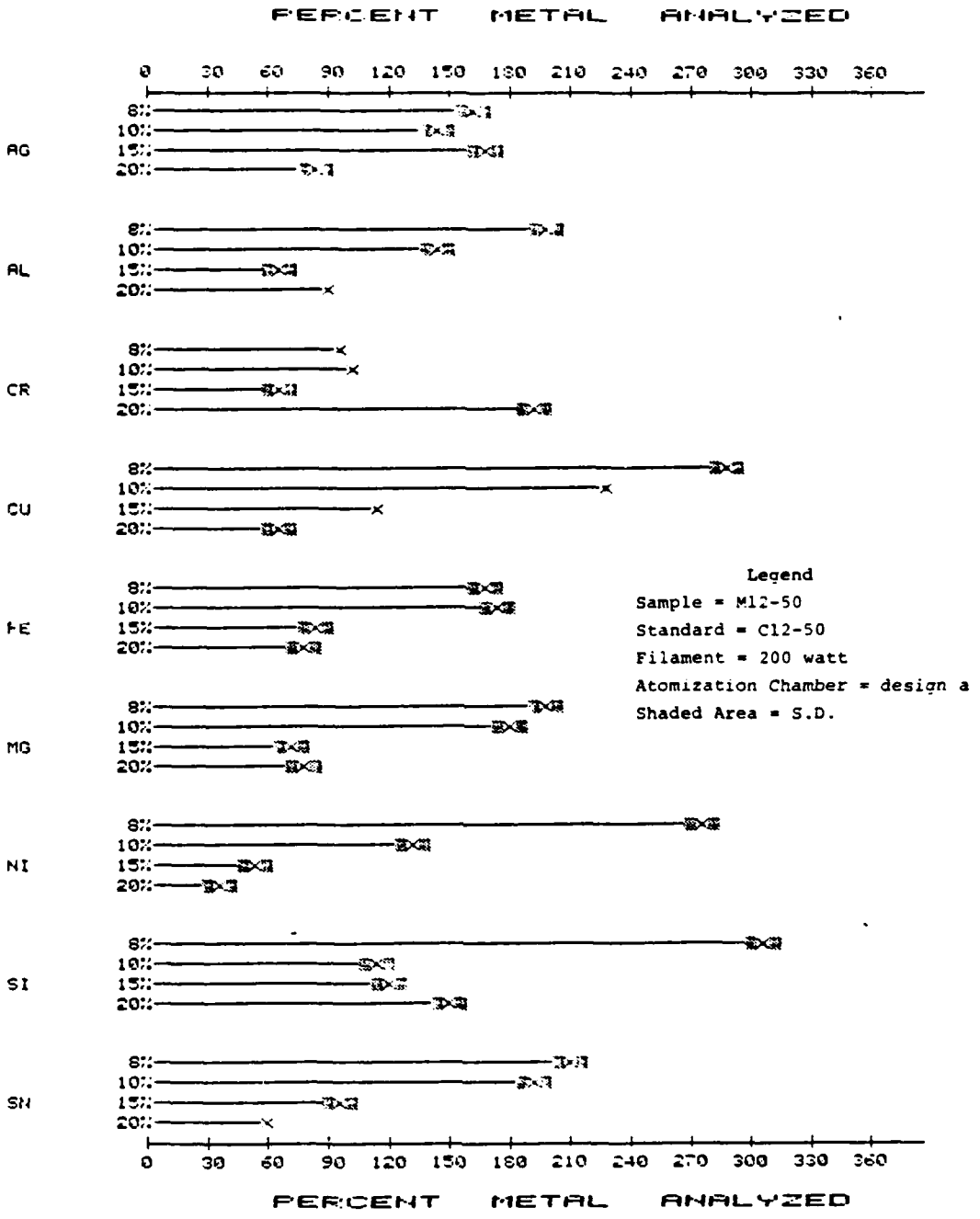

Figure 39. The Effects of the Initial Percent Voltage Setting on the Percent Metal Analyzed by the Two Step Atomization SIVM.

Except for Cr, increasing the percent setting of the initial atomization step decreased the percent metal analyzed for the M12-50 suspension. Regardless of the initial atomization temperature, the two step atomization increased the filament's life from 20 analyses (instantaneous atomization step) to 35-40 analyses.

(e) The two step atomization produced better agreement between the C12-50 standard and M12-50 suspension emission readouts than either the instantaneous or ramped atomization procedures (Figure 38). The repeatibilities for the two step atomization procedure are similar to those of the instantaneous atomization procedure (Figure 38).

c. Effect of Gas Flow Rate and Atomization Chamber Configuration.

(1) Although the two step atomization procedure improved the agreement between the emission readouts for the C12-50 standard and M12-50 suspension, the effect was dependent on the metal being analyzed. The fact that ramping the atomization temperature enhanced the emission readouts produced by the SIVM (Figure 37) implies that ramping the temperature increased the residence time of the metal vapor in the spark source resulting in higher emission readouts.

(2) Another experimental factor which has an effect on the residence time of the metal vapor in the spark source is the gas flow rate. The instantaneous atomization procedure was investigated using the three atomization chambers a, b, and c shown in Figure 8 with argon flow rates of 0.2-1.5 l/min. The A/E35U-1 emission readouts for the C12-50 standard and the percent metal analyzed of the M12-50 suspension for the different atomization chamber-argon flow rate combinations are listed in Tables 27 and 28, respectively.

(3) The results listed in Table 27 show that decreasing the argon flow rate and size of the atomization chamber increases the values and repeatibilities of the emission readouts for the C12-50 standard. As the data in Table 28 indicates, decreasing the argon flow rate and chamber size increased the agreement between the C12-50 standard and M12-50 suspension. The best results were obtained with the design c atomization chamber and an argon flow rate of 0.2 l/min. Atomization chamber design c was used for the remainder of the work unless specified otherwise.

(4) A modification of design b is shown in Figure 40 in which the argon supply tube is centered in the bottom of the chamber instead of on the side of the chamber. The design modification did not make any differences in the analytical results of the SIVM.

TABLE 27. THE EFFECTS OF THE ARGON FLOW RATE ON THE A/E35U-1 READOUTS OF THE SIVM FOR THE C12-50 STANDARD

Atomization Chamber Design *	Argon Flow Rate (l/min.)	Ag	Al	Cr	Cu	Fe	Mg	Ni	Si	Sn
a	1.5	68±3	92±8	25±1	24±2	73±2	42±4	48±3	32±3	89±4
	0.5	47±5	28±9	53±2	15±6	48±3	37±6	15±6	41±4	45±8
b	1.5	59±3	88±7	15±6	31±3	61±3	48±8	40±6	16±3	70±1
	0.5	83±2	95±4	44±3	43±4	85±3	59±7	61±7	31±5	115±4
c	1.5	50±3	69±3	8±7	20±4	49±6	32±6	21±4	8±4	65±2
	0.5	88±4	84±3	34±2	29±2	73±4	59±2	42±2	20±5	110±4
	0.2	111±3	134±5	90±1	42±6	144±3	74±3	63±4	48±5	118±5

Ashing Conditions - Time: 10 seconds
Voltage Setting: 8% (10 amp, 115V transformer)

Atomizing Conditions - Time: 3 seconds
Voltage Setting: 60% (10 amp, 115V transformer)

*a = 1.5" I.D. atomization chamber)
b = 1.0" I.D. atomization chamber) see Figure 8.
c = 0.75" I.D. atomization chamber)

TABLE 28. THE EFFECTS OF THE ARGON FLOW RATE ON THE PERCENT METAL ANALYZED BY THE SIVM FOR THE M12-50 SUSPENSION

Atomization Chamber Design	Argon Flow Rate (l/min.)	Ag	Al	Cr	Cu	Fe	Mg	Ni	Si	Sn
a	1.5	147±5	123±11	116±4	260±7	178±9	248±10	117±7	153±7	224±20
	0.5	149±6	168±13	134±6	267±8	148±7	136±12	207±8	78±6	222±14
b	1.5	148±5	126±7	133±11	167±9	164±7	162±9	120±7	250±9	257±18
	0.5	119±6	124±8	122±9	160±10	124±5	139±10	112±8	135±6	170±11
c	1.5	178±5	132±8	175±9	305±7	155±10	206±10	195±7	363±8	169±14
	0.5	99±5	119±11	144±4	238±5	141±5	120±7	152±5	195±7	136±15
	0.2	102±8	89±7	105±5	207±8	110±8	94±6	109±7	122±6	110±14

Ashing Conditions - Time: 10 seconds
Voltage Setting: 8% (10 amp, 115V transformer)
Atomizing Conditions - Time: 3 seconds
Voltage Setting: 60% (10 amp, 115V transformer)

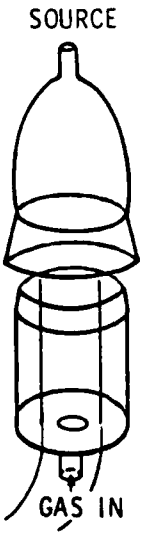

Figure 40. Modified Design b Atomization Chamber.

d. Effect of Sample Size.

(1) As indicated by the data presented thus far, the repeatibility of the SIVM is better for the C12-50 standard than for the M12-50 suspension, indicating the 20 µl is not consistently producing a representative sample of the heterogeneous M12-50 suspension. Therefore, the effects of the sample size on the repeatibility of the A/E35U-1 readouts for the M12-50 suspension were studied using sample volumes between 7.5 and 45 µl deposited on the 300 watt filament supported inside atomization chamber c. The 300 watt filament was required to support samples greater than 30 µl.

(2) The results in Figure 41 show that the standard deviations of the emission readouts for the M12-50 suspension are similar for sample sizes up to approximately 35 µl. For the 45 µl sample the repeatibility of the results decreased slightly. This decrease is most likely due to the overloading of the filament causing the oil to run off the ends of the filament when not exactly centered. As expected, the relative error decreases with increasing sample size and is approaching the specifications of the spectrometer (±10%) at sample sizes of 35-45 µl.

e. Effect of Atomization Chamber Atmosphere.

(1) Introduction. The ashing and atomizing processes as well as the stability of the spark source are affected by the gas used to transport the metal vapor from the chamber to the source. Therefore, the effects of the inert gases, nitrogen, helium, and argon, and the reactive gas, carbon dioxide, on the emission readouts of the C12-50 standard were studied.

(2) Effect of an Inert Gas Atmosphere. The effects of an inert gas atmosphere on the emission readouts of the C12-50 standard were studied using the inert gases, nitrogen, helium, and argon. As illustrated in Figure 42, nitrogen greatly reduces the emission readouts of all the metals

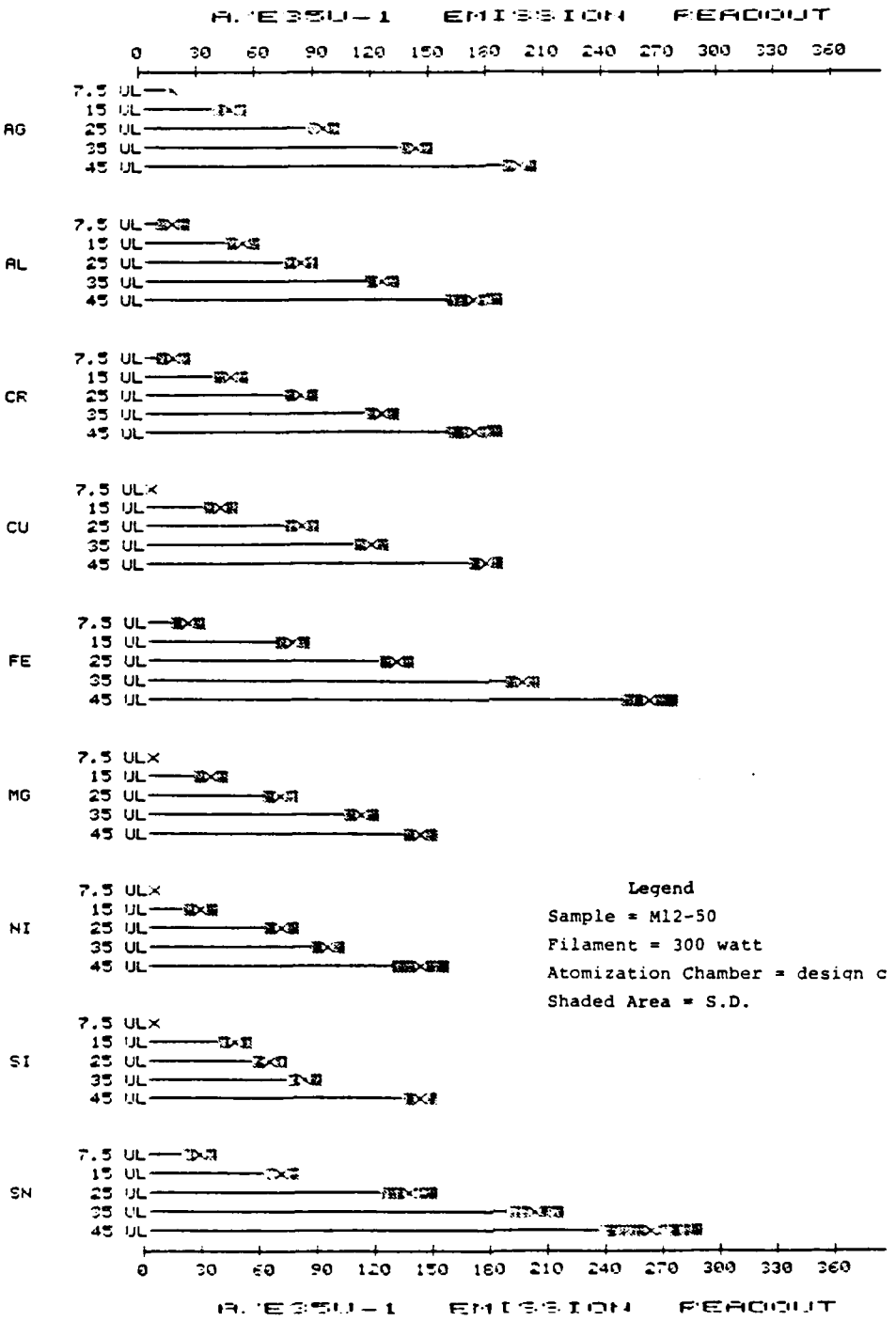

Figure 41. The Effects of Sample Size (µl) on the A/E35U-1 Readouts for the SIVM.

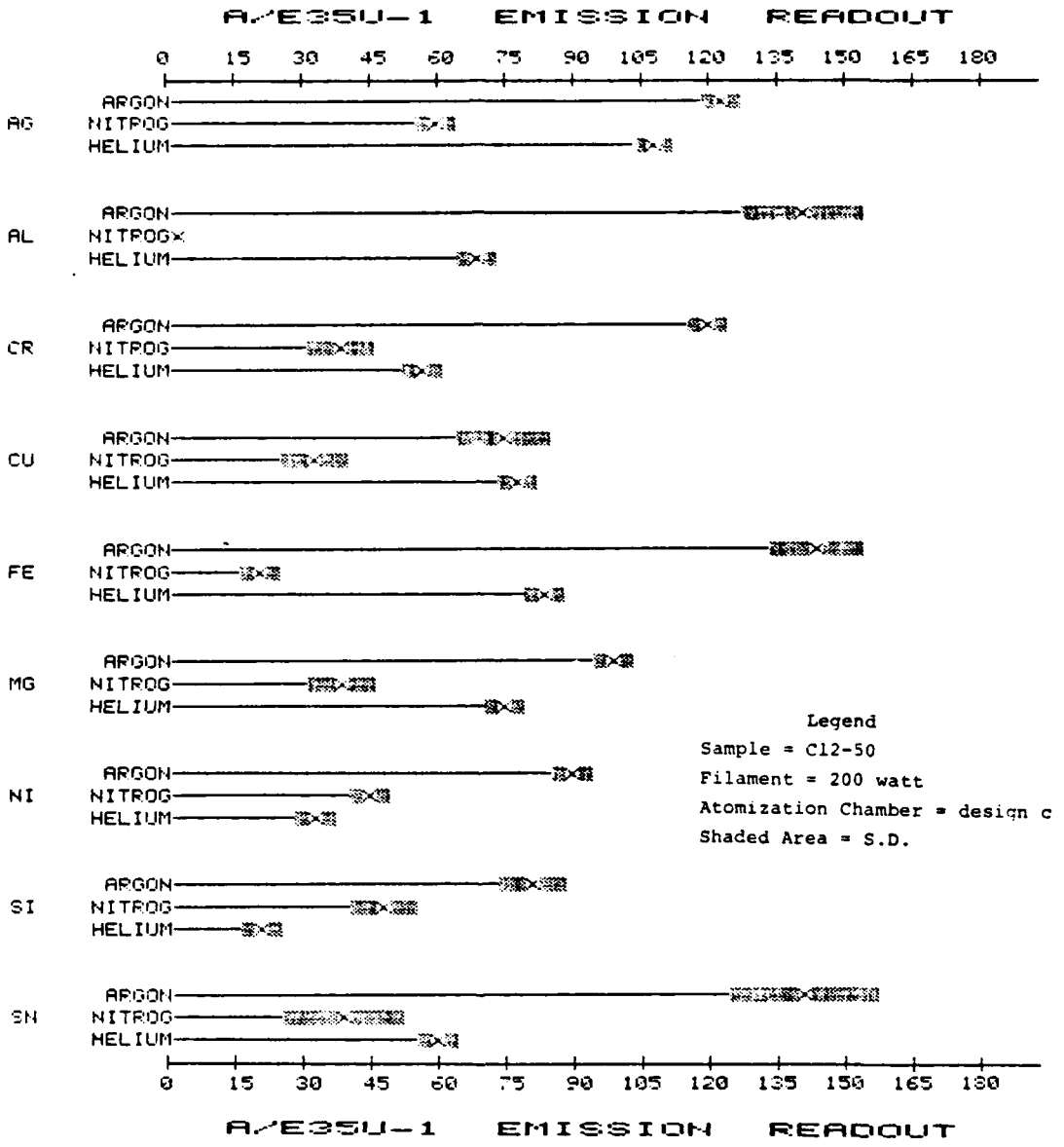

Figure 42. The Effects of Atomization Chamber Atmosphere on the A/E35U-1 Readouts for the SIVM Using Argon, Nitrogen, and Helium.

relative to the emission readouts obtained using argon. The repeatibilities of the results using helium are improved compared to those obtained using argon. One reason for the improved repeatibility of the helium results is that the blank signals of Al, Cr, Fe, Ni, and Sn are lower for helium than argon (Table 29). Therefore, it appears that background emission from argon interferes with the emission lines of Al, Cr, Fe, Ni, and Sn so that small variations in the argon gas flow will cause changes in their respective emission readouts reducing the reliability of the SIVM. Although helium produces better repeatibility, argon will be used in the SIVM due to the enhanced emission readouts obtained in argon.

(3) Effect of a Carbon Dioxide Atmosphere.

(a) A reactive gas that has been used to stabilize spark sources and reduce background emission is carbon dioxide, CO_2. Another advantage of CO_2 is that it decomposes in the spark source to produce C. The background radiation produced at 3897A reduces the burn time of the A/E35U-1 spectrometer from 25 to 18 seconds.

(b) However, during the atomization step the CO_2 caused the tungsten filament to rapidly oxidize and break. Emission from the tungsten oxide that was transported to the source strongly interferred with the emission lines of Fe causing high Fe readouts.

5. EFFECT OF ELECTRODE CONFIGURATION.

a. Introduction.

(1) The effects of various configurations (tip angles) of the counter (upper) electrode and the vapor transporting (lower) electrode were the next experimental variables investigated. The two configurations of the counter-electrode studied during this investigation are shown in Figure 6. The configurations will be referred to as the 160° and 15° electrodes, where the angles refer to the tip angles of the electrodes. The 160° electrode (which has been used in all of the previous studies) is the one recommended for the A/E35U-3 spectrometer, and the 15° tapered electrode is the one recommended for the A/E35U-1.

(2) Two different vapor transporting electrodes, the boiler cap electrode (BC) and the modified D-2 rotating disk electrode illustrated in Figure 6, were also studied during this phase of the investigation. The effects of electrode configuration and the boiler cap electrode's upper orifice (G in Figure 6) diameter of the different vapor transporting electrodes on the analytical results of the SIVM were studied.

b. Effect of Counter-Electrode Configuration. The two counter-electrode configurations used in this study, 160° and 15°, are illustrated in Figure 6. The counter-electrode configuration study was carried out using the boiler cap (BC-1) electrode as received. The results for the C12-50 standard shown in Figure 43 indicate that the counter-electrode's configuration has a significant effect on the results of the SIVM. The emission readouts produced

TABLE 29. RELATIVE EMISSION BACKGROUND SIGNALS OF ARGON WITH RESPECT TO HELIUM* ON THE A/E35U-1 SPECTROMETER

Ag	Al	Cr	Cu	Fe	Mg	Ni	Si	Sn
1	16	12	1	9	1	31	2	60

*Relative Emission Background Signal = Emission Background Signal of Ar - Emission Background Signal of He

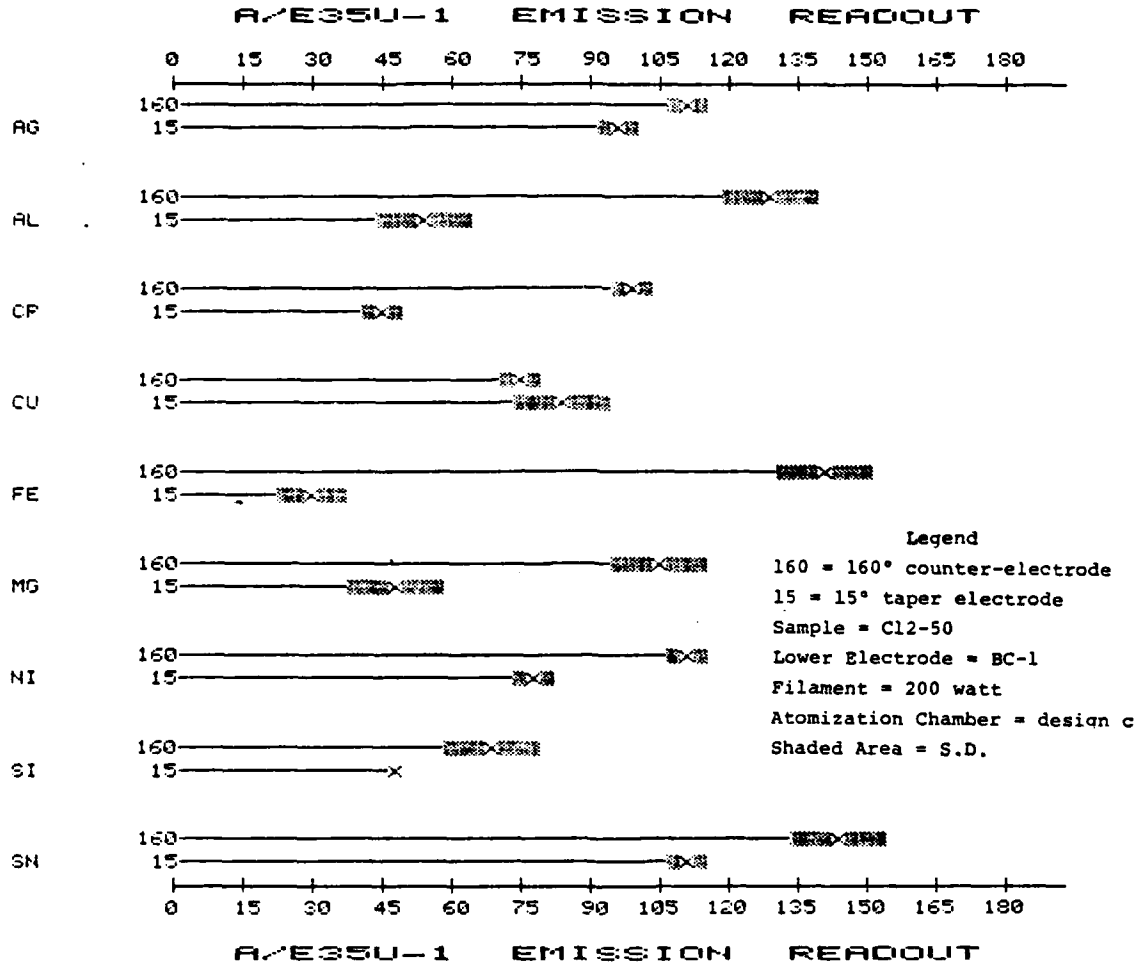

Figure 43. The Effects of the Counter-Electrode's Configuration on the A/E35U-1 Readouts for the SIVM.

by the 160° tip electrode are greatly enhanced compared to those produced by the 15° electrode.

c. Effect of Vapor Transporting Electrode Orifice Diameter and Configuration.

(1) The BC electrode was studied with upper orifice diameters of 1.0 (BC-1), 2.1 (BC-2), and 3.2 (BC-3) mm in combination with the 160° counter-electrode. As seen in Figure 44, the emission readouts of the C12-50 standard decreases as the diameter of the BC electrode's upper orifice increases.

(2) The modified RDE (D-2) electrode with a 3.2 mm diameter orifice was then investigated. The D-2 electrode was modified by enlarging the lower half of the hole (see Figure 6) in order to obtain a tight fit on the upper opening of the atomization chamber.

(3) As seen in Figure 44, the emission readouts obtained with the modified RDE (D-2) electrode for the C12-50 standard are greatly reduced in comparison to those produced by the BC electrodes with the 1.0 and 2.1 mm orifices but are similar to those produced by the BC electrode with a 3.2 mm orifice. Therefore, it appears that the emission signal is greatly affected by the orifice diameter but only slightly by the configuration of the vapor transporting electrode.

(4) Although the BC electrode with the 2.1 mm diameter upper orifice produced lower emission readouts than the BC electrode with the 1.0 mm diameter orifice, the larger orifice allows the ashing step to be performed during a predetermined portion of the burn cycle. The 2.1 mm orifice is the smallest diameter which will allow the ashed oil to be flushed efficiently (8-10 seconds) from the atomization chamber.

6. EFFECTS OF PARTICLE SIZE DISTRIBUTION.

a. Introduction.

(1) The metal powders used to produce the M12-50 multielement suspension have an approximate maximum particle size of 45 µm. As previously discussed, the repeatibility of the C12-50 emission readouts are higher than those for the M12-50 multielement suspension regardless of sample sizes less than 45 µl. Also, the agreement between the C12-50 standard and M12-50 suspension are affected by the rate of the gas flow and other experimental parameters.

(2) Single element suspensions of Fe (M1-Fe), with particle size distributions of -45+30, -30+20, and -20 microns, were prepared to study the effects of particle size on the analytical results of the SIVM. Iron was chosen for this study since it is the most important and most common wear metal found in used lubricating oils.

(3) The effects of particle size on the analytical results were studied using 30 µl samples of the C1-Fe-50 standard and M1-Fe-50 suspensions

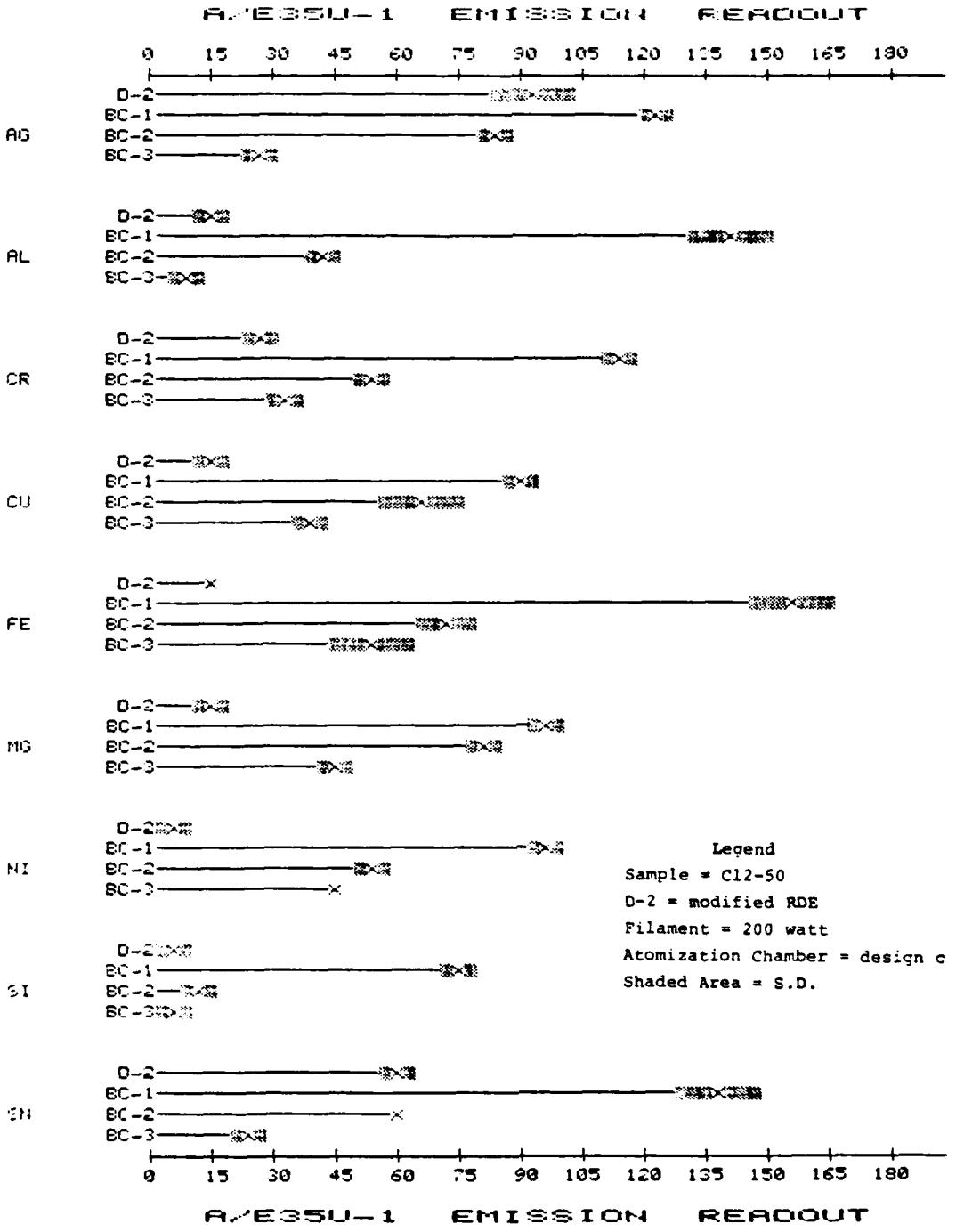

Figure 44. The Effects of the Vapor Transporting Electrode's Upper Orifice Diameter and Configuration on the A/E35U-1 Readouts for the SIVM Using the Modified RDE (D-2), BC-1, BC-2, and BC-3 Electrodes.

on the 300 watt filament using an argon flow rate of 0.2 l/min. through the atomization chamber design c (Figure 8).

b. Working Curve for Fe.

(1) Before the particle size distribution study could be initiated, a working curve of Fe emission versus concentration was needed. The working curve is necessary to evaluate the agreement between the emission readouts of the C1-Fe standard and M1-Fe suspensions since the working curve may not be linear throughout the 0-100 ppm range.

(2) The working curve for the Fe analyses was produced by plotting the emission readouts versus concentration for the Fe standards prepared in MIL-L-23699 at 10, 20, 50, 75, and 100 ppm concentrations using an argon flow rate of 0.2 l/min. As seen in Figure 45, the working curve is linear to approximately 50 ppm but begins to deviate from linearity between 50 and 75 ppm.

c. Effect of Particle Size Distribution on Fe Analyses.

(1) Samples (30 µl) of the M1-Fe-50 suspensions and the C1-Fe-50 standard were analyzed and the results listed in Table 30. The results in Table 30 show that the reproducibility of and agreement between the emission readouts of the M1-Fe-50 suspensions and the C1-Fe-50 standard are affected by the Fe's particle size distribution.

(2) As the data in Table 30 shows, the agreement between the M1-Fe-50 suspensions' and C1-Fe-50 standard's readouts decreases as the maximum particle size of the Fe powder increases. With an argon flow rate of 0.2 l/min., the emission readouts for Fe particles with sizes up to 30 µm have good reproducibility and are in good agreement with those of the C1-Fe standard. For Fe particles in the range -45+30 µm, the emission readouts of the Fe particles and dissolved standard are still in fair agreement but the reproducibility for samples containing particles is poor.

(3) The data in Table 30 show that the emission readouts for the M1-Fe-50 suspensions increase with particle size. Although the reproducibility of the M1-Fe-50 readouts is affected by the particle size of the Fe suspension, the agreement between the readouts of the M1-Fe suspensions and C1-Fe standard at an argon flow rate of 0.2 l/min. is good for Fe particles up to 30 µm.

7. INTERFERENCES FOR THE SIVM ANALYSES.

a. Introduction.

(1) Multielement spectrometric analyses are subject to numerous physical, chemical, and spectral interferences. Chemical and spectral interferences have been observed [references (f) and (g)] for analyses on the A/E35U-1 and A/E35U-3 spectrometers.

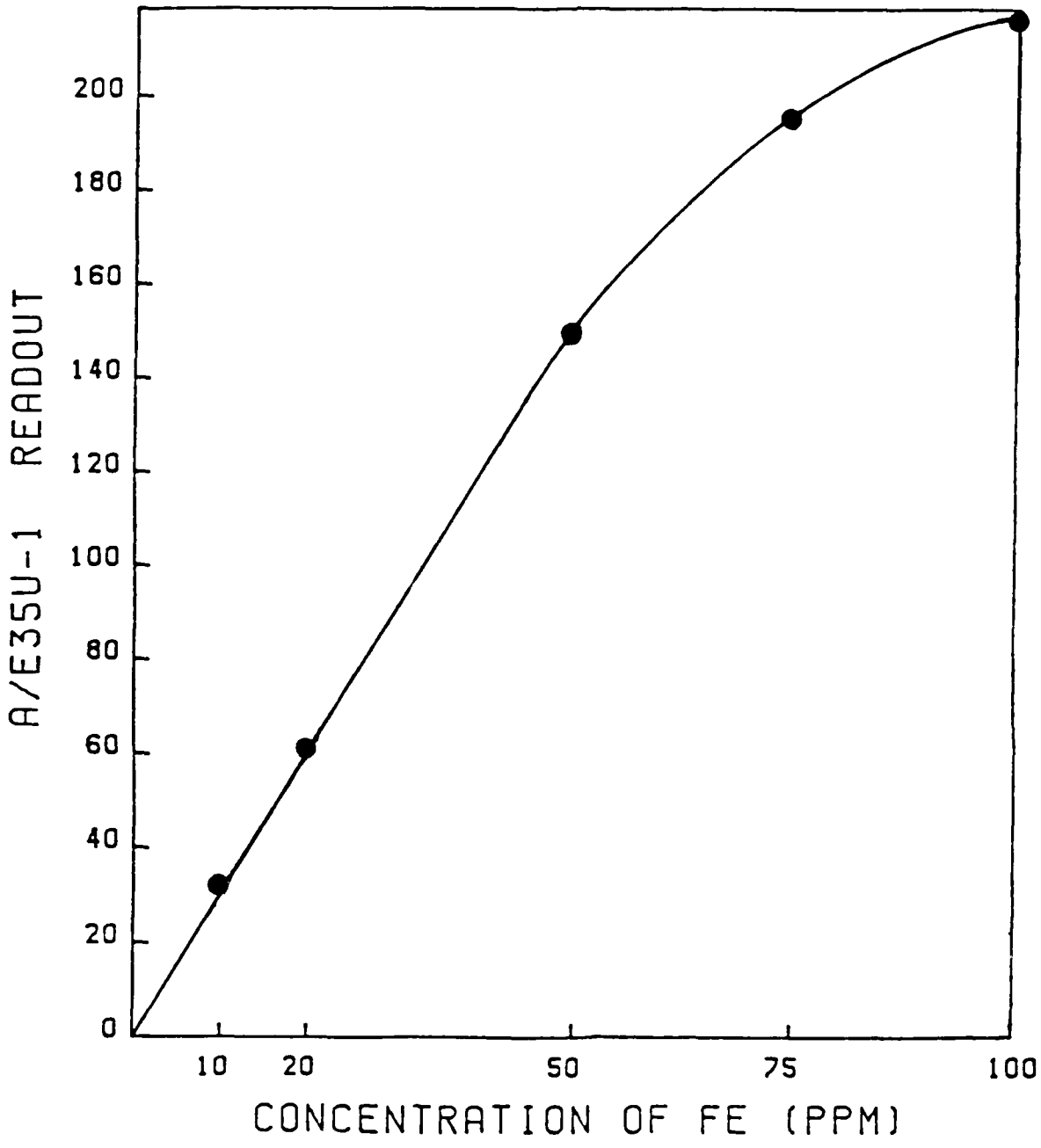

Figure 45. The Working Curve for the Determination of Fe by the SIVM on the A/E35U-1.

TABLE 30. THE EFFECTS OF THE PARTICLE SIZE DISTRIBUTION ON THE FE A/E35U-1 READOUTS FOR THE SIVM

Sample	Particle Size Distribution (μm)	A/E35U-1 Readout
C1-Fe-50	Standard (Dissolved)	154±5
M1-Fe-50	-20	157±10
	-30+20	168±15
	-45+30	189±35

Ashing Conditions - Time: 10 seconds
Voltage Setting: 8% (10 amp, 115V transformer)
Atomizing Conditions - Time: 3 seconds
Voltage Setting: 60% (10 amp, 115V transformer)
Argon Flow Rate - 0.2 l/min.
Atomization Chamber - Design c

(2) Although the SIVM cannot improve the spectral interferences for the emission spectrometer, the SIVM has the potential of reducing the chemical interferences. By ashing the oil matrix prior to analysis, the SIVM should eliminate the oil matrix effects observed for the RDE-SSAE spectrometers, even though the accuracy of the spark-to-residue methods were affected by matrix effects. Also, since the metals are vaporized from the filament atomizer and introduced into the spark source in the order of their sublimation or evaporation temperatures, the concomitant element effects observed for the RDE-SSAE spectrometers should be greatly reduced.

(3) To examine the affects due to concomitant elements, single and multielement standards were prepared in MIL-L-23699, MIL-L-7808, and Conostan 1100 hydrocarbon oils. The analyses were performed using 30 µl samples, the 300 watt filament and an argon atmosphere in design c (Figure 8) atomization chamber with a flow rate of 0.2 l/min.

b. Effect of Matrix. The effect of matrix was studied by preparing 12-element Conostan standards in MIL-L-23699, 245 hydrocarbon, and light hydrocarbon oils. The results in Figure 46 show that, as expected, the SIVM essentially eliminates the effect of matrix from the analyses of the A/E35U-1 spectrometer.

c. Effect of Concomitant Elements.

(1) To study the effect of concomitant elements, single element and 12-element Conostan standards prepared in MIL-L-23699 oil were analyzed. The initial investigation of concomitant element effects was performed on single element Fe standards.

(2) The results in Table 31 indicate that there is a concomitant element effect but the effect is less than the effect experienced by the RDE-SSAE spectrometric analyses [references (f) and (g)].

E. EVALUATION OF THE DEVELOPED METHODS FOR USE ON THE A/E35U-3.

1. INTRODUCTION.

a. The ultimate goal of this investigation was to develop methods capable of making the wear metal analyses of the A/E35U-3 spectrometer particle size independent. For this reason a multielement MIL-L-23699 oil suspension containing Ag, Al, Cr, Cu, Fe, Mg, Mo, Ni, Pb, Si, Sn, and Ti metal powders with maximum particle size of approximately 45 µm was used to optimize and evaluate the capabilities of the different analytical techniques.

b. The percent metal analyzed, the percent errors, and the suitability for use on the A/E35U-3 were used as the evaluation criteria to prioritize the developed methods for final evaluation on the A/E35U-3 spectrometer.

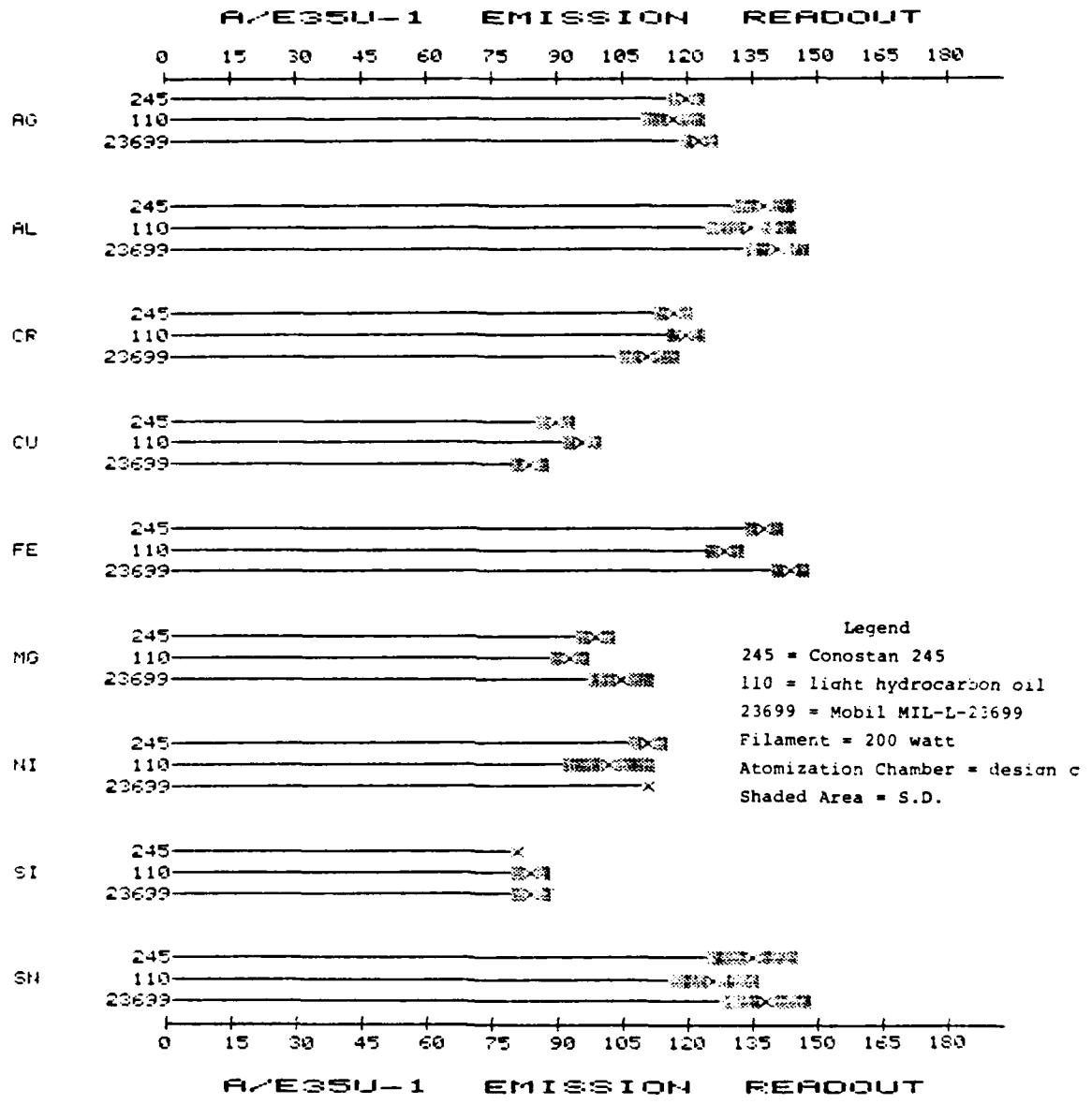

Figure 46. The Effects of the Matrix on the A/E35U-1 Readouts for the SIVM.

TABLE 31. THE EFFECTS OF CONCOMITANT ELEMENTS ON THE FE A/E35U-1 READOUTS FOR THE SIVM

Standard	A/E35U-1 Readout
C12-100	265±8
C1-Fe-100	250±6
C12-50	165±6
C1-Fe-50	154±5
C12-20	75±2
C1-Fe-20	66±3

Ashing Conditions - Time: 10 seconds
Voltage Setting: 8% (10 amp, 115V transformer)
Atomizing Conditions - Time: 3 seconds
Voltage Setting: 60% (10 amp, 115V transformer)
Argon Flow Rate - 0.2 l/min.
Atomization Chamber - Design c

2. COMPARISON OF DEVELOPED METHODS' ANALYTICAL RESULTS.

a. The percent metal analyzed for the optimized methods are listed in Table 32 along with those for the analysis with the rotating disk electrode. As seen in Table 32, all of the developed methods greatly improve the particle detection capabilities of the A/E35U-1 spectrometer in comparison to direct analysis with the rotating disk electrode.

b. Of the techniques developed so far the acid dissolution/spark-to-residue method (AD-STRM) and spark-in-vapor method (SIVM) produce the most accurate results for the metals of study. The precision of the analytical results for the AD-STRM and SIVM are also similar.

3. SUITABILITY OF THE METHODS FOR TESTING ON THE A/E35U-3.

a. Since evaluating methods on the A/E35U-3 required traveling to Lakehurst, New Jersey, only the methods with the most potential could be investigated. In order for the developed methods to be suitable for investigation on the A/E35U-3, they must improve the particle detection capabilities of the A/E35U-1 spectrometer. Of the developed methods, the SIVM is considered to have the most potential for the reasons listed in Table 33. The spark-to-residue methods also have potential for improving the particle detection capabilities of the A/E35U-3 and were investigated.

b. The SIVM also has the potential for providing valuable information on the particle size distribution and oxidation states of the wear debris present in used oil samples. Research by UDRI has demonstrated [reference (dd)] that the particle size distribution and oxidation state of Fe wear debris is more indicative of the severity of wear present in operating jet engines than the concentration of the Fe wear debris. Methods have been reported which employ electrothermal atomization to obtain information on the particle size distribution [reference (ee)] and oxidation states [reference (ff)] of metal species in solid, powdered samples.

F. OPTIMIZATION OF THE DEVELOPED METHODS ON THE A/E35U-3 SPECTROMETER.

1. INTRODUCTION. All of the methods described in this report were developed and optimized on the A/E35U-1 spectrometer. Previous research

---

Ref: (dd) AFWAL Report No. TR-81-4184 of January 1982: Research and Development of Wear Metal Analysis.

(ee) Goldberg, J. and Sacks, R. "Direct Determination of Metallic Elements in Solid Powder Samples with Electrically Vaporized Thin Film Atomic Emission Spectrometry". Anal. Chem., V. 54, P. 2179, 1982.

(ff) Prack, E. R. and Bastiaans, G. J. "Metal Specification by Evolved Gas/Inductively Coupled Plasma Atomic Emission Spectrometry". Anal. Chem., V. 55, P. 1654, 1983.

TABLE 32. SUMMARY OF METHODS USED TO ANALYZE PARTICLES ON THE A/E35U-1 SPECTROMETER

Method	Percent Metal Analyzed								
	Ag	Al	Cr	Cu	Fe	Mg	Ni	Si	Sn
RDE-Direct[e]	50±3	35±15	50±8	2±50	40±10	55±8	9±20	10±10	40±15
ADM[a,e]	102±5	139±14	102±4	93±9	105±5	117±9	112±5	56±5	95±5
STRM[b,e]	156±4	76±10	220±8	99±16	214±11	110±6	89±9	120±7	220±8
AD-STRM[c,e]	102±2	74±14	103±8	105±2	95±10	98±6	101±5	102±5	119±7
SIVM[d,f]	102±4	94±8	105±5	207±4	110±7	94±6	109±6	122±5	125±12

[a]Dissolution with HNO_3/HCl/p-Toluene sulfonic acid for 5 minutes at 65°C - 160° counter-electrode - RDE.
[b]160° Counter-electrode - RDE - Rotated counterclockwise 3 times - Ashed at 600°C for 1 minute.
[c]Dissolution with HNO_3/HCl/HF for 3 minutes at 65°C - 160° counter-electrode - RPE - Ashed at 400°C for 1 minute.
[d]Ashed 8 seconds - Atomized 3 seconds at an argon flow rate of 0.2 l/min.
[e]Standard = C13-50
[f]Standard = C12-50

TABLE 33. COMPARISON OF SIVM AND AD-STRM FOR USE IN JOAP

	SIVM	AD-STRM
Particle Size Limit	~30 μm	None
Sample Size Requirements	Limited[a]	>1 ml
Sample Preparation	None	React with concentrated acid mixture for three minutes at 65°C
Sample Preparation Time	None	7-8 minutes
Matrix Effect	None	Moderate
Concomitant Element Effect	Slight	Not determined
Information on Particle Size Distribution	Possible	No
Incorporation into Sample Analysis Chamber of A/E35U-3 Spectrometer	Yes	No

[a]Upper Limit Determined by Atomizer Design (Tungsten Filament, Carbon Braid, Boats, etc.), Lower Limit Dependent upon Spectrometer Sensitivity.

[reference (g)] demonstrated that the particle detection capabilities of the A/E35U-1 and A/E35U-3 spectrometers were different and limited by the inefficient particle transport of the rotating disk electrode and by the energy of their respective spark sources. Although the developed methods eliminate inefficient particle transport by direct sample deposition, the optimum experimental parameters of each developed method will depend upon the nature of the spark source. Since the goal of this investigation is to improve the particle detection capabilities of the A/E35U-3 spectrometer, the final optimization of the developed ashing methods was performed on the A/E35U-3 spectrometer. Due to its detrimental effects on the rotating disk electrode's spindle, the acid dissolution method was not tried on the A/E35U-3 spectrometer.

2. OPTIMIZATION OF SPARK-TO-RESIDUE METHODS.

a. When the ashed rotating platform electrode was analyzed on the A/E35U-3 spectrometer, the burn time exceeded 50 seconds and the A/E35U-3 was stopped manually. Adjustment of the CV reference gain did not reduce the burn time. This result was expected since the A/E35U-3 spectrometer monitors the 4861A spectral line of H in order to determine the length of the burn time. During normal operation the spectralline of H originates from the excitation of the lubricating oil. Since the oil matrix is vaporized prior to analysis for the spark-to-residue method, the source of the H emission is eliminated making the A/E35U-3 spectrometer incapable of controlling the burn time.

b. In an attempt to control the burn time of the A/E35U-3 spectrometer, Be and Na were tried as internal standards. The output of the Be photomultiplier tube was connected to the input of the CV reference channel. A 30 µl sample of the Be concentrate (0.526%) was deposited onto the rotating platform electrode and ashed on a hot plate for 30 seconds. The presence of Be shortened the burn time of the A/E35U-3 spectrometer, but the repeatability of the burn time was low, 35 $\pm$ 15 seconds. The results for a Na concentrate were similar.

c. Due to the problems associated with producing a burn time of the required length and repeatability, no further work with the spark-to-residue method was performed on the A/E35U-3 spectrometer. Once the burn time can be controlled, further work on this method should be conducted.

3. OPTIMIZATION OF THE SPARK-IN-VAPOR METHOD.

a. Introduction. As previously discussed, the spark-in-vapor method has the best potential for improving the capabilities of the A/E35U-3. In order to determine the optimum experimental parameters of the SIVM on the A/E35U-3 spectrometer, the effects of the analytical gap parameters (frequency and energy of the analytical spark, upper orifice diameter of the boiler cap electrode, and argon flow rate), atomization temperature, two step versus one step atomization procedure, and in situ versus manual SIVM (sample introduction port diameter and ashing during the burn cycle) on the analytical results of the A/E35U-3 spectrometer were studied. The SIVM was optimized using the C13-100 standard and M12-100 suspension prepared in MIL-L-23699 lubricating

oil. Unless stated otherwise, the ashing step was performed prior to the analysis on the A/E35U-3 (manual SIVM) and 25 μl samples were analyzed.

b. Effect of Analytical Gap Parameters.

(1) Introduction.

(a) As previously discussed in paragraph II.B.1.c, the electronic nature of the spark source employed by the A/E35U-3 spectrometer is different from that of the A/E35U-1 spectrometer's spark source. It has been shown [reference (g)] that the spark source of the A/E35U-1 analyzes particles more efficiently than the spark source of the A/E35U-3. Two of the most important source characteristics are the energetics and frequency of the spark discharges. The auxiliary spark gap distance controls both of these characteristics.

(b) The analytical spark gaps of the A/E35U-1 and A/E35U-3 spectrometers are ignited in a similar manner. The capacitor connected in parallel with the auxiliary gap of each RDE-SSAE spectrometer charges until it attains the voltage required to break down the auxiliary gap.

(c) When the auxiliary spark gap distance is shortened, the voltage required to break down the gap is lowered, resulting in a spark discharge at the analytical gap of lower energy. Since the rate at which the capacitor is charged is unaffected by the distance of the auxiliary spark gap and the capacitor charges to a lower voltage before discharging, the frequency of the spark discharges at the analytical gap increases as the auxiliary gap is shortened.

(d) Other parameters expected to affect the efficiency of the spark source are the upper orifice diameter of the boiler cap electrode and the argon flow rate. As the orifice diameter of the boiler cap electrode increases, the concentration of metal vapor per volume decreases since the volume of argon entering the spark is directly proportional to the orifice diameter. Increasing the orifice diameter, decreased the emission readouts of the A/E35U-1 spectrometer (Paragraph III.D.5.c.(1)).

(e) On the A/E35U-1 spectrometer, the rate of argon flow affected the shape of the spark and the emission readout of the spectrometer. As the argon flow rate was increased the spark source was condensed into a well-defined column between the tip of the boiler cap electrode and the center of the upper electrode (Paragraph III.C.2.j.(1)). Increasing the argon flow rate also decreased the emission readouts of the studied elements (Paragraph III.C.2.j.(3)).

(f) Therefore, the effects of the frequency and energy of the analytical spark, boiler cap electrode upper orifice diameter, and argon flow rate on the emission readouts of the spark source of the A/E35U-3 spectrometer were studied.

(2) Effects of the Frequency and Energy of the Analytical Spark.

(a) The effects of the frequency and energy of the analytical spark on the emission readouts of the C13-100 standard prepared in MIL-L-23699 oil were studied using the modified boiler cap electrode (diameter = 2.1 mm) with an argon flow rate of 0.5 1/min. The experimental set-up used to optimize the SIVM on the A/E35U-3 is shown in Figure 47. The ashing step of the manual SIVM, used for this study, is shown in Figure 48.

(b) In contrast to the spark-to-residue methods, the CV reference gain could be used to control the burn time of the A/E35U-3 spectrometer and the burn times were repeatable to approximately one second with the spark-in-vapor method (SIVM).

(c) The ammeter reading from the A/E35U-3 spectrometer was used as a reference for the auxiliary gap distance. When the auxiliary spark gap was shortened, the current reading increased, and conversely, when the gap was lengthened the current reading decreased. The spark gap distances studied for this investigation produced ammeter readings of 1.0 to 3.5 amps. Above 3.5 amps the fuse protecting the circuit blew.

(d) The results in Table 34 show that the emission readouts of the spark source depend strongly on the width of the auxiliary spark gap. At currents below 2.0 amps (widest auxiliary spark gap), the source is unable to excite any of the elements. The emission readouts of all the elements except Mo and Ti increase as the current readings increase from 1.5 to 3.5 amps (as the auxiliary gap is shortened). Mo and Ti were not detected under these experimental parameters.

(e) Although the current readings observed for the SIVM are similar to those observed for direct analysis using the rotating disk electrode ($\sim$2.0 amps), the auxiliary spark gap is much wider for the SIVM. When the rotating disk electrode was replaced by the electrothermal chamber, the current reading went off scale (>5.0 amps). The auxiliary gap had to be widened from that used for direct analysis to obtain a current reading of 2.0 amps for the SIVM. Since at a current reading of 2.0 amps all of the elements are detectable by direct analysis, but none are by the SIVM, the changes in the nature of the source, not the current, are responsible for the effects of the auxiliary spark gap width on the emission readouts of the C13-100 standard.

(f) Since the energy of the spark is decreasing as the emission readouts increase, the faster frequency of the spark is most likely responsible for the increased emission readout for the C13-100 standard. Also, the effect of the auxiliary spark gap on the energy of each spark is nullified to a certain extent by the voltage supplied across the analytical gap by the low voltage circuit. Therefore, the information obtained for the SIVM during this study shows that the sensitivity of the spark source is improved by increasing the frequency of spark discharges. The optimum frequency was not reached since the emission readouts were still increasing at the highest spark frequency obtainable which was limited by the current rating of the fuse protecting the spark circuit.

Figure 47. The Spark-in-Vapor Method with the A/E35U-3 Spectrometer.

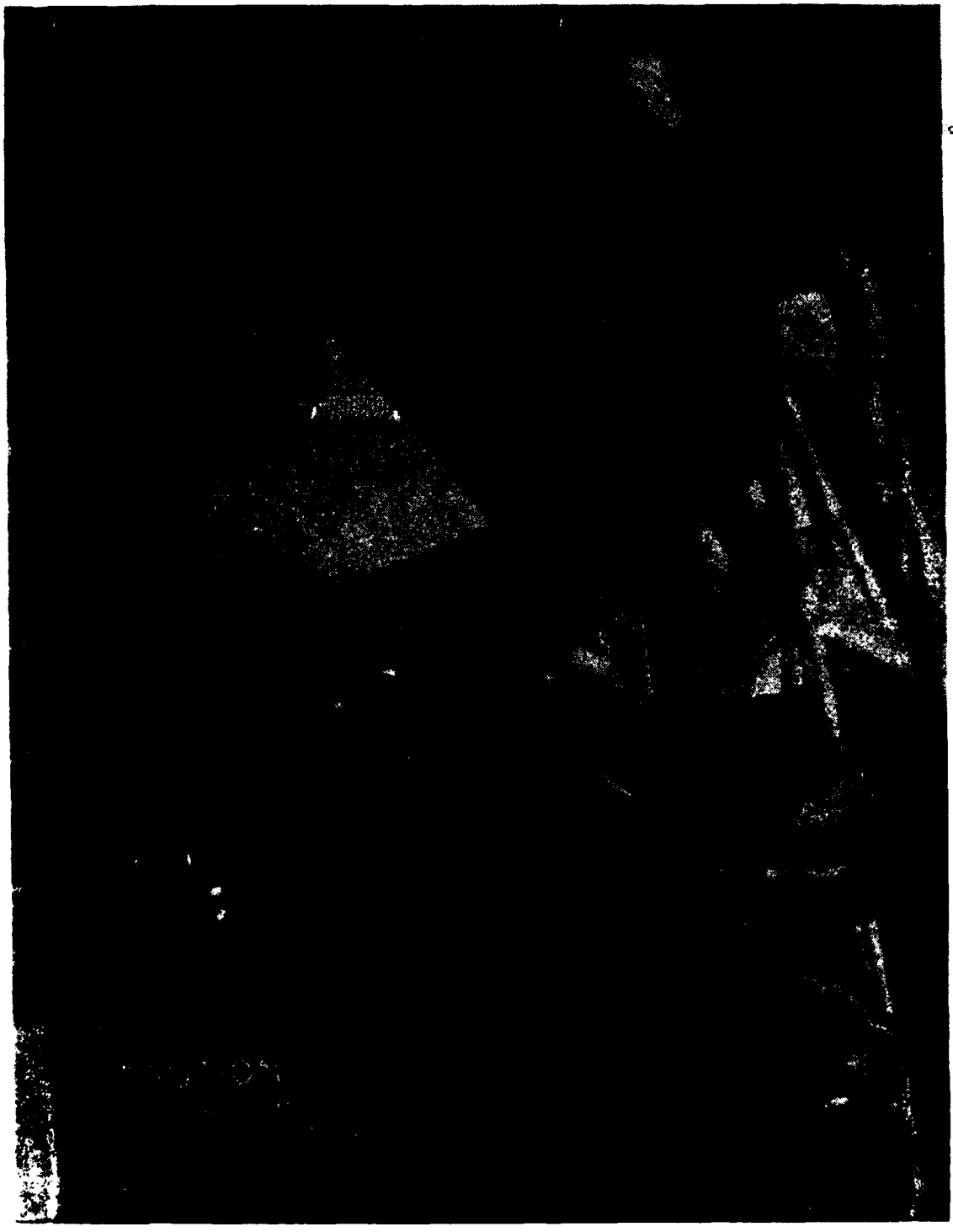

Figure 48. Ashing Step for the Spark-in-Vapor Method with the A/E35U-3 Spectrometer.

TABLE 34. THE EFFECT OF THE AUXILIARY SPARK GAP DISTANCE ON THE A/E35U-3 READOUTS FOR THE C13-100 STANDARD

Current Reading (Amps)*	Ag	Al	Cr	Cu	Fe	Mg	Mo	Ni	Pb	Si	Sn	Ti
1.5	--**	--	--	--	--	--	--	--	--	--	--	--
2.0	--	--	--	--	--	--	--	--	--	--	--	--
2.5	18±1	38±3	8±4	37±2	68±5	35±3	--	45±1	22±1	44±4	40±5	--
3.0	47±2	85±3	37±6	87±4	150±5	83±3	--	88±1	37±3	128±3	70±4	--
3.5	89±4	130±2	106±5	99±2	366±10	100±4	--	205±2	47±4	140±4	96±5	--

* Current Inversely Related to the Auxilary Spark Gap Separation.
** -- Not Detected
Ashing Conditions - Time: 15 seconds
Rheostat (R1) Setting: 170 ohms (see Figure 11)
Atomizing Conditions - Time: 5 seconds
Total Resistance: 15 ohms
Atomization Chamber - Design c
Argon Flow Rate - 0.5 l/min.

(g) This study also indicates that the energy of the A/E35U-3's source is adequate for the SIVM since the emission readouts were still increasing as the energy of the sparks' discharges were decreasing. The SIVM requires a less energetic spark source than direct analysis by the rotating disk electrode. The spark is only required to excite metal vapor in the SIVM, while for direct analysis the spark must vaporize the oil matrix, then atomize and excite the metal species (dissolved and particles).

(h) The auxiliary spark gap distance which produced a current of 3.0 amps was used for all of the following research on the A/E35U-3 spectrometer. Due to the variations in the spark source's current during an analysis, the gap distance giving 3.5 amps caused the fuse protecting the circuit to blow after every two to five analyses and, therefore, could not be used to obtain consistent data.

(3) Effect of the Upper Orifice Diameter of the Boiler Cap Electrode.

(a) The effect of the boiler cap electrode's upper orifice diameter on the emission readouts for the C13-100 standard was studied using the regular boiler cap electrode (BC-1, upper orifice diameter = 1.0 mm) and the modified boiler cap electrode (BC-2, upper orifice diameter = 2.1 mm) [Figure 6] at an argon flow rate of 0.5 l/min.

(b) The results in Table 35 show that, except for Ag, none of the elements were detected with the BC-1 electrode. Also, the burn time increased from 20 seconds (BC-2) to 35 seconds for the BC-1 electrode.

(c) The results for the A/E35U-3 spectrometer are opposite of those produced by the A/E35U-1 spectrometer. For the A/E35U-1 spectrometer the emission readouts of the elements decreased as the orifice diameter increased while the burn time was not affected by the orifice diameter (Paragraph III.D.5.c.(1)).

(d) Therefore, the BC-2 electrode was used for all of the following research on the A/E35U-3 spectrometer. As with the frequency of the spark source, the optimum orifice diameter may not have been reached during this initial investigation.

(4) Effect of the Argon Flow Rate.

(a) The effect of the argon flow rate on the emission readouts for the C13-100 standard and M12-100 suspension prepared in MIL-L-23699 was studied at flow rates from 0.5-2.0 l/min. using a single step atomization procedure and a sample size of 25 µl. The results in Figure 49 show that the emission readouts for all the elements (except Mo and Ti which were not detected at any flow rate) increase with the argon flow rate. The burn time decreased from 27 seconds to 17 seconds as the argon flow rate increased from 0.5-2.0 l/min. The appearance of the A/E35U-3's spark source was not changed by any of flow rates used in this study. The spark source of the A/E35U-3 during the atomization cycle of the SIVM with a flow rate of 2.0 l/min. is shown in Figure 50.

TABLE 35. THE EFFECTS OF THE UPPER ORIFICE DIAMETER OF THE BOILER CAP ELECTRODE ON THE A/E35U-3 READOUTS FOR THE C13-100 STANDARD

Boiler Cap Electrode	Ag	Al	Cr	Cu	Fe	Mg	Mo	Ni	Pb	Si	Sn	Ti	Mo
BC-1	12±3	--*	--	--	--	--	--	--	--	--	--	--	--
BC-2	47±2	85±3	37±6	87±4	150±5	83±3	--	88±1	47±3	128±3	70±4	--	--

* -- Not Detected
Ashing Conditions - Time: 15 seconds
Rheostat (R1) Setting: 170 ohms (see Figure 11)
Atomizing Conditions - Time: 5 seconds
Total Resistance: 15 ohms
Atomization Chamber - Design c
Argon Flow Rate - 0.5 l/min.

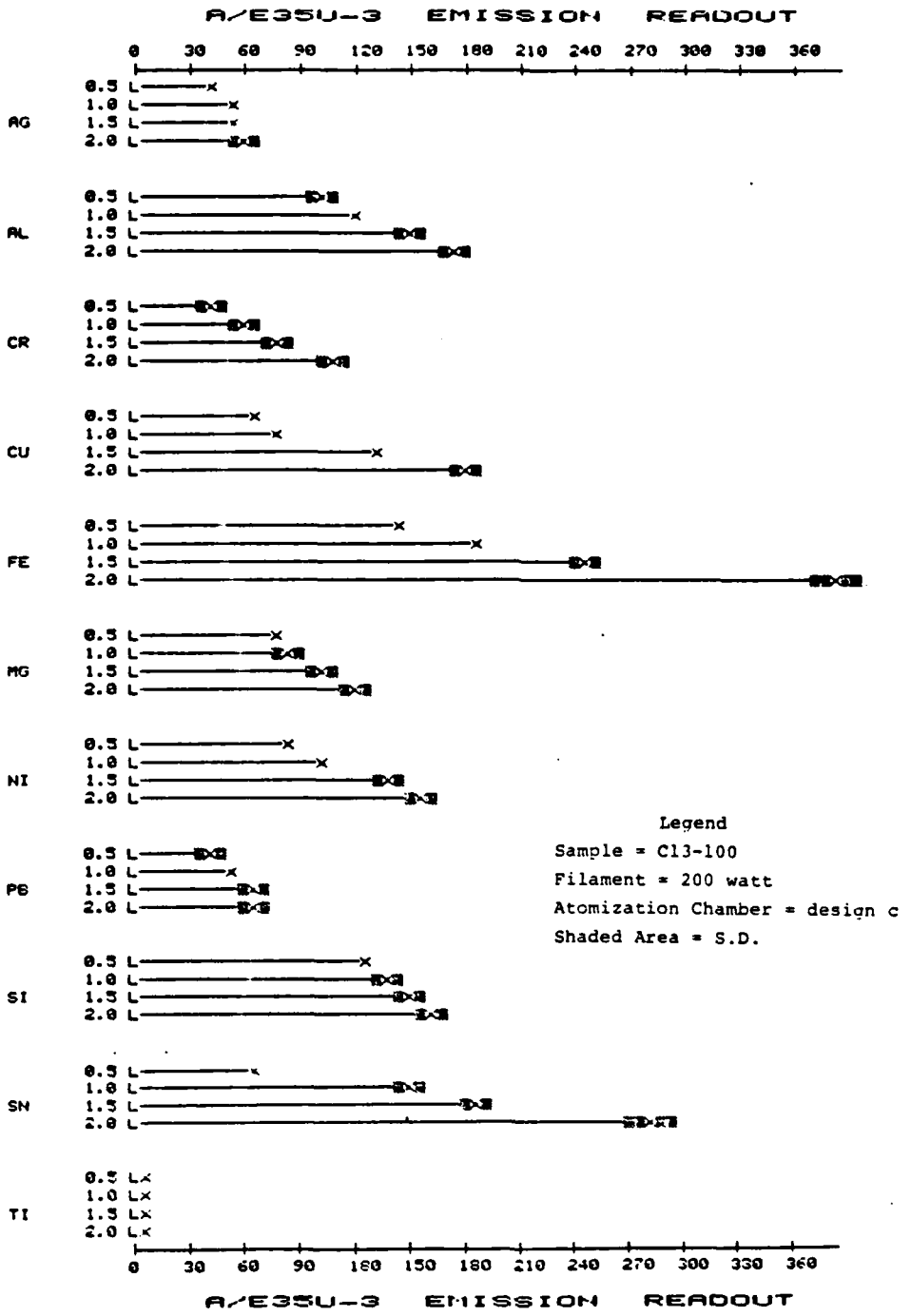

Figure 49. The Effects of the Argon Flow Rate (1/min.) on the A/E35U-3 Readouts of the SIVM.

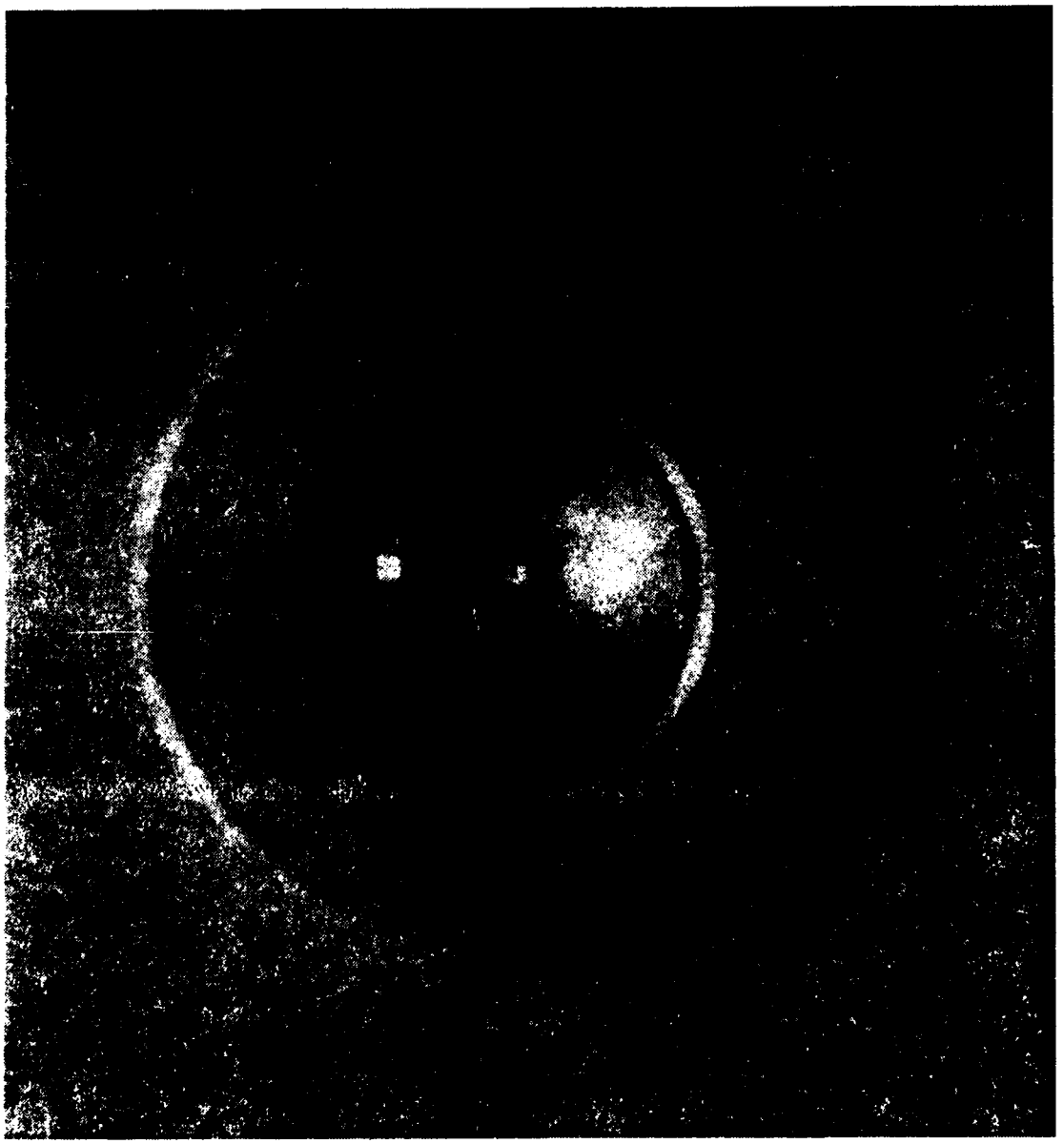

Figure 50. Spark Source of the A/E35U-3 with Electrothermal Atomizer.

(b) However, the agreement between the A/E35U-3 readouts of the C13-100 standard and M12-100 suspension decreased as the argon flow rate increased (Figure 51), i.e., the percent metal analyzed diverged from 100 percent as the argon flow rate increased. At flow rates below 1.5 l/min., the percent metal analyzed for Al, Cr, Fe, and Ni are essentially 100 percent. With increasing argon flow rates, the percent metal analyzed for the M12-100 suspension decreased for Al and Pb, but increased for Ag and Sn.

(c) In contrast to the A/E35U-3, the A/E35U-1 readouts of the elements studied decreased with the argon flow rate. However, in agreement with the A/E35U-1, the percent metal recoveries for the A/E35U-3 improved as the argon flow rate was decreased.

(d) The optimum argon flow rate for the SIVM on the A/E35U-3 is complicated by the fact that decreasing the argon flow increases the accuracy but reduces the sensitivity of the SIVM on the A/E35U-3 spectrometer. However, problems with sensitivity could be overcome by analyzing larger samples which have the additional benefit of producing more representative samples when particles are present.

c. Effect of Atomization Temperature. Since Mo and Ti were not detected by the SIVM on the A/E35U-3, one problem could be that the atomization temperature was too low. However, temperatures greater than 3000°C, which caused the tungsten filament to melt and break, did not enable the A/E35U-3 to detect Mo or Ti. Since Mo is detectable at atomizer temperatures above 2500°C in graphite furnace - multielement atomic absorption spectrometry [reference (gg)], the atomization temperature cannot be solely responsible for the inability of the SIVM to analyze Mo and Ti.

d. Effect of Two Step Versus One Step Atomization Procedure.

(1) The effect of a two step versus one step atomization procedure on the emission readouts of the C13-100 standard and M12-100 suspension was studied at a flow rate of 1.5 l/min. The two step atomization procedure was accomplished by incorporating the time delay relay timer (TD3) into the power supply of the tungsten filament (Figure 11). After a delay, the atomization step was initiated, TD3 closed the circuit to R3 causing the total circuit resistance to drop and the atomization temperature to increase.

(2) The results for the C13-100 standard listed in Table 36 show that the two step atomization procedure decreased the emission readouts of Al, Fe, and Si relative to the one step procedure. However, the two step atomization procedure enabled the A/E35U-3 spectrometer to detect Ti.

(3) The results listed in Table 36 also show that the two step atomization procedure increased or did not change the agreement between the

---

Ref: (gg) Harnly, J. M. and Kane, J. S. "Optimization of Electrothermal Atomization Parameters for Simultaneous Multielement Atomic Absorption Spectrometry". Anal. Chem., V. 56, P. 48, 1984.

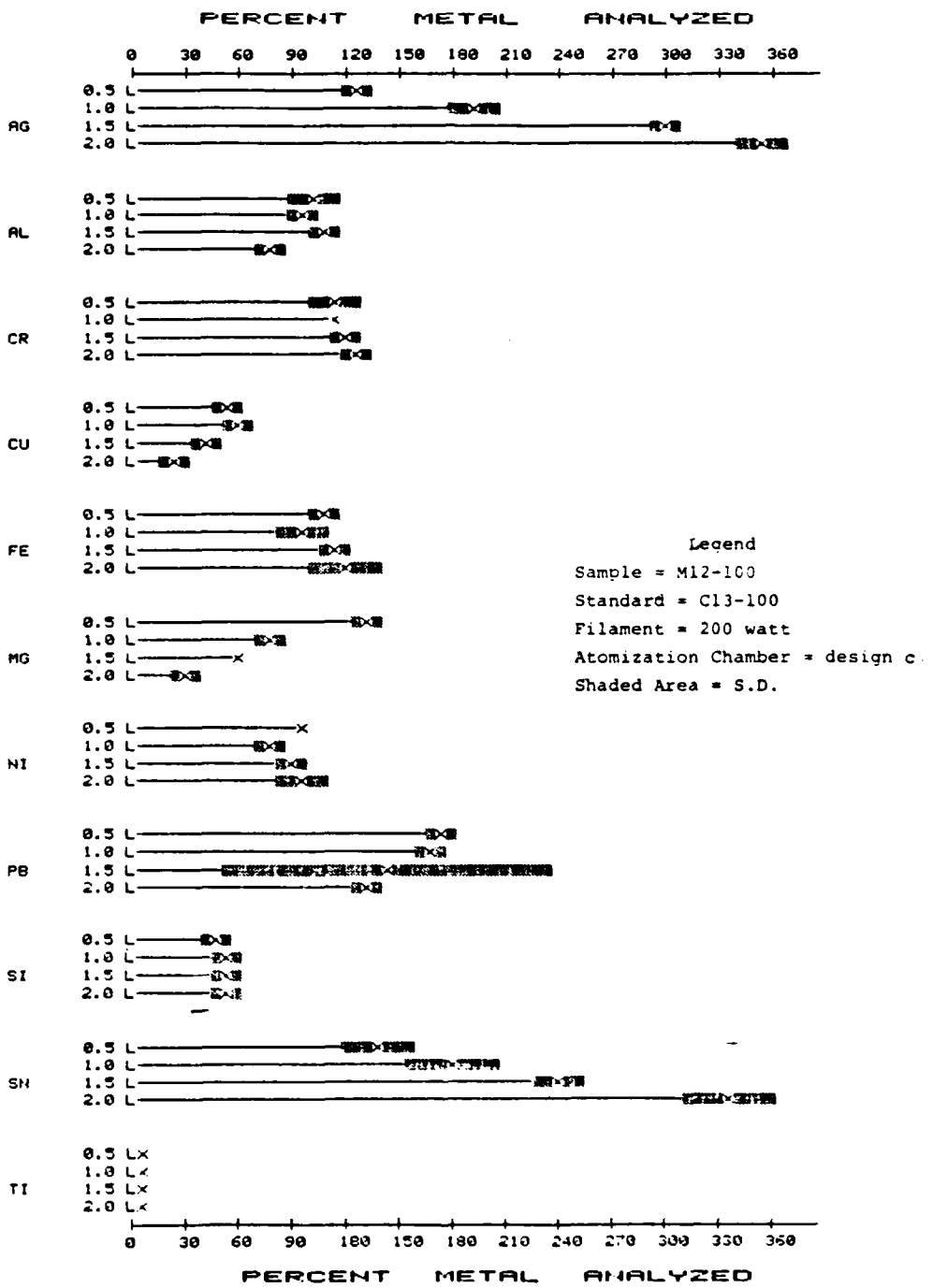

Figure 51. The Effects of the Argon Flow Rate (l/min.) on the Percent Metal Analyzed by the SIVM.

TABLE 36. THE EFFECTS OF THE TWO STEP VERSUS ONE STEP ATOMIZATION PROCEDURE ON THE ANALYTICAL RESULTS FOR THE SIVM

	Atomization Procedure	Ag	Al	Cr	Cu	Fe	Mg	Mo	Ni	Pb	Si	Sn	Ti
Readout (C13-100)	One Step	60±2	151±8	80±8	135±4	190±6	107±8	--*	144±6	72±4	156±8	182±4	--
	Two Step	52±3	53±6	81±2	132±3	146±2	99±2	--	157±1	71±2	68±3	180±2	37±6
A% (M12-100)	One Step	402±8	112±10	125±10	48±6	102±6	64±5	--	94±7	168±10	57±6	341±6	--
	Two Step	84±6	93±7	112±4	73±6	97±8	71±6	--	104±6	76±6	194±8	115±8	103±5

* -- Not Detected
Ashing Conditions - Time: 15 seconds
Rheostat (R1) Setting: 170 ohms (see Figure 11)
Atomizing Conditions - One Step Time: 5 seconds
Total Resistance: 15 ohms
Two Step Time 1: 2 seconds
Total Resistance: 57 ohms
Time 2: 3 seconds
Total Resistance: 15 ohms
Atomization Chamber - Design c
Argon Flow Rate - 1.5 l/min.

emission readouts of the C13-100 standard and M12-100 suspension for all elements except Si.

(4) As observed for decreasing the argon flow rate, the optimum atomization procedure is complicated by the fact the the two step atomization increases the accuracy but decreases the sensitivity of the SIVM on the A/E35U-3.

e. Effect of In Situ SIVM.

(1) Introduction.

(a) In order to make the SIVM more suitable for routine analysis, a sample introduction port was put into the top half of the atomization chamber as shown in Figure 9. The sample is then deposited onto the electrothermal atomizer through the introduction port eliminating the need to remove the top half of the chamber each time a sample is deposited. This also reduces the exposure of the filament to the atmosphere which should result in an increase in the filament's life.

(b) The SIVM was made even more suitable for routine analysis by ashing the sample during the burn cycle of the A/E35U-3 spectrometer. The SIVM employing the sample introduction port and ashing during the burn cycle is referred to as the "in situ" SIVM.

(c) Therefore, the effects of the sample introduction port diameter and ashing during the burn cycle on the A/E35U-3 readouts for the SIVM were studied.

(2) Effect of Sample Introduction Port Diameter.

(a) The effects of the sample introduction port diameter on the emission readouts of the C13-100 standard and M12-100 suspension were studied using ports with diameters of 4.0, 2.1, and 1.0 mm. The effect of closing off the introduction port after sample introduction was also studied. The effect of the sample introduction port diameter was studied at an argon flow rate of 1.5 l/min. and with the two step atomization procedure.

(b) The results in Figure 52 show that the diameter of the sample introduction port has a very strong effect on the emission readouts of the C13-100 standard. At a diameter of 4.0 mm, Fe, Ni, Pb, Si, Sn, and Ti were not detected by the A/E35U-3 spectrometer. As the sample introduction port diameter was decreased, the emission readouts of all the elements except Mo increased, with the closed port producing the highest A/E35U-3 readouts. Mo was not detected.

(c) The results illustrated in Figure 53 show that the agreement between the emission readouts of the C13-100 standard and M12-100 suspension improves (percent metal recoveries converge on 100 percent) as the diameter of the sample introduction port is decreased. Therefore, the emission readouts of the M12-100 suspension are affected more by the sample introduction port diameter than the C13-100 standard.

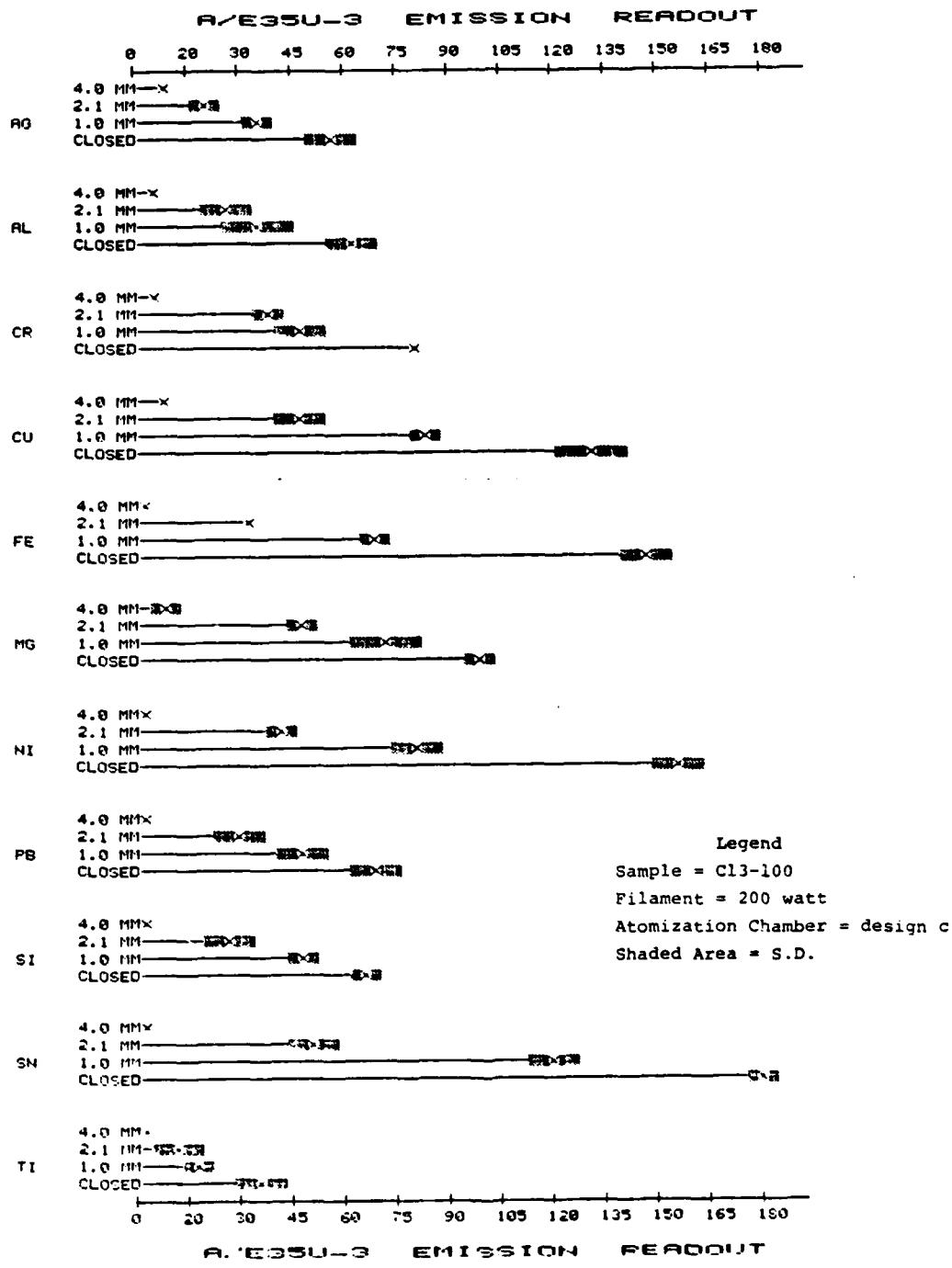

Figure 52. The Effects of the Sample Introduction Port Diameter (mm) on the A/E35U-3 Readouts for the SIVM.

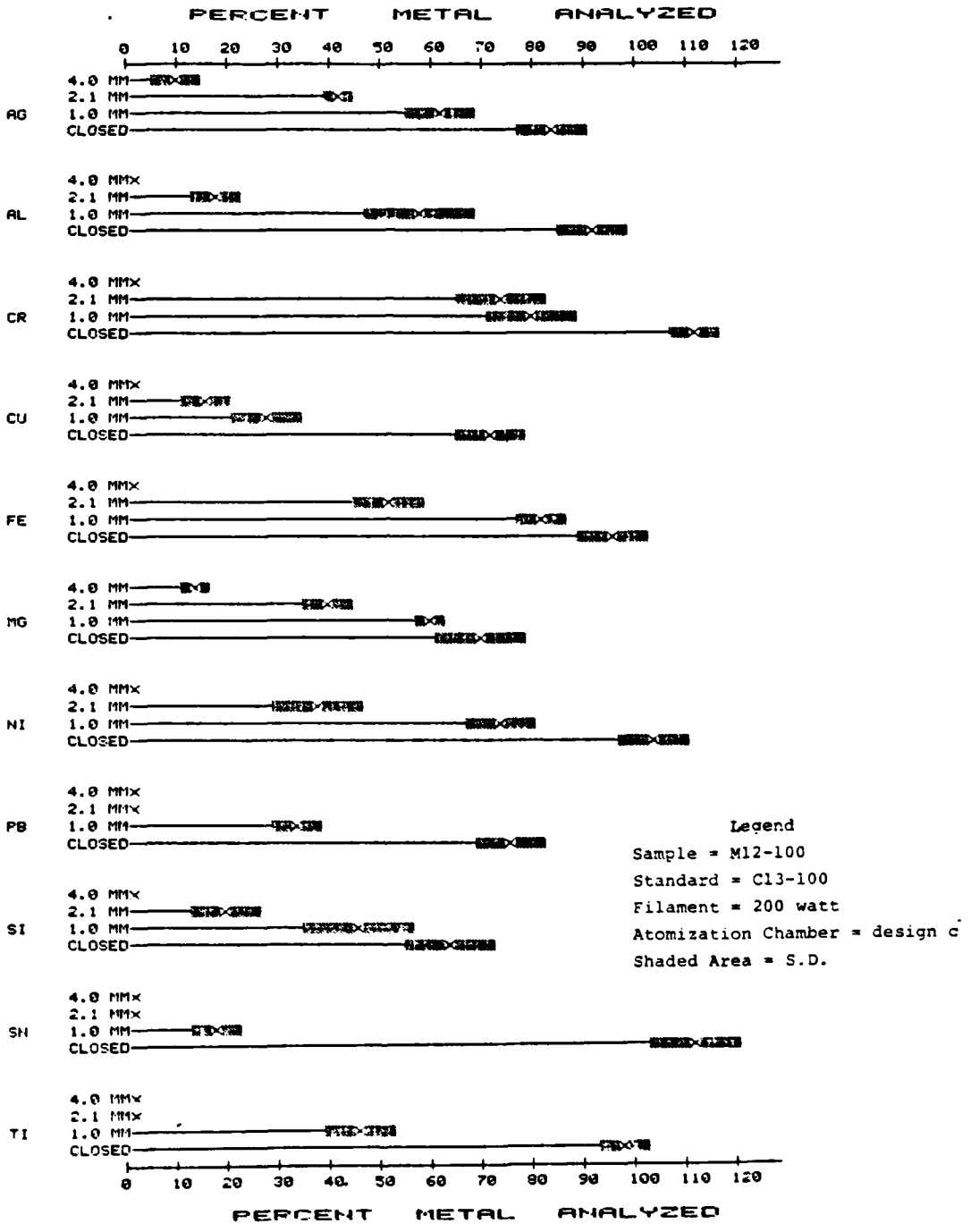

Figure 53. The Effects of the Sample Introduction Port Diameter (mm) on the Percent Metal Analyzed by the SIVM.

(d) The results of this study show that the optimum analytical results are obtained when the sample introduction port is closed after deposition of the sample.

(3) Effect of Ashing During the Burn Cycle.

(a) To study the effect of ashing during the burn cycle on the emission readouts of the C13-100 standard and M12-100 suspension, the ashing step of the SIVM was started immediately before the purge cycle of the A/E35U-3 analysis was begun. The 25 µl sample required approximately 13 seconds to be completely ashed so that the ashing of the sample was completed at the same time that the preburn cycle of the A/E35U-3 analysis ended.

(b) During the preburn cycle, the current reading of the analytical spark gap circuit dropped from 3.0 amperes to below 2.0 amperes due to the introduction of the oil vapor into the spark. The start of the first atomizing step was, therefore, delayed (2 seconds) until the current was restabilized at 3.0 amperes. A two step atomization cycle was then conducted (first step - 2.0 seconds; second step - 3.0 seconds).

(c) After the atomization cycle was completed, the A/E35U-3's burn cycle was completed (integration period of $\sim$ 6 seconds) resulting in a total burn cycle of 19 seconds as compared to 33 seconds for analyses of lubricants using the rotating disk electrode. Therefore, the in situ SIVM actually shortens the sample analysis time, as compared to the STRM and ADM, which lengthen the analysis time by several minutes. When the ashing step is performed prior to analysis (manual SIVM) the analysis time of the SIVM is approximately the same as required by analysis of lubricants with the rotating disk electrode.

(d) The results listed in Table 37 show that for the C13-100 standard, the magnitudes and the precision of the emission readouts for Ag, Cu, Mg, and Pb are less for the in situ SIVM than for the manual SIVM. The other metals are essentially unaffected by the timing of the ashing cycle. The percent metal recoveries for the Ag, Cu, Mg, and Pb particles of the M12-100 suspension are also reduced in magnitude and precision by the in situ SIVM. The elements whose emission readouts are affected by the in situ SIVM (Ag, Cu, Mg, and Pb) atomize at the lowest temperatures, while the elements which atomize at higher temperatures are unaffected.

(e) To determine if the effects of the in situ SIVM are a result of the ashing/atomizing processes or the instability of the A/E35U-3's source, the in situ SIVM was run on the A/E35U-1 spectrometer. The results in Table 38 show that the magnitude and precision of the A/E35U-1 readouts for the C13-100 standard are essentially unaffected by the in situ SIVM, except for Si whose readout increased in comparison to the manual SIVM. Also, during the ashing of the oil into the source the current reading remained constant at 3.5 amps.

TABLE 37. COMPARISON OF THE A/E35U-3 READOUTS OBTAINED FOR THE C13-100 STANDARD WITH THE MANUAL AND IN SITU SIVM

	SIVM	Ag	Al	Cr	Cu	Fe	Mg	Mo	Ni	Pb	Si	Sn	Ti
Readout (C13-100)	Manual	52±3	53±6	81±2	132±3	146±6	99±2	--	157±1	71±2	68±3	180±2	37±6
	In Situ	24±4	60±9	78±10	61±8	159±10	58±8	--	160±10	30±8	77±9	170±16	43±8
A% (M12-100)	Manual	84±6	93±7	112±4	73±6	97±6	71±8	--	104±6	76±6	194±8	115±8	103±5
	In Situ	50±8	88±12	105±8	50±9	105±12	39±10	--	95±11	21±10	188±16	130±18	108±12

* -- Not Detected
Ashing Conditions - Time: 13 seconds
Rheostat (R1) Setting: 140 ohms (see Figure 11)
Atomizing Conditions - Time 1: 2 seconds
Total Resistance: 57 ohms
Time 2: 3 seconds
Total Resistance: 15 ohms
Atomization Chamber - Design c With Sample Introduction Port
Argon Flow Rate - 1.5 l/min.

TABLE 38. COMPARISON OF THE A/E35U-1 READOUTS OBTAINED FOR THE C13-100 STANDARD WITH THE MANUAL SIVM AND IN SITU SIVM

	Ag	Al	Cr	Cu	Fe	Mg	Ni	Si	Sn
Manual	89±3	138±6	48±4	96±10	148±6	106±8	90±4	28±2	129±6
In Situ	94±1	130±2	46±6	88±6	150±8	118±6	84±2	46±3	140±8

Ashing Conditions - Time: 13 seconds
Rheostat (R1) Setting: 140 ohms (see Figure 11)
Atomizing Conditions - 1st Step Time: 2 seconds
Total Resistance: 57 ohms
2nd Step Time: 3 seconds
Total Resistance: 15 ohms
Atomization Chamber: Design c With Sample Introduction Port
Argon Flow Rate: 0.3 l/min.

(f) Therefore, it appears that characteristics of the A/E35U-3's spark source are responsible for the lower accuracy and reproducibility of the in situ SIVM in comparison to the manual SIVM. The analytical results obtained with the A/E35U-1 spectrometer (Table 38) show that with the correct spark characteristics, the in situ SIVM should be suitable for use with the A/E35U-3.

(4) Comparison of SIVM on the A/E35U-1 and A/E35U-3 Spectrometers.

(a) As discussed in the preceding paragraphs, the size and directions of the effects that the experimental parameters have on the analytical results of the SIVM are dependent upon the RDE-SSAE spectrometer used. A summary of the experimental parameters studied on the A/E35U-1 and A/E35U-3 and their effects on the SIVM is presented in Table 39.

(b) The percent metal analyzed of the SIVM on the A/E35U-1 and A/E35U-3 spectrometers decrease as the argon flow rate increases. However, the effects of all of the other experimental parameters are in opposite directions and differ in magnitude. As the argon flow increases, the emission readout for the SIVM on the A/E35U-3 increases as the A% decreases, while the emission readout for the SIVM on the A/E35U-1 decreases as the A% decreases. However, as the diameter of the boiler cap orifice increases, the emission readout for the SIVM on the A/E35U-3 increases significantly, while the emission readout for the SIVM A/E35U-1 decreases significantly.

(c) Therefore, it appears that a source is needed which is optimized for the SIVM. Other differences between the RDE-SSAE spectrometers such as the length of burn time, purge cycle, and the background correction used by the A/E35U-3 spectrometer [reference (h)] could also contribute to the effects observed during this study.

G. EVALUATION OF THE MANUAL SIVM ON THE A/E35U-3 SPECTROMETER.

1. INTRODUCTION.

a. In the final phase of this investigation the manual SIVM was evaluated on the A/E35U-3 spectrometer. The particle size dependence of the manual SIVM was determined for Ag, Al, Cu, Fe, Mg, and Ti metal powder suspensions prepared in MIL-L-23699 lubricating oil with metal powders with particle size distributions of -45+30, -30+20, and -20 µm. The manual SIVM was also evaluated by comparing the analytical results from authentic used MIL-L-23699 oil samples with the concentrations determined by the particle size independent method (PSIM) [reference (j)] and by direct analysis on the A/E35U-3. The PSIM was used to determine the actual metal content in each used oil sample.

b. To determine the potential of the SIVM to analyze materials which may be used in the manufacture of future engine components, Si_3N_4 and TiC ceramic powder suspensions prepared in MIL-L-23699 oil were analyzed by the manual SIVM. The potential of the SIVM to differentiate between the different

TABLE 39. SUMMARY OF THE ANALYTICAL RESULTS OF THE SIVM ON THE A/E35U-1 AND A/E35U-3 SPECTROMETERS

Experimental Parameter	A/E35U-3	A/E35U-1
Effect of Increase in Argon Flow Rate		
Percent Metal Analyzed	Decrease	Decrease
Emission Readout	Increase	Decrease
Effect of Increase in Discharge Frequency		
Emission Readout	Increase	Not Investigated
Effect of An Increase in the Diameter of the Boiler Cap Electrode Orifice		
Emission Readout	Increase	Decrease
Effect of Vaporizing Oil Into Spark During Burn Cycle		
Emission Readout	Decrease	No Effect
Two Step versus One Step Atomization Procedure		
Percent Metal Analyzed	Two Step Procedure Improved Ag, Cu, Sn, and Ti,	Slight Effect

oxidation states of metal species present as wear debris in used oil samples was assessed by determining the experimental parameters of the SIVM required to detect Fe and Fe_2O_3 particles.

2. DETERMINATION OF THE PARTICLE SIZE LIMITATIONS OF THE SIVM.

a. To determine the particle size limitations of the SIVM single element standards and metal powder suspensions of Ag, Al, Cu, Fe, Mg, and Ti were analyzed on the A/E35U-3 spectrometer. Mo was not studied since it could not be detected using the present SIVM on the A/E35U-3. The experimental conditions used to evaluate the manual SIVM consisted of a two step atomization procedure, an argon flow rate of 1.5 l/min. and 25 µl samples deposited onto a 300 watt tungsten filament. The atomization chamber (design c) modified with the sample introduction port (Figure 9) was used for this study. The sample introduction port was closed off after the oil sample was ashed.

b. The results in Figure 54 show that the SIVM accurately determined the concentration of particles below 20 µm for all of the metals studied and below 30 µm for Al and Mg. Metal particles larger than 45 µm are detected by the SIVM but produce attenuated A/E35U-3 readouts in comparison to the single element standards. The precision for the analytical results decreased with particle size as expected.

c. For comparison, the analytical results for direct analysis on the A/E35U-3 are also included in Figure 54. As illustrated in Figure 54, direct analysis is only capable of detecting less than 20 percent of the metal particles below 20 µm and is completely blind to particles greater than 20 µm for all of the metals studied, except Mg, which is detectable up to 20-30 µm.

d. Therefore, the SIVM enables the A/E35U-3 to detect metal particles larger than 45 µm for all of the metals studied (except Mo) and to accurately determine the concentrations of metal particles below 20-30 µm. This is a significant improvement over direct analysis on the A/E35U-3 spectrometer which is only capable of detecting particles less than 8-20 µm and accurately determining the concentrations of metal particles below 3-10 µm [reference (g)].

3. ANALYSIS OF AUTHENTIC USED MIL-L-23699 OIL SAMPLES.

a. Since JOAP analyzes used oil samples, authentic used MIL-L-23699 oil samples obtained from T56 engines were analyzed with the SIVM on the A/E35U-3. The experimental conditions described in Paragraph III.G.2.a were used for this study. The actual metal concentration for each used oil sample, were obtained from reference (f). These values were determined using the PSIM with a dc plasma AE spectrometer.

b. To compare the analytical results, the concentrations determined by the SIVM and direct analysis were plotted versus the concentration determine by the PSIM for each used oil sample. The results for Cu, Fe, and Mg were plotted and are shown in Figures 55, 56, and 57, respectively. None of the samples contained more than 2 ppm of Ag, Al, or Ti. As illustrated in Figures 55, 56, and 57, the SIVM gives higher wear metal analyses than direct

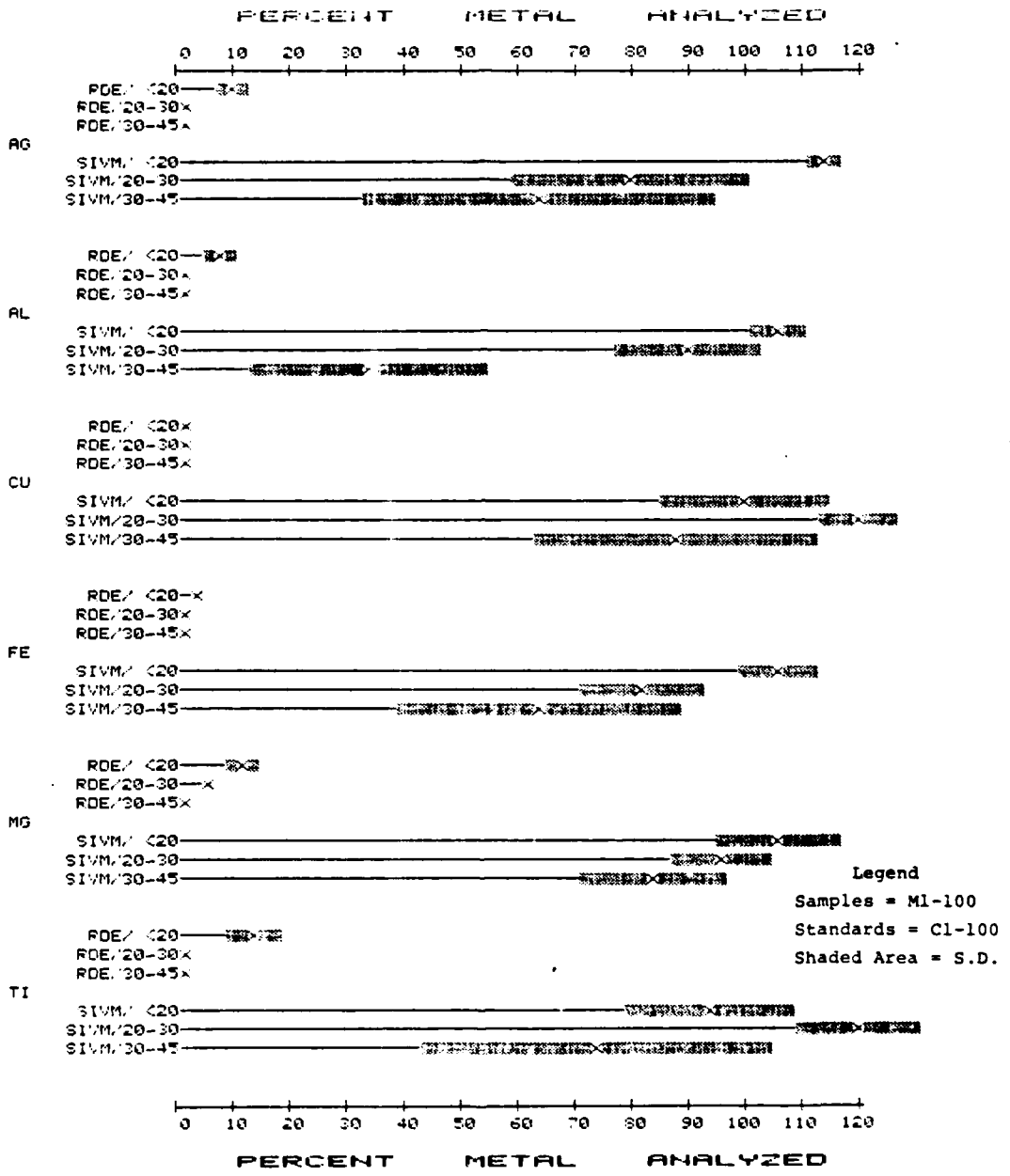

Figure 54. The Effects of Particle Size (μm) on the Percent Metal Analyzed by the SIVM and Direct Analysis (RDE).

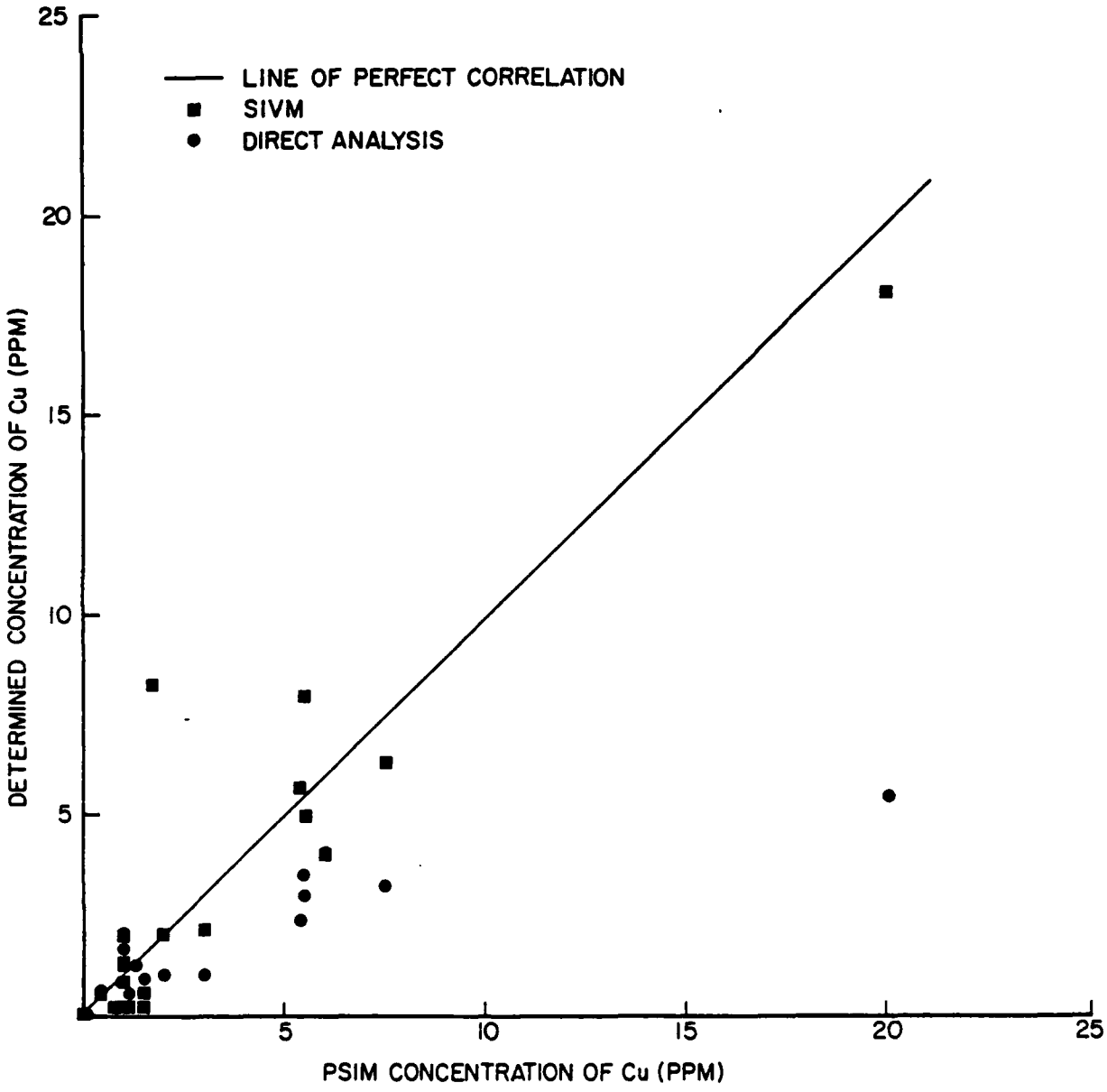

Figure 55. Comparison of the SIVM and Direct Analyses with the PSIM Analyses of Cu in Used MIL-L-23699 Oil Samples.

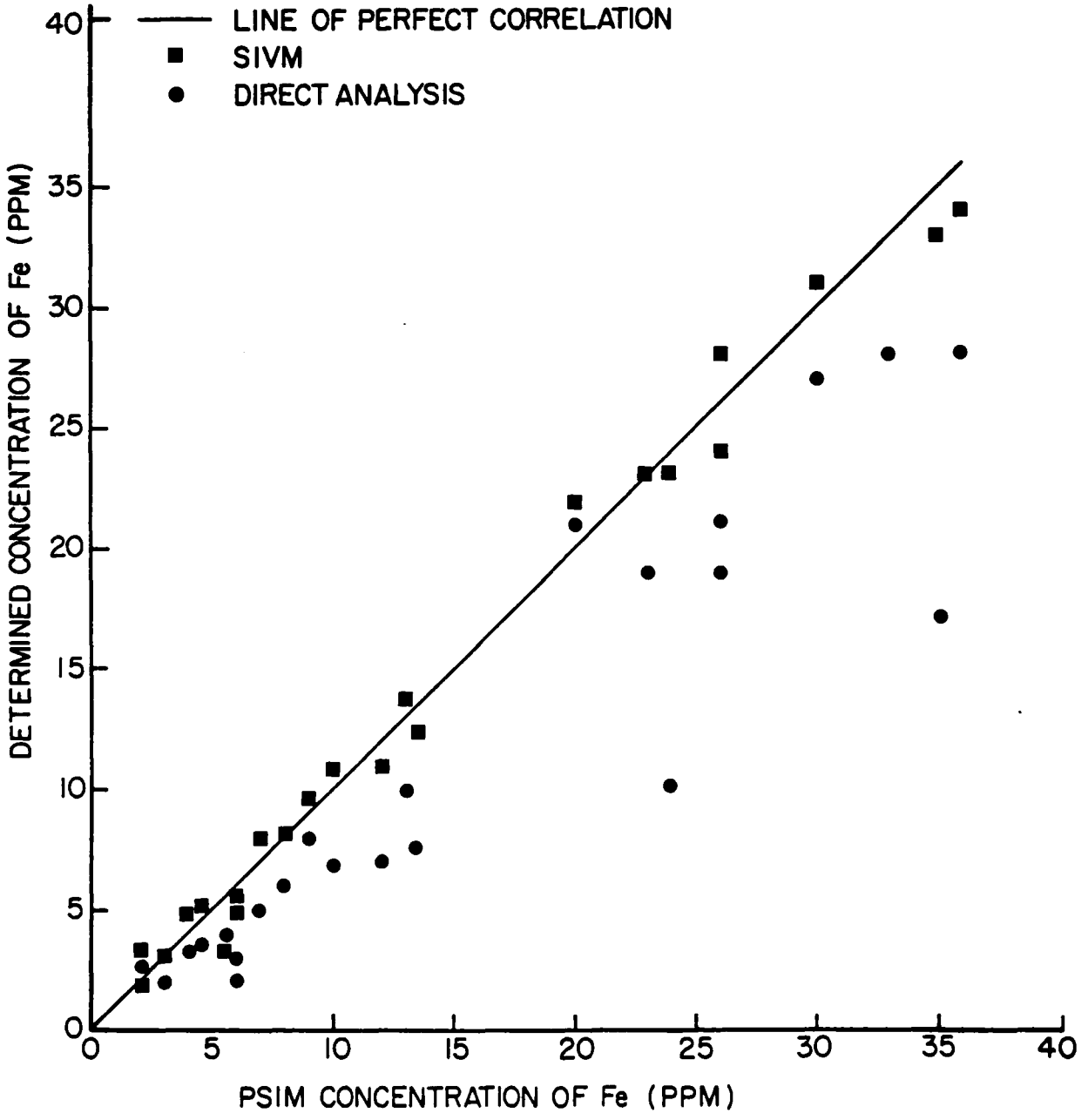

Figure 56. Comparison of the SIVM and Direct Analyses with the PSIM Analyses of Fe in Used MIL-L-23699 Oil Samples.

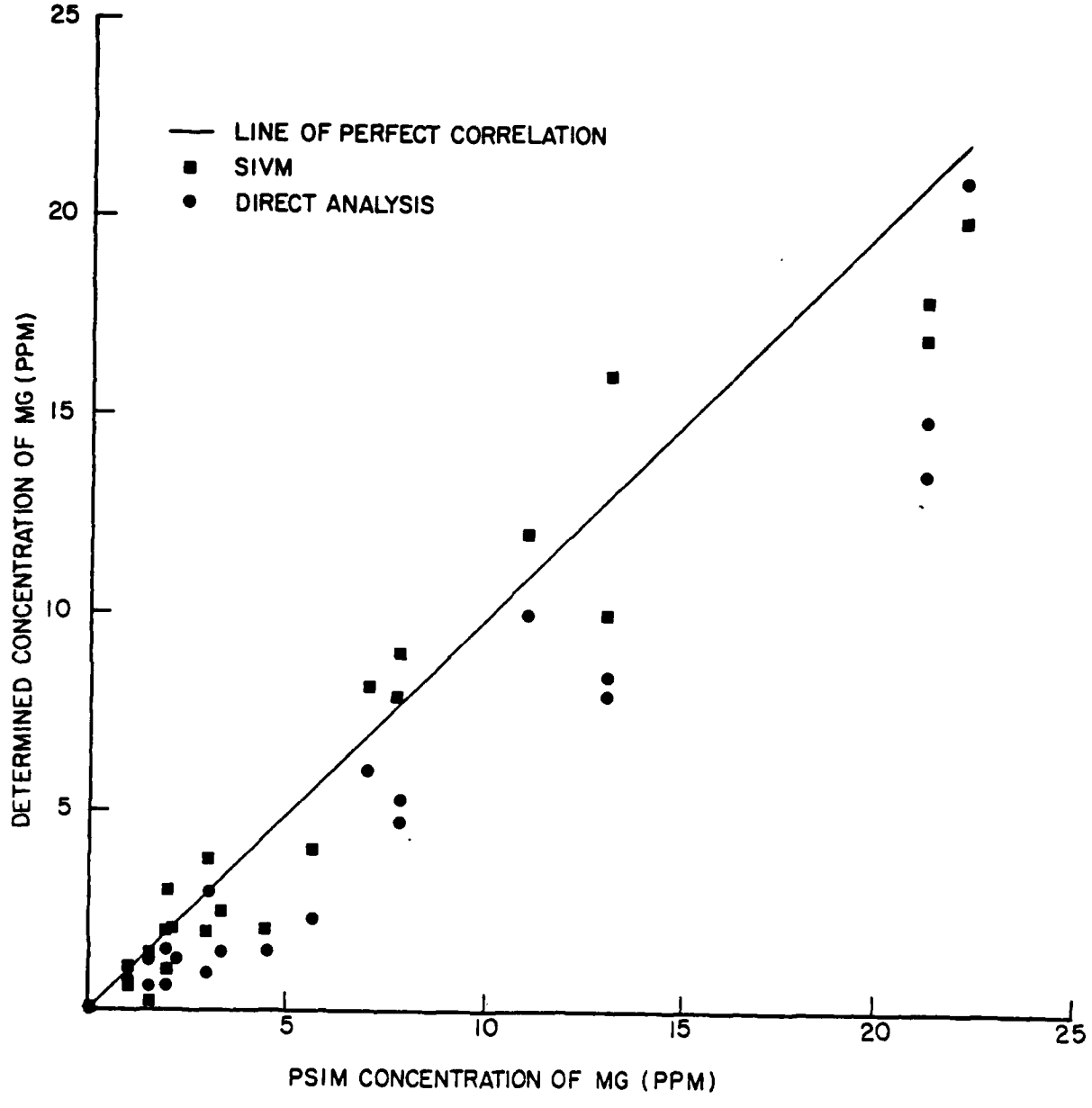

Figure 57. The Comparison of the SIVM and Direct Analyses with the PSIM Analyses of Mg in Used MIL-L-23699 Oil Samples.

analysis with the RDE. The correlation is best for Fe, which is to be expected since the experimental condition were optimized for its analysis. In general, the SIVM produces comparable results to direct analysis on the A/E35U-3 for samples containing small particles (<1 μm) but produces more accurate concentrations than direct analysis for samples containing larger (>10 μm) particles.

c. Therefore, even though the SIVM produced particle size limited analyses of the single metal powder suspensions, the SIVM enabled the A/E35U-3 spectrometer to perform particle size independent analyses of the authentic used oil samples. When compared to metal powder suspensions, the authentic used oil samples normally contain a lower concentration of wear metal particles which are usually smaller than 10 μm and may be oxidized or metallo-organic in nature [reference (dd)]. Also, the upper limit of the wear metal particles' size is controlled by the sampling procedure which may allow most of the larger particles (greater than 50 μm) to settle out.

4. ANALYSIS OF THE Si_3N_4 AND TiC CERAMIC POWDERS.

a. To determine the potential of the SIVM for analyzing ceramic wear particles, Si_3N_4 and TiC ceramic powders suspended in MIL-L-23699 lubricating oil were analyzed with the manual SIVM on the A/E35U-3. The results in Table 40 show that Si_3N_4 is readily analyzed by the SIVM.

b. However, the results in Table 40 show that the TiC is detected by the SIVM but only after a second atomization of the sample. This result cannot be explained at this time.

5. CAPABILITY OF THE SIVM TO DIFFERENTIATE OXIDATION STATES OF IRON WEAR DEBRIS.

a. It has been reported [reference (dd)] that the chemical nature of the iron wear debris present in used oil samples is dependent upon the severity and mechanism of the wear producing the debris. Therefore, information on the chemical nature of the iron wear debris could be used to improve maintenance recommendations. The results presented in Table 26 (page 110) showed that the iron particles and metallo-organic standards atomize at approximately the same temperatures. Therefore, the SIVM will probably not be capable of differentiating between metallic and metallo-organic wear debris.

b. To determine if the SIVM is capable of differentiating between iron and ferric oxide, Fe_2O_3, MIL-L-23699 suspensions of Fe and Fe_2O_3 were analyzed under various atomization temperatures and timing sequences. The results in Table 41 show that none of the atomization conditions investigated were capable of completely separating the Fe and Fe_2O_3 signals. However, complete atomization of the Fe_2O_3 powder could be accomplished while atomizing less than 20 percent of the Fe_2O_3 particles. Therefore, the SIVM possesses the potential for differentiating between the oxidation states of Fe wear debris once finer control of the atomization conditions is achieved.

TABLE 40. ANALYSES OF SILICON NITRIDE AND TITANIUM CARBIDE CERAMIC POWDERS BY THE SIVM AND DIRECT ANALYSIS (RDE)

Sample	Repetitive Analysis (SIVM)	A/E35U-3 Readout (SIVM)	% Metal Analyzed[a] SIVM	RDE
Si_3N_4	1	70	85	40
	2	2		
TiC	1	--[b]		
	2	80	72	10
	3	2		

[a]Single Element Si and Ti Standards Used
[b]-- Not Detected
Ashing Conditions - Time: 13 seconds
Rheostat (R1) Setting: 140 ohms (see Figure 11)
Atomizing Conditions - 1st Step Time: 2 seconds
Total Resistance: 57 ohms
2nd Step Time: 3 seconds
Total Resistance: 15 ohms
Atomization Chamber - Design c With Sample Introduction Port
Argon Flow Rate - 1.5 l/min.

TABLE 41. THE EFFECTS OF ATOMIZATION CONDITIONS ON THE A/E35U-3 READOUTS OF THE SIVM FOR IRON AND FERRIC OXIDE

Rheostat R2 Setting[a] (Ohms)	Repetitive Analysis	A/E35U-3 Readout Fe[c]	A/E35U-3 Readout Fe_2O_3[d]
85	1	--[b]	--
	2	--	4
70	1	30	319
	2	160	6
55	1	210	285
	2	80	2

[a]Decreasing Resistance - Increases Atomization Temperature
[b] -- Not Detected
Ashing Conditions - Time: 13 seconds
Rheostat (R1) Setting: 140 ohms (see Figure 11)
Atomizing Conditions - Time: 5 seconds
Total Resistance: 57 ohms (R2=85 ohms) to 42 ohms (R2=55 ohms)
Atomization Chamber - Design c With Sample Introduction Port
Argon Flow Rate - 1.5 l/min.
[c]Fe = 100 ppm
[d]Fe_2O_3 = 70 ppm Fe

6. COMPARISON OF THE MANUAL SIVM AND DIRECT ANALYSIS ON THE A/E35U-3 SPECTROMETER.

a. In order to evaluate the SIVM's capability for improving the particle detection capabilities of the A/E35U-3, the analytical results and experimental parameters for the SIVM and direct analysis on the A/E35U-3 are summarized in Table 42.

b. As seen in Table 42 the SIVM provides significant improvement in the particle detection capabilities for the A/E35U-3. The SIVM has the additional benefits of using smaller amounts of the calibration standard, eliminating the need for sample holders, and it can be used to analyze small oil samples when necessary. The SIVM also has the potential of providing information on the particle size and oxidation state of the wear debris present in used oil samples.

c. Once the problems identified for the SIVM have been solved or minimized, i.e., detection of Mo, effects of vaporized oil on the stability of the A/E35U-3's spark source, and the precision of the analytical results, the SIVM should be very suitable for use with the A/E35U-3.

TABLE 42. COMPARISON OF THE MANUAL SIVM AND DIRECT ANALYSIS (RDE) ON THE A/E35U-3 SPECTROMETER

	SIVM	RDE
Particle Size Limit		
Analyze Accurately	20-30 μm	3-10 μm
Detection	>45 μm	8-20 μm
Sample Requirements	Limited[a]	>2 ml
Sample Preparation	15 second ashing	None
A/E35U-3 Burn Cycle	18 second	33 seconds
Total Analysis Time	33 seconds	33 seconds
Use of Inert Gas	0.5 l/min.	None
Matrix Effect	None	Strong
Concomitant Element Effect	Slight	Strong
Information on Particle Size Distribution of Wear Metal	Possible	None
Information on Oxidation State of Wear Metal	Possible	None

[a]Upper Limit Determined by Atomizer Design, Lower Limit Dependent on Spectrometer Sensitivity

IV. CONCLUSIONS

A. ACID DISSOLUTION METHODS.

1. During this project, research was conducted to develop acid dissolution methods which could be used with the RDE spectrometers. The best method previously available [reference (1)] used a mixture of HF, HCl and HNO_3 in a ratio of 1:8:1. The presence of HF is undesirable because of its detrimental effects on glass components and its toxic properties. Therefore, a replacement for HF was needed.

2. Giering and Lukas [reference (k)] reported that sulfonic acids dissolve Mo and Ti in the presence of an oxidizing agent. Acid mixtures employing HNO_3, HCl, and p-toluene sulfonic acid (PTS) were investigated and the optimum ratio of the acids was found to be 1:8.5:0.5 [Paragraph III.B.2.b.(3)]. For optimum results, the acid was added to the oil, heated at 65°C for 5 minutes and then diluted with Neodol 91-8 to obtain a homogeneous solution for analysis [Paragraph III.B.2b.(2)].

3. The method does not give excellent results on the A/E35U-1 because of matrix differences between the sample and the standards [Paragraph III.B.2.d.(1)]. Heating the standard at 65°C for 5 minutes did not significantly improve the agreement between standards and acid treated suspensions of metal powders [Paragraph III.B.2.d.(2)].

4. Another acid method (ADM-2) was investigated where the acids are diluted with surfactant and the acid-surfactant solution is added to the oil. In this case, the optimum acid mixture was a 4:3 ratio of HNO_3 and PTS [Paragraph III.B.3c.(1)]. The dilution of the acids with surfactant reduced the method's effectiveness [Paragraph III.B.3.b].

5. Since the acid solutions eventually dissolved the metal spindle for the RDE [Paragraph III.B.3.d.(1)], the acid treated samples were analyzed using alternative electrodes that do not require any metal parts such as the porous cup electrode and the vacuum cup electrode. The presence of water in the acid treated samples caused the oil to boil out of the porous cup electrodes [Paragraph III.B.3.d.(2)]. Therefore, the porous cup electrodes could not be used to analyze acid treated samples. Results obtained with the vacuum cup electrode were more encouraging. The agreement between samples and standards was poor but the precision was very good [Paragraph III.B.3d.(3).(a)].

B. SPARK-TO-RESIDUE METHODS.

1. During this project research was conducted to develop a spark-to-residue method for improving the particle detection capabilities of spark source emission spectrometers. Spark-to-residue methods involve depositing the oil sample on a graphite electrode, heating the electrode to ash the oil, and analyzing the residue with the spark source.

2. The rotating platform electrode was especially designed for spark-to-residue methods and was investigated for the analysis of wear metal particles.

The best metal particle recoveries were obtained using the 160° electrode after ashing the oil for 1 minute at 400°C [Paragraphs III.C.2.c and III.C.2.c(2)]. The RPE gave poor agreement between samples containing particles and the Conostan standards [Paragraph III.C.2.h.(1)] and none of the variables studied improved the results to an acceptable level.

3. Two ashing methods were investigated and ashing in a furnace was found to give the best results. Laser ashing was found to be impractical since the oil moved away from the laser beam [Paragraph III.C.2.g.(1)].

4. Two additional electrodes, the RDE and RSE, were investigated for use with spark-to-residue methods. For the rotating disk electrode, the oil was deposited on the rim of the rotating disk electrode, ashed, and the residue analyzed. The RDE was not rotated during the preburn cycle to reduce the amount of metal vaporized prior to the integration cycle. A switch was installed in the circuit controlling the RDE's motor so that its rotation could be controlled.

5. There are problems with ashing the oil on the rotating disk electrode. The best results were obtained using a furnace temperature of 600°C [Paragraph III.C.3.b.(1).(a)]. Above this temperature the oil ignited and below this temperature the oil dripped off the electrode.

6. The ashing step can be performed with the electrode rotating or stationary. Either approach can be used without affecting the analytical results significantly [Paragraph III.C.3.b.(2)]. However, if the electrode is ashed while stationary its orientation in the spectrometer is important.

7. If the electrode is held stationary during the ashing step, the sample concentrates at the bottom of the electrode and should be placed in the spectrometer in the same orientation used for ashing. Since the electrode is held stationary during the preburn cycle, none or very little wear metal is vaporized prior to integration of the emission signal [Paragraph III.C.3b.(1).(b)].

8. As was observed for the RPE, the emission readouts for the C13 standards and the M12 suspension analyzed on the RDE, were in very poor agreement [Paragraph III.C.3.f.(1)]. However, in contrast to the RPE, the emission readouts for all of the metals analyzed in the M12 suspension (except Cu) are higher than those for the C13 standard [Paragraph III.C.3.g.(2)].

9. The other electrode investigated was the reciprocating semicylindrical electrode. This electrode suffered from the same limitations observed for the other electrodes, and the emission readouts for the M12 suspensions and the C13 standards were in the least agreement [Paragraph III.C.4.c].

10. Although the STRM improves the particle detection capabilities of the A/E35U-1, the metal recoveries produced by the different STRMs are superficially high.

11. The enchanced analyses for particles are caused by the fact that the metal particles and Conostan standards behave differently in the spark source (Paragraphs III.C.2.h, III.C.3.f, and III.C.4.c). Although the metal

recoveries are enchanced by shorter burn times [Paragraphs III.C.2.i and III.C.3.g] and by the 160° electrode [Paragraph III.C.2.c and III.C.3.d), the effects of the other factors studied depended on the type of electrode used and the metal being analyzed (Paragraph III.C.2, III.C.3, and III.C.4). Of the electrodes tested, the highest metal recoveries for all of the metals studied are produced by the RDE, followed by the RSE, and then the RPE (Table 22).

12. Normally the RDE is rotated clockwise at 30 rpm. In this work, the effect of rotation direction was studied using C13-50 and M12-50 samples. The rotation direction of the RDE or counter-electrode configuration had no effect on the emission signals measured for the C13-50 standards. However, when the 160° counter-electrode was used to analyze the M12-50 suspensions, higher percent metal recoveries for all the metals except Cu were obtained when the RDE was rotated counterclockwise [Paragraph III.C.3.e.(2)].

C. ACID DISSOLUTION - SPARK-TO-RESIDUE METHOD.

1. Since the spark-to-residue method did not give the desired results, other approaches were investigated. The main difference between the C13 standards and M12 suspension is that the standards are dissolved metallo-organic compounds and the suspension contains metallic particles. Therefore, the differences between samples and standards can be reduced by dissolving the metal particles prior to analysis by using an acid dissolution procedure.

2. The best results were obtained using the 1:8:1 acid mixture of HNO_3, HCl and HF to dissolve the metal particles [Paragraph III.C.5.a]. The dissolution process was carried out at 65°C for 3 minutes [Paragraph III.C.5.b). After dissolution the amine sulfonate stabilizer and Neodol 91-8 were added and samples ashed on the RPE in the furnace.

3. The analytical results for the M12 suspension and C13 standard give the best agreement for this method (Paragraph III.C.6.d). All of the metals analyzed gave 100 percent recoveries except Al which was 74 percent and Sn which was 119 percent (Table 22).

D. SPARK-IN-VAPOR METHOD.

1. Spark-in-vapor methods involve depositing the oil onto an electrothermal atomization device. The device is heated to vaporize the oil and then heated to a higher temperature to atomize any metal species present. The metal vapor is carried to the source by the stream of gas flowing through the device.

2. Of the atomizers studied, the tungsten filaments have the most potential for use as an electrothermal atomizer. They can be used without a high current power supply and can be heated to 2900°C to vaporize all the metals [Paragraph III.D.2.e.(1)].

3. The optimum conditions for ashing samples on the tungsten filament

involve using samples smaller than 25 µl [Paragraph III.D.3.e], small atomization chambers [Paragraph III.D.3.f] and argon flow rates of 1.5 l/min. [Paragraph III.D.3.d].

4. The optimum conditions for the ashing step are not consistent with those required for optimum metal analyses on the A/E35U-1 spectrometer. The best analytical results were obtained with the small atomization chamber and slow flow rates of argon [Paragraph III.D.4.c.(3)]. The best atomization procedure involved increasing the filaments temperature in two steps [Paragraph III.D.4.b.(3).(e)]. The vapor transporting electrode with an orifice of 1.0 mm diameter (BC-1) [Paragraph III.D.5.c.(1)] and the 160° counter-electrode gave the best emission intensities for the metals analyzed [Paragraph III.D.5.b] on the A/35U-1 spectrometer.

5. The optimum conditions for analyses on the A/E35U-3 spectrometer were different. The different results were attributed to the differences in the spark sources used on the A/E35U-1 and the A/E35U-3 (Paragraph IIIF3b(1)(a)). For analysis on the A/E35U-3 the small atomization chamber (design c) was used and the auxiliary gap was set to give an ammeter reading of 3.0 amperes. For best results the ashing step was conducted prior to starting the burn cycle.

6. Higher readouts were obtained using the vapor transporting electrode with the 2.1 mm orifice [Paragraph III.F.3.b.(3).(c)] and high flow rates of argon (~3.0 l/min.) [Paragraph III.F.3.b.(4).(a)]. At the maximum filament temperatures, Mo and Ti were not detected [Paragraph III.F.3.c] using a one step atomization procedure. However, Ti could be detected by using a two step atomization procedure [Paragraph III.F.3.d.(2)].

7. The particle size capabilities of the spark-to-vapor method were determined on the A/E35U-3. The SIVM improved the particle detection capabilities of the A/E35U-3 so that the spectrometer can detect greater than 45 µm particles of all the metals studied and provide accurate analyses of particles smaller than 20-30 µm [Paragraph III.G.2.d].

8. Authentic used oils were analyzed using the SVIM on the A/E35U-3. Excellent results were obtained for Fe analysis giving concentrations that agreed with those determined by the particle size independent method (PSIM) (Paragraph IIIG3b).

9. Samples of Fe and Fe_2O_3 suspended in MIL-L-23699 oils were analyzed under various atomization conditions. The results (Table 41) showed that the emission signals for Fe and Fe_2O_3 could not be completely separated. However, the Fe_2O_3 could be completely atomized while only partially atomizing the Fe particles. Therefore, the SIVM possesses the potential for differentiating between Fe and iron oxides [Paragraph III.G.5.b].

E. COMPARISON OF METHODS. Both the AD-STRM and the SIVM have potential for improving the performance of the RDE-SSAE spectrometers. However, neither of these methods gave totally acceptable results because the spark source has not been optimized for these methods [Paragraph III.F.3.e.(4).(c)].

V. RECOMMENDATIONS

A. The research conducted for this project has shown that the particle detection capabilities of the RDE-SSAE spectrometers can be improved by acid dissolution, spark-to-residue and spark-in-vapor methods. Although good results were obtained for the AD-STRM and SIVM, further research is needed to optimize these methods.

B. The best results for analyses on the A/E35U-1 were obtained using the AD-STRM with the amine sulfonate stabilizer present. The results were encouraging giving 100 percent recoveries for all metals except Al and Sn. Additional research is recommended to optimize this procedure and improve the analyses for Al and Sn. With slight modifications to the dissolution or ashing procedure, this method should give good results for all the metals.

C. Unfortunately, the AD-STRM was not adequately tested on the A/E35U-3 because of problems with the burn time. Further work is recommended to develop an AD-STRM for use with the A/E35U-3.

D. Good results were also obtained with the spark-in-vapor methods. This method has the advantage that no sample preparation is required and analyses can be conducted rapidly. However, some matrix problems remain and the accuracy of determinations for samples containing particles is not as high as desired. Samples containing large particles of Cu, Si, and Sn give superficially high results on the A/E35U-1.

E. The SIVM also works well with the A/E35U-3 but has not been optimized for use with the source on the A/E35U-3. Further work should be conducted to improve the accuracy of the method on the A/E35U-3.

F. The spark source used on these instruments has not been optimized for the spark-to-residue or spark-in-vapor methods. Therefore, research should be conducted to investigate the properties of the spark sources. The properties of the spark which affect metal recoveries by direct analysis, by spark-to-residue analysis, and by spark-in-vapor analysis, should be delineated. Once the spark's characteristics are known, a spark source can be designed which gives optimum metal analyses for each method.

G. The spark-in-vapor methods have the most potential for routine use with the spark source instruments since no sample preparation is required. With further work the method could be used to get an approximate particle size distribution of the wear debris and may also be able to provide information concerning the chemical composition of the wear debris.

VI. REFERENCES

(a) AFLC Historical Study No. 393 of December 1982: The Air Force Spectrometric Oil Analysis Program 1963-1980.

(b) Beerbower, A. "Spectrometry and Other Analysis Tools for Failure Prognosis". J. American Soc. of Lub. Engineers, V. 32, No. 6, P. 285, 1975.

(c) Seifert, W. W. and Wescott, V. C. "Investigation of Iron Content of Lubricating Oils Using a Ferrograph and an Emission Spectrometer". Wear, V. 23, No. 2, P. 239, 1973.

(d) Naval Aviation Integrated Logistic Support Center Report No. 03-41 of 27 May 1976: An Investigation of the Navy Oil Analysis Program (NOAP).

(e) Lee, R., Technical Support Center, Naval Air Station, Pensacola, Florida, Private Communication, 1979.

(f) AFWAL Report No. TR-82-4017 of February 1982: Evaluation of Plasma Source Spectrometers for the Air Force Oil Analysis Program.

(g) NAEC Report No. 92-169 of April 1983: Spectrometer Sensitivity Investigations on the Spectrometric Oil Analysis Program.

(h) Naval Air Systems Command Report No. NA17-15-50 of 1 May 1977: Joint Oil Analysis Program Laboratory Manual.

(i) Baird Corp. Report No. FSN6650-937-4401 of 15 May 1972: Spectrometer, Engine Oil Analysis, A/E35U-1 Technical Manual.

(j) Baird Corp. Report No. FSN6650-251-0712 of 1 February 1973: Operation Instructions, Maintenance Instructions, Fluid Analysis Spectrometer (FAS-2).

(k) Giering, L. P. and Lukas, M. "A Method for the Analysis of Lubricating Oils Containing Large Wear Metal Particles". Symposium No. 95a on Military Technology Oil Analysis 1978; Materialpruefstelle der Bundeswehr und Bundesakademie fur Wehruerwaltung und Wehrtechnik: Erding, West Germany, July 1978.

(l) Kauffman, R. E.; Saha, C. S.; Rhine, W. E.; and Eisentraut, K. J. "Quantitative Multielement Determination of Metallic Wear Species in Lubricating Oils and Hydraulic Fluid". Anal. Chem., V. 54, P. 975, 1982.

(m) Gassman, A. and O'Neill, W. "The Use of a Porous-Cup Electrode in the Spectrographic Analyses of Lubricating Oils". Proceedings, Amer. Petrol. Inst., V. 29M, P. 79, 1949.

(n) Feldman, C. "Direct Spectrochemical Analysis of Solutions Using Spark Excitation and the Porous Cup Electrode". Anal. Chem., V. 21, P. 1041, 1949.

(o) MacGowan, R. J. "Spectrochemical Analysis of Oils Using Vacuum Cup Electrode". Appl. Spectrosc., V. 15, P. 179, 1961.

(p) Zink, T. "A Vacuum Cup Electrode for the Spectrochemical Analysis of Solutions". Appl. Spectrosc., V. 13, P. 94, 1959.

(q) Baer, W. and Hodge, E. "The Spectrochemical Analysis of Solutions, A Comparison of Five Techniques". J. Appl. Spectry., V. 14, P. 141, 1960.

(r) Hodge, E. "Spectrographic Tricks", J. Appl. Spectry., V. 15, P. 21, 1961.

(s) Wynn, T. F.; et al. "Wavelength-Modulated, Continuum-Source Excited Atomic Fluorescence Spectrometric System for Wear Metals in Jet-Engine Lubricating Oils Using Electrothermal Atomization". Anal. Chim. Acta, V. 124, P. 155, 1981.

(t) Chuang, F.S. and Winefordner, J. P. "Jet Engine Oil Analysis by Atomic Absorption Spectrometry with a Graphite Filament". Appl. Spectrosc., V. 28, P. 215, 1974.

(u) Hall, G.; Bratzel, M. P.; and Chakrabarti, C. L. "Evaluation of a Carbon-Rod Atomizer for Routine Determination of Trace Metals by Atomic-Absorption Spectroscopy: Applications to Analysis of Lubricating Oil and Crude Oil". Talanta, V. 20, P. 755, 1973.

(v) Patel, B. M. and Winefordner, J. D. "Graphite Rod Atomization and Atomic Fluorescence for the Simultaneous Determination of Silver and Copper in Jet Engine Oils". Anal. Chim. Acta, V. 64, P. 135, 1973.

(w) Reeves, R. D.; et al. "Determination of Wear Metals in Engine Oils by Atomic Absorption Spectrometry With a Graphite Rod Atomizer". Anal. Chem., V. 44, P. 2205, 1972.

(x) Reeves, R. D.; Molnar, C. J.; and Winefordner, J. D. "Rapid Atomic Absorption Determination of Silver and Copper by Sequential Atomization From a Graphite Rod". Anal. Chem., V. 44, P. 1913, 1982.

(y) Alder, J. F. and West, T. S. "Atomic Absorption and Fluorescence Spectrophotometry with a Carbon Filament Atom Reservior: Part IX. The Direct Determination of Silver and Copper in Lubricating Oils". Anal. Chim. Acta, V. 58, P. 331, 1972.

(z) Everett, G. L.; West T. S.; and Williams, R. W. "The Determination of Manganese in Lubricating Oils by Carbon Filament Atomic Absorption Spectrometry". Anal. Chim. Acta, V. 70, P. 204, 1974.

(aa) Dodge, W. B. and Allen, R. O. "Trace Analysis by Metastable Energy Transfer for Atomic Luminescence". Anal. Chem., V. 53, P. 1279, 1981.

(bb) Williams, M. and Piepmeir, E. H. "Commercial Tungsten Filament Atomizer for Analytical Atomic Spectrometry". Anal. Chem., V. 44, P. 1342, 1972.

(cc) Montaser, A.; Goode, S. R.; and Crouch, S. R. "Graphite Braid Atomizer for Atomic Absorption and Atomic Fluoresence Spectrometry". Anal. Chem., V. 46, P. 599, 1974.

(dd) AFWAL Report No. TR-81-4184 of January 1982: Research and Development of Wear Metal Analysis.

(ee) Goldberg, J. and Sacks, R. "Direct Determination of Metallic Elements in Solid Powder Samples with Electrically Vaporized Thin Film Atomic Emission Spectrometry". Anal. Chem., V. 54, P. 2179, 1982.

(ff) Prack, E. R. and Bastiaans, G. J. "Metal Specification by Evolved Gas/Inductively Coupled Plasma Atomic Emission Spectrometry". Anal. Chem., V. 55, P. 1654, 1983.

(gg) Harnly, J. M. and Kane, J. S. "Optimization of Electrothermal Atomization Parameters for Simultaneous Multielement Atomic Absorption Spectrometry". Anal. Chem., V. 56, P. 48, 1984.

VII. BIBLIOGRAPHY

A. ELECTROTHERMAL ATOMIZERS.

1. Aggett, J. "The Determination of Gold in Serum by Atomic Absorption Spectrometry With a Carbon Filament Reservoir". Anal. Chim. Acta, V. 63, P. 473, 1972.

2. Aggett, J. and Sprott, A. J. "Non-Flame Atomization in Atomic Absorption Spectrometry". Anal. Chim. Acta, V. 72, P. 49, 1974.

3. Alder, J. F. and West, T. S. "Atomic Absorption and Fluorescence Spectrophotometry With a Carbon Filament Atom Reservoir: Part IX. The Direct Determination of Silver and Copper in Lubricating Oils". Anal. Chim. Acta, V. 58, P. 331, 1972.

4. Alder, J. F. and West, T. S. "Atomic Absorption and Fluorescence Spectroscopy With a Carbon Filament Atomic Reservoir: Part XII. The Determination of Nickel in Crude and Residual Fuel Oils by Atomic Absorption Spectrometry". Anal. Chim. Acta, V. 61, P. 132, 1972.

5. Amos, M. D.; et al. "Carbon Rod Atomizer in Atomic Absorption and Fluorescence Spectrometry and Its Clinical Application". Anal. Chem., V. 43, P. 211, 1971.

6. Belyaev, Y. I.; Karyakin, A. V.; and Pchelintsev, A. M. "Increasing the Sensitivity of the Atomic-Fluorescent Determination of Traces of Elements by Using an Arc Pulse Atomizer for Solid Samples". J. Anal. Chem. USSR, V. 25, P. 735, 1970.

7. Belyaev, Y. I.; et al. "The Use of a DC Arc for the Atomic Absorption Determination of Traces of Elements". J. Anal. Chem. USSR, 23, P. 432, 1968.

8. Blac, M. S.; Glenn, T. H.; Bratzel, M. P.; and Winefordner, J. D. "Atomic Fluorescence Spectrometry With Continuous Nebulization into a Platinum Furnace". Anal. Chem., V. 43, P. 1769, 1971.

9. Bratzel, M. P.; Dagnall, R. M.; and Winefordner, J. D. "A New Simple Atom Reservoir for Atomic Fluorescence Spectrometry". Anal. Chim. Acta, V. 48, P. 197, 1969.

10. Brodie, K. G. and Matousek, J. P. "Application of the Carbon Rod Atomizer to Atomic Absorption Spectrometry of Petroleum Products". Anal. Chem., 43, P. 1557, 1971.

11. Caruso, J. A. and NG, K. C. "Microliter Sample Introduction Into an Inductively-Coupled Plasma by Electrothermal Carbon Cup Vaporization". Anal. Chim. Acta, V. 143, P. 209, 1982.

12. Chauvin, J. V.; Newton, M. P.; and Davis, D. G. "The Determination of Lead and Nickel by Atomic-Absorption Spectrometry With a Flameless Wire Loop Atomizer". Anal. Chim. Acta, V. 65, P. 291, 1973.

13. Chuang, F. S. and Winefordner, J. D. "Jet Engine Oil Analysis by Atomic Absorption Spectrometry Witn a Graphite Filament". Appl. Spectrosc., V. 28, P. 215, 1974.

14. Dewey, D. R.; Lincoln, Kopito, L. "Excitation Source for Emission Spectroscopy". U. S. Patent No. 3,1174,393; March 23, 1965.

15. Dittrich, K. and Borzym, K. "Bestimmung von Spuren Seltener Erden in Anderen Seltenen Erden Durch Atomabsorption mit Elecktrothermischer Atomisierung and Emissionsspecktrographie mit dem Gleichstromdauerbogen". Anal. Chim. Acta, V. 94, P. 83, 1977.

16. Donega, H. M. and Burgess, T. E. "Atomic Absorption Analysis by Flameless Atomization in a Controlled Atmosphere". Anal. Chem., V. 42, P. 1521, 1970.

17. Everett, G. L. and West, T. S. "Atomic Absorption and Fluorescence Spectrometry With a Carbon Filament Atomic Reservoir: Part XIV. The Determination of Vanadium in Fuel Oils". Anal. Chim. Acta, V. 66, P. 301, 1973.

18. Everett, G. L.; West, T. S.; and Williams, R. W. "The Determination of Manganese in Lubricating Oils by Carbon Filament Atomic Absorption Spectrometry". Anal. Chim. Acta, V. 70, P. 204, 1974.

19. Fricke, F. L.; Rose, O.; and Caruso, J. A. "Simultaneous Multielement Determination of Trace Metals by Microwave Induced Plasma Coupled to Vidicon Detector: Carbon Cup Sample Introduction". Anal. Chem., V. 47, P. 2018, 1975.

20. Gilbert, T. R. and Hildebrand, K. J. "A Graphite Filament Plasma/Echelle Spectrometer System: An Advance Report". Amer. Lab., P. 72, February 1982.

21. Gregoire, D. C.; Chakrabarti, C. L.; and Bertels, P. C. "Effects of Heating Rates in Graphite Furnace Atomic Absorption Spectrometry". Anal. Chem., V. 50, P. 1731, 1978.

22. Grime, J. K. and Vickers, T. J. "Determination of Lithium in Microliter Samples of Blood Serum Using Flame Atomic Emission Spectrometry With a Tantalum Filament Vaporizer". Anal. Chem., V. 47, P. 432, 1975.

23. Grushko, L. F.; Ivanov, N. P.; and Chupakhim, M. S. "Analytical Possibilities of an Atomizer With a Tantalum Ribbon as Vaporizer". J. Anal. Chem. USSR, V. 29, P. 1584, 1974.

24. Hall, G.; Bratzel, M. P.; and Chakrabarti, C. L. "Evaluation of a Carbon-Rod Atomizer for Routine Determination of Trace Metals by Atomic-Absorption Spectroscopy: Applications to Analysis of Lubricating Oil and Crude Oil". Talanta, V. 20, P. 755, 1973.

25. Hasegawa, T.; Yanagisawa, M.; and Takeuchi, T. "The Atomization Processes of Calcium, Aluminum and Manganese Oxides on a Molybdenum Filament". Anal. Chim. Acta, V. 89, P. 217, 1977.

26. Hwang, J. Y.; Mokeler, C. J.; and Ullucci, P. A. "Maximization of Sensitivities in Tantalum Ribbon Flameless Atomic Absorption Spectrometry". Anal. Chem., V. 44, P. 2018, 1972.

27. Hwang, J. Y.; Ullucci, P. A.; Smith, S. B.; and Malenfant, A. L. "Microdetermination of Lead in Blood by Flameless Atomic Absorption Spectrometry". Anal. Chem., V. 43, P. 1319, 1971.

28. Kirkbright, G. F. "The Application of Non-Flame Atom Cells in Atomic Absorption and Atomic Fluorescence Spectorscopy". Analyst, V. 96, P. 609, 1971.

29. Kirkbright, G. F. and Snook, R. D. "The Determination of Some Trace Elements in Uranium By Inductively Coupled Plasma Emission Spectroscopy Using a Graphite Rod Sample Introduction Technique". Appl. Spectrosc., V. 37, P. 11, 1983.

30. Kyuregyan, S. K. and Marenova, M. M. "A Direct Spectral Method for Determining Wear Products in Lubricating Oils". Chem. Tech. Oils Fuels, V. 7, P. 527, 1967.

31. L'vov, B. V. "The Analytical Use of Atomic Absorption Spectra". Spectrochim. Acta, V. 17, P. 761, 1961.

32. L'vov, B. V. "The Potentialities of the Graphite Crucible Method in Atomic Absorption Spectroscopy". Spectrochim. Acta, V. 24B, P. 53, 1969.

33. Massman, H. "Vergleich von Atomabsorption and Atomfluoreszenz in der Graphitkuvette". Spectrochim. Acta, V. 23B, P. 215, 1968.

34. Molnar, C. J.; et al. "Construction and Evaluation of a Versatile Graphite Filament for Atomic Absorption Spectrometry". Appl. Spectrosc., V. 26, P. 606, 1972.

35. Molnar, C. J. and Winefordner, J. D. "Vitreous Carbon Furnace With Continuous Sample Introduction for Atomic Fluorescence Spectrometry". Anal. Chem., V. 46, P. 1419, 1974.

36. Montaser, A.; Goode, S. R.; and Crouch, S. R. "Graphite Braid Atomizer for Atomic Absorption and Atomic Fluorescence Spectrometry". Anal. Chem., V. 46, P. 599, 1974.

37. Murphy, M. K.; Clyburn, S. A.; and Veillon, C. "Comparison of Lock-In Amplification and Photon Counting With Low Background Flames and Graphite Atomizers in Atomic Fluorescence Spectrometry". Anal. Chem., V. 45, P. 1468, 1973.

38. Nixon, D. E.; Fassel, V. A.; and Kniseley, R. N. "Inductively Coupled Plasma-Optical Emission Analytical Spectroscopy: Tantalum Filament Vaporization of Microliter Samples". Anal. Chem., V. 46, P. 210, 1974.

39. Ohta, K. and Suzuki, M. "Trace Metal Analysis of Rocks by Flameless Atomic Absorption Spectrometry With a Metal Microtube Atomizer". Talanta, V. 22, P. 465, 1975.

40. Omang, S. H. "The Determination of Vanadium and Nickel in Mineral Oils by Flameless Graphite Tube Atomization". Anal. Chim. Acta, V. 56, P. 470, 1971.

41. Patel, B. M. and Winefordner, J. D. "Graphite Rod Atomization and Atomic Fluorescence for the Simultaneous Determination of Silver and Copper in Jet Engine Oils". Anal. Chim. Acta, V. 64, P. 135, 1973.

42. Puschell, P.; et al. "Electrothermal Atomization from Metallic Surfaces: Part 3. Some New Developments in Design and Performance of a Tungsten-Tube Atomizer". Anal. Chim. Acta, V. 127, P. 109, 1981.

43. Reeves, R. D.; et al. "Determination of Wear Metals in Engine Oils by Atomic Absorption Spectrometry With a Graphite Rod Atomizer". Anal. Chem., V. 44, P. 2205, 1972.

44. Reeves, R. D.; Mrlnar, C. J.; and Winefordner, J. D. "Rapid Atomic Absorption Determination of Silver and Copper by Sequential Atomization From a Graphite Rod". Anal. Chem., V. 44, P. 1913, 1972.

45. Siemer, M.; Ohta, K.; Yamakita, T.; and Katsuno, T. "Electrothermal Atomization With a Metal Micro-Tube in Atomic Absorption Spectrometry". Spectrochim. Acta, V. 36B, P. 679, 1981.

46. Sychria, V.; et al. "Electrothermal Atomization From Metallic Surfaces: Part I. Design and Performance of a Tungsten-Tube Atomizer". Anal. Chim. Acta, V. 105, P. 263, 1979.

47. Thelin, B. "The Use of a High Temperature Hollow Cathode Lamp for the Determination of Trace Elements in Steels, Nickel-Base Alloys, and Ferroalloys by Emission Spectrometry". Appl. Spectrosc., V. 35, P. 302, 1981.

48. Takeuchi, T.; Yanagisawa; and Suzuki, M. "Trace Analysis by Flameless Atomic-Absorption Spectrometry". Talanata, V. 19, P. 465, 1972.

49. Vogel, R. S. "A Semiautomated Device for Controlled Atmospheres in Optical Emission Spectroscopy". Appl. Spectrosc., V. 30, P. 436, 1976.

50. West, T. S. and Williams, X. K. "Atomic Absorption and Fluorescence Spectroscopy With a Carbon Filament Atom Reservoir; Part I. Construction and Operations of Atom Reservoir". Anal. Chim. Acta, V. 45, P. 27, 1969.

51. Williams, M. and Piepmeier, E. H. "Commercial Tungsten Filament Atomizer for Analytical Atomic Spectrometry". Anal. Chem., V. 44, P. 1342, 1972.

52. Wynn, T. F.; et al. "Wavelength-Modulated, Continuum-Source Excited Atomic Fluorescence Spectrometric System for Wear Metals in Jet-Engine Lubricating Oils Using Electrothermal Atomization". Anal. Chim. Acta, V. 124, P. 155, 1981.

B. LASER PROBE ANALYZERS

1. Barton, H. N. "Laser Microprobe Toxic Sample Cell". Appl. Spectrosc., V. 23, P. 519, 1969.

2. Beatrice, E. S.; Harding-Barlow, I.; and Glick, D. "Electric Spark Cross-Excitation in Laser Microprobe-Emission Spectroscopy for Samples of 10-25 μm Diameter". Appl. Spectrosc., V. 23, P. 257, 1969.

3. Blackburn, W. H.; Pelletier, Y. J. A.; and Dennen, W. H. "Spectrochemical Determinations in Garnets Using a Laser Microprobe". Appl. Spectrosc., V. 22, P. 278, 1968.

4. Brech, F. and Cross, L. "Optical Micromission Stimulated by a Ruby Maser". Appl. Spectrosc., V. 16, P. 59, 1962.

5. Brokeshoulder, S. F. and Robinson, F. R. "Laboratory Experience With In Situ Detection of Beryllium in Biological Specimens". Appl. Spectrosc., V. 22, P. 758, 1968.

6. Carr, J. W. and Horlick, G. "Laser Vaporization of Solid Metal Samples into an Inductively Coupled Plasma". Spectrochim. Acta, V. 37, P. 1, 1982

7. Dittrich, K. and Wennrich, R. "Atomabsorptionsspektrometrie durch Laser Verdampfung mit Nachfolgender Electrothermischer Atomisierung". Spectrochim. Acta, V. 35B, P. 731, 1980.

8. Grishko, V. I. and Yudelevick, I. G. "Application of Lasers in Analytical Chemistry (Review)". Ind. Lab. - USSR, V. 48, P. 321, 1982.

9. Kagawa, K. and Yokoi, S. "Application of the N-2 Plasma Microprobe Spectrochemical Analysis". Spectrochim. Acta, V. 37, P. 789, 1982.

10. Karyakin, A.; Akhmanova, M.; and Kaigorodov, V. "Spectrographic Analysis of Nonmetallics by Means of a Laser". J. Anal. Chem. USSR, V. 23, P. 1610, 1968.

11. Katsuno, Y.; et al. "Emission Spectroscopy With Laser Excitation". NASA Technical Translation No. NASA TT F-12, 681 of November 1969: Translated from Buneski Kagaku, V. 3, P. 376, 1968.

12. Katsuno, Y.; et al. "Spectroscopic Analysis With the Laser Microscope". NASA Technical Translation No. NASA TT F-12, 677 of November 1969: Translated from Bunko-Kenkyu, V. 16, P. 151, 1968.

13. Leis, F. and Laqua, K. "Emissionsspektralanalyse mit Anregung des durch Laserstrahlung Erzeugten Dampfes Fester Proben in einer Mikrowellenentladung - I. Grundlagen der Methode und Experimentelle Verwirklichung". Spectrochim. Acta, V. 33B, P. 727, 1978.

14. Leis, F. and Laqua, K. "Emissionsspektralanalyse mit Anregung des durch Laserstrahlung erzeugten Dampfes Fester Proben in einer Mikrowellenentladung - II. Analytische Anwendungen". Spectrochim. Acta, V. 34B, P. 307, 1979.

15. Lyons, D. J. and Roofayel, R. L. "Determination of Molybdenum in Plant-Material Using Inductively Coupled Plasma Emission-Spectroscopy". Analyst, V. 107, P. 331, 1982.

16. Macoy, N. H. and Zweibaum, F. "Laser Flash Heating Techniques for Atomic Absorption Spectroscopy". Report No. AFML-TR-67-287 of November 1967, Air Force Materials Laboratory, Research and Technology Division, Air Force Systems Command, Wright-Patterson Air Force Base, Ohio.

17. Morton, K. L.; Nohe, J. D.; and Madsen, B. S. "The Relationship of Spectral Line Intensity to the Weight of Sample Vaporized With the Laser Microprobe". Appl. Spectrosc., V. 27, P. 109, 1973.

18. Nickel, H.; Peuser, F. A.; and Mazurkiewicz, M. "Evaporation of Material and Influence of Auxiliary Spark Gap on the Spectral Excitation by Means of Laser Emission Spectroscopy for Local Analysis of Graphite". Spectrochim. Acta, V. 33B, P. 675, 1978.

19. Osten, D. E. and Piepmeier, E. H. "Atomic Absorption Measurements in [illegible]-Switched Laser Plume Using Pulsed Hollow Cathode Lamps". Appl. Spectrosc., V. 27, P. 165, 1973.

20. Panteleyev, V. N. and Yankouskiy, A. A. "Possibilities for Using Lasers in the Monopulse Mode for Spectral Analysis". NASA Technical Translation No. NASA TT F-12,697 of November 1969: Translated from Zh. Prik. Spektr., V. 8, P. 905, 1968.

21. Peppers, N. A.; et al. "Q-Switched Ruby Laser for Emission Microspectroscopic Elemental Analysis". Anal. Chem., V. 40, P. 1178, 1968.

22. Rasberry, S. D.; Scribner, B. F.; and Margoshes, M. "Laser Probe Excitation in Spectrochemical Analysis. I: Characteristics of the Source". Appl. Optics, V. 6, P. 81, 1967.

23. Rasberry, S. D.; Scribner, B. F.; and Margoshes, M. "Laser Probe Excitation in Spectrochemical Analysis. II: Investigations of Quantitative Aspects". Appl. Optics., V. 6, P. 87, 1967.

24. Rosan, R.; Brech, F.; and Glick, D. "Spectrographic Analysis of Nanogram Samples by Improved Laser Microprobe Techniques". Federation Proc., V. 23, P. 174, 1964.

25. Rosan, R.; Healy, M.; and McNary, W. "Spectroscopic Ultramicroanalysis With a Laser". Science, V. 142, P. 236, 1963.

26. Runge, E. F.; Minck, R. W.; and Bryan, R. F. "Spectrochemical Analysis Using A Pulsed Laser Source". Spectrochim. Acta, V. 20, P. 733, 1964.

27. Scott, R. H. and Strasheim, A. "Laser Induced Plasmas for Analytical Spectroscopy". Spectrochim. Acta, V. 25B, P. 311, 1970.

28. Scott, R. H. and Strasheim, A. "Laser Emission Excitation and Spectroscopy". Appl. At. Spectrosc., P. 73, 1978.

29. Talmi, Y.; Sieper, H. P.; and Moenkebankenburg, L. "Laser-Microprobe Elemental Determinations With an Optical Multichannel Detection System". Anal. Chim. Acta, V. 127, P. 71, 1981.

30. Thompson, M.; Goulter, J. E.; and Sieper, F. "Laser Ablation for the Introduction of Solid Samples Into an Inductively Coupled Plasma for Atomic Emission Spectrometry". Analyst, V. 106, P. 32, 1981.

31. VanDeijck, W.; Balke, J.; and Maessen, F. J. "An Assessment of the Laser Microprobe Analyzer as a Tool for Quantitative Analysis in Atomic Emission Spectrometry". Spectrochim. Acta, V. 34B, P. 359, 1979.

32. Whitehead, A. B. and Heady, H. H. "Laser Spark Excitation of Homogeneous Powdered Materials". Appl. Spectrosc., V. 22, P. 7, 1968.

33. Yamane, T. and Matsushita, S. "Influence of a Spark Plasma on a Sample Surface in Laser Emission Microspectral Analysis". Spectrochim. Acta, V. 27B, P. 27, 1982.

34. Yamane, T.; Suzuki, S.; and Matsushita, S. "Laser Microemission Spectroscopic Analysis of Metals and Nonmetals". NASA Technical Translation No. NASA TT F-13,971 of November 1971: Translated from Bunko Kenkyu, V. 19, P. 147, 1970.

35. Zlotowska, Z. "Application of Laser for Spectral Analysis". Foreign Technology Division Translation No. FTD-HT-23-721-67 of October 1967, Wright-Patterson Air Force Base, Ohio: Translated from Przeglad Elecktroniki, V. 9, P. 445, 1966.

DISTRIBUTION LIST

NAVAIRENGCEN
- 1115 (2)
- 9011
- 92A1C
- 92A3 (25)
- 92713
- 92623

NAVAIRSYSCOM
- AIR-00D4 (2)
- AIR-310G (2)
- AIR-411
- AIR-417
- AIR-530
- AIR-536
- AIR-552
- AIR-55232D

DTIC (12)

JOAP-TSC Director
Building 780
Naval Air Station
Pensacola, FL 32508 (2 copies)

Air Force Program Manager/OAP
San Antonio Air Logistics
Center/MMETP
Kelly AFB, TX 78241

Commanding Officer
Naval Air Rework Facility (440)
Naval Air Station
Pensacola, FL 32508
Attn: Navy Program Manager/OAP

Commander
US Army DARCOM Material Readiness
Support Activity
Attn: DRXMD-MS
Lexington, KY 40511

REVISION LIST

REVISION	PAGES AFFECTED	DATE OF REVISION

DISTRIBUTION LIST

NAVAIRENGCEN
- 1115 (2)
- 9011
- 92A1C
- 92A3 (25)
- 92713
- 92623

NAVAIRSYSCOM
- AIR-00D4 (2)
- AIR-310G (2)
- AIR-411
- AIR-417
- AIR-530
- AIR-536
- AIR-552
- AIR-55232D

DTIC (12)

JOAP-TSC Director
Building 780
Naval Air Station
Pensacola, FL 32508 (2 copies)

Air Force Program Manager/OAP
San Antonio Air Logistics
Center/MMETP
Kelly AFB, TX 78241

Commanding Officer
Naval Air Rework Facility (440)
Naval Air Station
Pensacola, FL 32508
Attn: Navy Program Manager/OAP

Commander
US Army DARCOM Material Readiness
Support Activity
Attn: DRXMD-MS
Lexington, KY 40511

REVISION LIST

REVISION	PAGES AFFECTED	DATE OF REVISION

END

FILMED

3-85

DTIC